



Universitat de Girona

ASSESSMENT OF VIRTUAL DESIGN AND MANUFACTURING TECHNIQUES FOR FIBRE REINFORCED COMPOSITE MATERIALS

Marc GASCONS TARRÉS

Dipòsit legal: GI-74-2012

<http://hdl.handle.net/10803/52864>

ADVERTIMENT. La consulta d'aquesta tesi queda condicionada a l'acceptació de les següents condicions d'ús: La difusió d'aquesta tesi per mitjà del servei [TDX](#) ha estat autoritzada pels titulars dels drets de propietat intel·lectual únicament per a usos privats emmarcats en activitats d'investigació i docència. No s'autoritza la seva reproducció amb finalitats de lucre ni la seva difusió i posada a disposició des d'un lloc aliè al servei TDX. No s'autoritza la presentació del seu contingut en una finestra o marc aliè a TDX (framing). Aquesta reserva de drets afecta tant al resum de presentació de la tesi com als seus continguts. En la utilització o cita de parts de la tesi és obligat indicar el nom de la persona autora.

ADVERTENCIA. La consulta de esta tesis queda condicionada a la aceptación de las siguientes condiciones de uso: La difusión de esta tesis por medio del servicio [TDR](#) ha sido autorizada por los titulares de los derechos de propiedad intelectual únicamente para usos privados enmarcados en actividades de investigación y docencia. No se autoriza su reproducción con finalidades de lucro ni su difusión y puesta a disposición desde un sitio ajeno al servicio TDR. No se autoriza la presentación de su contenido en una ventana o marco ajeno a TDR (framing). Esta reserva de derechos afecta tanto al resumen de presentación de la tesis como a sus contenidos. En la utilización o cita de partes de la tesis es obligado indicar el nombre de la persona autora.

WARNING. On having consulted this thesis you're accepting the following use conditions: Spreading this thesis by the [TDX](#) service has been authorized by the titular of the intellectual property rights only for private uses placed in investigation and teaching activities. Reproduction with lucrative aims is not authorized neither its spreading and availability from a site foreign to the TDX service. Introducing its content in a window or frame foreign to the TDX service is not authorized (framing). This rights affect to the presentation summary of the thesis as well as to its contents. In the using or citation of parts of the thesis it's obliged to indicate the name of the author.



Universitat de Girona
Escola Politècnica Superior
Dept. d'Enginyeria Mecànica i de la Construcció Industrial

Assessment of virtual design and manufacturing techniques for fibre reinforced composite materials

A thesis submitted for the degree of Doctor of Philosophy

by

Marc Gascons i Tarrés

2011



Universitat de Girona
Escola Politècnica Superior
Dept. d'Enginyeria Mecànica i de la Construcció Industrial

Assessment of virtual design and manufacturing techniques for fibre reinforced composite materials

A thesis submitted for the degree of Doctor of Philosophy
by

Marc Gascons i Tarrés

2011

Advisors

Dr. Norbert Blanco
Universitat de Girona, Spain

Dr. Koen Matthys
Brunel University London, United Kingdom

To whom it might concern,

Dr. Norbert Blanco, Assistant Professor of the Department of Mechanical Engineering and Industrial Construction of Universitat de Girona.

Dr. Koen Matthys, Lecturer in the School of Engineering and Design at Brunel University London.

CERTIFY that the study entitled "Assessment of virtual design and manufacturing techniques for fibre reinforced composite materials" has been carried out under their supervision by Marc Gascons i Tarrés to obtain the doctoral degree, and accomplishes all the requirements to be considered for the European Mention.

Girona, June 2011

Acknowledgements - Agraïments

The author of this work wants to acknowledge the Department of Mechanical Engineering and Industrial Construction of the University of Girona for the support provided throughout the doctorate period, and particularly to the research group Analysis of Advanced Materials for Structural Design (AMADE) for the opportunity given. The author further acknowledges the support of the Mechanical Engineering Subject Area from the School of Engineering and Design at Brunel University London.

Also, this thesis would not have been possible without the expertise of Prof. Suresh Advani and the computational support of Dr. Pavel Simacek of the Center for Composite Materials of the University of Delaware, both of whom kindly acted as external advisor to the project.

The experimental work was realized with kind assistance of Mr. Jaume Vives in the laboratories of the Parc Científic i Tecnològic of the Universitat de Girona, and in the facilities of Airborne Composites B.V., The Hague, The Netherlands, through collaboration with Mr. Marco Brinkman, Mr. Alex Verduyn and Mr. Maarten van Vliet.

This doctoral research endeavour has been funded through the research group AMADE; however, partial funding and specific support have been received from private companies such as Poltank SAU or Airborne Composites B.V., and public funding bodies such as the Spanish government (through research projects CICYT MAT2006-14159-C02-01 and MAT2009-07918).

Vull que aquesta pàgina serveixi per retornar tot el que he rebut durant aquests anys i que no puc escriure en els capítols que venen a continuació.

Agraeixo als meus tutors el temps invertit en aquest projecte, el qual no hagués sortit endavant sense la seva especial implicació. A en Joan Andreu, per la oportunitat i a en Norbert i en Koen per la implicació i l'esforç.

Vull remarcar el mèrit de tots els que m'han hagut d'aguantar els crits, emprenyades i canvis d'humor d'aquells dies que costa tant tirar endavant. Pep, Marta, Elio, Jordi, Albert, Pere, tota la gent del galliner i dels despatxos de dalt... neu n'hi dó quina paciència que teniu! Gràcies!. També remarcar tots els moments de desconexió que m'han ofert els meus amics, a en Xavi i en Carles, a la Natàlia i la Eli, a en Jan, els Jordis, en Xevi i la Jordina, als nois i noies del Club Rem Casinet i molt especialment a la Lierni per aquesta recta final. A tots i totes, moltes gràcies.

Per acabar, vull que aquesta pàgina sigui per aquells que m'han servit de patró. Pels que m'han ensenyat una actitud i una forma de fer, a ser massell i a no rendir-me. Per aquells que m'han escoltat quan calia i m'han plantat cara quan tocava. Al pare, a l'Anna, a en Ramon i a la mare. Tot el que implica aquest document és un reflex del que m'heu transmès.

Un cop més, al meu pare.

Summary

Virtual tools are commonly used nowadays to optimize product design and manufacturing process of fibre reinforced composite materials. The present work focuses on two areas of interest to forecast the part performance and the production process particularities.

The first part proposes a multi-physical optimization tool to support the concept stage of a composite part. The strategy is based on the strategic handling of information and, through a single control parameter, is able to evaluate the effects of design variations throughout all these steps in parallel.

The second part targets the resin infusion process and the impact of thermal effects. The numerical and experimental approach allowed the identification of improvement opportunities regarding the implementation of algorithms in commercially available simulation software.

Sumari

Les eines de disseny virtual son usades de forma habitual per optimitzar el disseny i el procés productiu de peces de material compost reforçades amb fibra. Aquest treball es centra en dos àrees d'interès per la predicció de les prestacions de la peça i les particularitats del seu procés productiu.

La primera part proposa una eina d'optimització multi-física per recolzar l'etapa de desenvolupament d'una nova peça. La estratègia es basa en la gestió intel·ligent de la informació a través d'un paràmetre de control comú, permeten l'avaluació dels canvis en totes les etapes en paral·lel.

La segona part es centra en la infusió de resina, i particularment en l'impacte dels efectes tèrmics. Aquesta investigació numèrica i experimental ha permès la identificació de possibilitats de millora en la implementació d'algoritmes usats actualment en codis comercials de simulació.

Preface

The initial motivation of this PhD thesis was due to the fact that the research group AMADE, Universitat de Girona, felt the necessity to complement its research and technology transference capabilities in the virtual assessment of structural performance of composite materials for aeronautical and aerospace applications with expertise in manufacturing processes of fibre reinforced thermoset materials.

The group sensed an increasing demand for knowledge in the manufacturing and design areas, both from its academic and industrial partners. In collaboration with Professor Suresh G. Advani, an identification of suitable research topics and the development of research activity was made. The support of industrial partners, such as Poltank SAU and Airborne Composites has been also vital to understand the real need of the surrounding industry, focus the new research activities and transfer the developed topics directly to the surrounding area, testing it in a real industrial environment.

The conclusion of this work supposes the achievement of a milestone for the hosting research group, AMADE, not only for the opening of a new research line, but also for the experience acquired in this field and the development of a manufacturing equipment for further research. The present work also establishes the bases for a production process research line, closely related to companies, as well as the establishment of an European collaborative framework of technology transfer between the hosting Universitat de Girona, the University of Brunel and the European companies that support this initiative.

Contents

1	Introduction	9
2	List of Papers	13
I	Part I. Production and design optimization	15
3	Manufacturing processes for FRP vessels	17
3.1	Introduction	18
3.2	Early beginnings	23
3.2.1	Hand laminating	23
3.2.2	Spray up	24
3.3	The impact of regulation	26
3.3.1	Preform making	27
3.3.2	Double-sided closed mould infusion systems	28
3.3.3	One-sided closed mould infusion systems	30
3.4	A need for volume	32
3.4.1	Compression moulding systems	32
3.5	A drive for quality	33
3.5.1	Pre-preg lay-up systems	34
3.6	A push for automation	35
3.6.1	Filament winding	35
3.7	The impact of innovation	37
3.7.1	Fibre placement	38
3.7.2	Roll wrapping	39
3.8	Discussion	39

3.9 Summary	44
4 Strategy to support design processes	55
4.1 Introduction	56
4.2 Methodology	58
4.3 Case study. Supporting the decisions into the design process . . .	62
4.3.1 Design step: Material selection and configuration	62
4.3.2 Design step: Structural analysis	66
4.3.3 Design step: Production process	67
4.3.4 Design step: Production rates and costs	71
4.3.5 Design step: Strategy application	73
4.4 Discussion	75
4.5 Conclusions	77
II Part II. Thermal effects in virtual manufacturing	85
5 Fibre bed impact on resin viscosity	87
5.1 Introduction	88
5.2 Background	90
5.3 Methodology	94
5.3.1 Analytical model	94
5.3.2 Experimental work	98
5.3.3 Experiment vs. simulation	102
5.4 Results	104
5.5 Discussion	105
5.6 Case Study	108
5.7 Conclusions	111
6 Through-the-thickness temperature model	117
6.1 Introduction	118
6.2 Methods	121
6.2.1 Analytical background	121
6.2.2 Implementation	123
6.3 Experimental set-up	126

6.4	Results	131
6.4.1	Outputs of the numerical analysis	131
6.4.2	Data treatment and post processing	132
6.4.3	Resin heated configuration	134
6.4.4	Mould heated configuration	137
6.5	Discussion	138
6.6	Conclusions	140
7	Heat dispersion coefficient analysis	147
7.1	Introduction	148
7.2	Analytical background	150
7.2.1	Model considered	150
7.2.2	Term by term analysis	153
7.3	Experimental setup	154
7.4	Results	157
7.4.1	Data handling	157
7.4.2	Through-the-thickness conduction and dispersion	160
7.4.3	Output analysis	160
7.4.4	Discussion	165
7.5	Conclusions	166
III	Conclusions	171

List of Figures

3.1	<i>Hand layup production scheme</i>	24
3.2	<i>Spray up production scheme</i>	25
3.3	<i>Preform production</i>	28
3.4	<i>Resin Transfer Moulding</i>	29
3.5	<i>Compression moulding</i>	33
3.6	<i>Autoclave cure cycle</i>	34
3.7	<i>Filament winding</i>	36
3.8	<i>Fibre placement machine</i>	38
3.9	<i>Suggested techniques vs. volumes</i>	42
4.1	<i>Block diagram for usual simulation-aided design process.</i>	59
4.2	<i>Block diagram of the background of the proposed strategy.</i>	60
4.3	<i>Range analysis representative example</i>	61
4.4	<i>Main elastic properties</i>	64
4.5	<i>Relative thickness decrease as a function of V_f</i>	67
4.6	<i>Gate and vent placement</i>	69
4.7	<i>Filling time for the different infusions considered.</i>	70
4.8	<i>Variation of the thickness along the filling path</i>	70
4.9	<i>Scheme and layout of the production process.</i>	72
4.10	<i>Cost and production time variation vs control parameter V_f.</i>	73
4.11	<i>Blocks of data handled in the proposed strategy.</i>	74
4.12	<i>Chart illustrating the strategy for the specific case study.</i>	75
5.1	<i>Thermoset polymer viscosity behaviour</i>	90
5.2	<i>Two-dimensional mesh</i>	98
5.3	<i>RTM6 viscosity behaviour</i>	99

5.4	<i>Resin flow front vs. infusion time</i>	101
5.5	<i>Schematic of the infused flat panel</i>	102
5.6	<i>Experimental flow front position vs. time</i>	105
5.7	<i>Fibre volume distribution over mesh elements</i>	106
5.8	<i>Flow front prediction with different fibre volumes</i>	107
5.9	<i>Effect of permeability on predictions accuracy</i>	108
5.10	<i>Vessel mesh geometry</i>	109
5.11	<i>Filling isochrones</i>	110
6.1	<i>RIFT and RTM schematics</i>	119
6.2	<i>Representation of the expected temperature profile</i>	126
6.3	<i>Real setup overview</i>	127
6.4	<i>Transversal section detail</i>	129
6.5	<i>Resin potlife according to accelerator content</i>	130
6.6	<i>Numerical temperature prediction</i>	132
6.7	<i>Comparison of results for resin heated configuration</i>	133
6.8	<i>Infrared image, resin heated sample</i>	136
6.9	<i>Comparison of infrared camera data vs analytical solution</i>	136
6.10	<i>Comparison of results for the heated mould configuration</i>	137
6.11	<i>Infrared image, mould heated sample</i>	139
6.12	<i>Comparison of infrared camera data vs analytical solution</i>	139
7.1	<i>Schematic representation of RIFT techniques</i>	148
7.2	<i>Scheme of a longitudinal cut of the experimental rig</i>	155
7.3	<i>Detail of a transversal section of the sample</i>	156
7.4	<i>Detail of a longitudinal cut of the sample</i>	159
7.5	<i>Infrared image of the upper surface of one of the samples</i>	159
7.6	<i>Temperature recorded from one of the infused samples</i>	161
7.7	<i>Velocity profiles for the different infusions conducted.</i>	162
7.8	<i>Result comparison with and without the fourth term</i>	163
7.9	<i>Through-the-thickness heat dispersion term vs. Péclet number</i>	163
7.10	<i>Different conduction and dispersion terms vs. Péclet number</i>	164

List of Tables

3.1	<i>Application and pressures</i>	21
3.2	<i>Temperature ranges</i>	30
3.3	<i>Comparison of evaluative parameters</i>	40
3.4	<i>Mechanical performance</i>	41
3.5	<i>Cost selection chart</i>	41
4.1	<i>Main mechanical properties</i>	63
4.2	<i>Production scenarios considered in the case study.</i>	72
5.1	<i>Basic non-linear viscosity expressions</i>	92
5.2	<i>Advanced non-linear viscosity expressions</i>	92
5.3	<i>Main panel dimensions and material description</i>	100
5.4	<i>Values for the time-dependent viscosity expressions</i>	104
5.5	<i>Filling times for three different vessel sizes</i>	110
6.1	<i>Properties of the used materials</i>	129
6.2	<i>Main dimensions and experimental program information</i>	131
7.1	<i>Main dimensions and experimental program description</i>	157
7.2	<i>Auxiliary data extracted from the test configuration.</i>	158

Chapter 1

Introduction

The presence of thermoset reinforced composite materials in an ever-growing list of engineering applications has today brought forward the need to better understand, control and improve the step-by-step aspects of the composites design process and the related manufacturing techniques. In this matter, virtual design and manufacturing simulation tools play an important role and are increasingly deployed in the industrial environment. The extent to which details of all process steps are to be modelled in order to obtain industrial useful results and the significance of including more physical phenomena such as thermal and curing effects are key focus points for the on-going research in this field.

The present work investigates the benefits of virtual design and manufacturing tools for composite production in a two-part approach.

In the first part of this study, optimization opportunities for the complete composite design and manufacturing process are explored by means of two studies. First, a review of state-of-the-art composite manufacturing techniques is presented. Its findings have been composed from an extensive literature review enhanced with valuable practical insights, gained from initiating hands-on manufacturing experience through support of local composite manufacturers such as Poltank SAU and Airborne Composites, B.V.. The review makes use of a common industrial application, pressure vessels, as a leitmotif throughout the story and touches upon aspects of historical evolution, properties of currently used techniques, and future tendencies.

Next, a virtual design and manufacturing optimization scheme is put forward that proposes to tweak every step of the entire process through the careful selection and use of a single control parameter. The proposed optimization strategy encompasses indeed the step of constituent and reinforcement architecture selection, manufacturing process simulation, structural analysis, as well as the cost and production volume validation. Also here a practical aspect sides with the proposed methodology: with fibre volume fraction as the chosen control parameter, the various steps in a composite design and liquid injection moulding manufacturing case study are being subjected to the theoretical optimization scheme.

The second part of this study targets specifically the composite manufacturing process of liquid injection moulding and the particular impact that the inclusion of thermal and curing effects can have on the results from a virtual design and manufacturing cycle. In turn, this approach also allowed identification of improvement opportunities regarding the implementation of selected algorithms in current commercially available simulation software. This second part is composed of three studies.

A first study pinpoints the precision drop observed in the prediction of resin flow front advance when filling time starts approaching resin gel time. A non-linear, empirically-based viscosity model is proposed which is able to take into account the fibre bed effect on resin parameters during flow propagation. It is demonstrated that the use of this model results in better flow propagation predictions than traditional non-linear models based on neat resin characterization.

A second study covers the existence of temperature gradients in non isothermal set-ups for thick composite parts. A 3D temperature prediction model is presented. This model has been constructed as a further evolution of an existing 2D temperature module module in the research code LIMS from the collaborating institute Center of Composite Materials (CCM), University of Delaware.. Experimental model validation was performed by infusion of composite specimens under different non-isothermal conditions. The developed 3D tool provides a temperature plot during infusion that can be used onwards in the virtual design and manufacturing process when residual stress predic-

tions are to be made.

Finally, a third study investigates the predictive power of a local thermal equilibrium energy balance model, specifically targeting the impact in RIFT set-ups. The work is based around an experimental analysis of the thermal behaviour during infusion of thick composite specimens instrumented with thermocouples. Findings report on the capability of the energy balance model to accurately reproduce the experimental trends.

With this work, the research group AMADE of Universitat de Girona (Spain) has met its objective to explore a new composites research area and diversify beyond their established endeavours in structural analysis. Through partnership with Brunel University London (UK), an initial knowledge transfer in virtual composites design and manufacturing has been achieved. Under continued joint supervision, a blend of analytical, computational and experimental results were produced by the PhD. candidate, thus enabling him to present this research work and lay a foundation for future efforts in this particular field of composites.

Chapter 2

List of Papers

The body of this dissertation consists of the following five manuscripts:

- M. Gascons, N. Blanco, J.A. Mayugo, K. Matthys, A strategy to support design processes for fibre reinforced thermoset composite materials, *Applied Composite Materials*. Accepted 20 April 2011.
DOI 10.1080/0740817X.2011.590177
- M. Gascons, N. Blanco, K. Matthys, Evolution of manufacturing processes for fiber reinforced thermoset tanks, vessels and silos: A review. *IIE Transactions*. Accepted 11 May 2011.
DOI 10.1007/s10443-011-9203-1
- M. Gascons, N. Blanco, P. Simacek, J. Peiro, S. Advani, K. Matthys, Impact of the fibre bed on resin viscosity in liquid composite moulding simulations. *Applied Composite Materials*. Accepted 28 June 2011.
DOI 10.1007/s10443-011-9218-7
- M. Gascons, N. Blanco, J. Vives, K. Matthys, Numerical implementation and experimental validation of a through-the-thickness temperature model for non-isothermal vacuum bagging infusion. *Journal of Reinforced Plastics and Composites*. Accepted 17 Aug 2011.
DOI 10.1177/0731684411423321

- M.Gascons, N.Blanco, K.Matthys, Study of through-the-thickness heat conduction and dispersion in Resin Infusion under Flexible Tooling (RIFT).
To be submitted to International Journal of Heat and Mass Transfer

Part I

Production and design optimization techniques

Chapter 3

Evolution of manufacturing processes for fibre reinforced thermoset tanks, vessels and silos: A review

M. Gascons, N. Blanco, K. Matthys, Evolution of manufacturing processes for fiber reinforced thermoset tanks, vessels and silos: A review, IIE Transactions. Accepted 11 May 2011.

DOI 10.1007/s10443-011-9203-1

3.1 Introduction

Tanks, vessels and silos come in all shapes and sizes and are defined in this paper as receptacles containing a fluid, solid or gas. Thermoset fibre reinforced polymer (FRP) composite vessels firstly emerged in the chemical industry in the 1950s and expanded from there towards a wide range of different applications such as storage and handling of flammable and combustible liquids [1], sewage systems [2], pressurized operator equipment [3], offshore infrastructure [4], aerospace fuel recipients [5], etc. It was during the 1960s that manufacturers began to develop recognized design standards and test methods for FRP storage. Today, there are a number of internationally recognized standards and specifications for FRP storage containers, such as the ones created by the the American Society for Testing and Materials (ASTM)[6, 7], the American Society of Mechanical Engineers (ASME)[8], the Steel Tank Institute (STI) [9] and others entities [10, 11].

During the formation of design approach and the selection of manufacturing process for the production of a vessel, several criteria have to be taken into account concurrently. In what follows, we address shape, size, service position, strength, materials and the working environment as key areas of importance. Regarding shape, vessel geometries are in most of cases achieved by a revolution of a defined section around a central axis, which ends either with a flat lid or with a spherical or dome-shaped end. The latter offers advantages in terms of load distribution, but requires special attention as it constitutes a critical point in the structural design analysis [12, 13]. Regarding size, vessel diameters can range from a few centimetres to a couple of meters. Indeed, some processing techniques will not achieve sharp curvatures as found on small tanks, and smart fibre draping strategies for such products will be critical for successful manufacturing. For large diameter vessels, the

amount of bulk material necessary has to be considered in order to propose a cost-efficient manufacturing solution for them.

As an example, consider the selection of resin material. It is found that small diameter or high performance vessels requiring a high strength-to-weight ratio will commonly use an epoxy resin system. This is the case for off-shore, cryogenic or high pressure vessels. The cost of the high-quality resin is justified because not much of it is needed and performance (such as damage tolerance) is a critical design parameter. Polyester and vinylester systems, on the other hand, are applied in large diameter vessels with less critical strength-to-weight ratio. Examples of applications could be water tanks or large industrial, atmospherical, storage tanks. Indeed, despite adding weight, mechanical strength can still be achieved using more volume of a less-expensive resin-type [14, 15]. Apart from Epoxy, Polyesters and Vinylesters, which represent the most commonly used resin families on the market, other thermosets are less common such as Cyanate Esters, Bismaleinide and Polyamide.

Composite vessels are further extremely resistant to a variety of corrosive environments, and that gives them a clear advantage over vessels constructed with a more traditional material such as steel. A common misconception is that FRP is unaffected by corrosion for all applications. Instead, corrosion resistance is a property that needs to be introduced by design via careful selection of composite constituents for a targeted application. In terms of such material selection, the reinforcement choice is based mainly on filament materials and the fibre arrangement. As an example, C-type glass fibre is often used in chemically resistant environments [16], E-type glass fibre is applied in alkali environments [17], while carbon fibre is found mostly for applications where the design is driven by a critical final weight or pressure accommodation [18]. In addition, properties of constituents can be altered by the way they are held, manipulated and consolidated during manufacturing. High resistance to corrosion is directly related to low maintenance and more favourable ageing properties, which is a critical point in large vessels, due to the difficulty to move, replace or repair once in service.

Apart from suitability to the working environment, the design brief for a composite vessel also enlists requirements from a purely mechanical perspec-

tive [19], with the most important item being the accommodation of an internal vessel pressure. The mechanical strength of an FRP product depends upon the amount, type and arrangement of fibre reinforcement. As FRP materials can be mainly considered as shell structures, in-plane and out-of-plane properties are generally defined. Several research groups, such Air Force Materials Laboratory Wright-Patterson, Washington University or West Virginia University, put their efforts to obtain different micromechanical models. The reader is invited to read the book of Barbero et al. [20] to obtain more information. As an example, the model presented in Equations 3.1-3.6 is often used by the authors of this work.

$$E_{in-plane} = C_{11}^* - \frac{2C_{12}^{*2}}{2C_{22}^* + 2C_{23}^*} \quad (3.1)$$

$$E_{out-of-plane} = \frac{(2C_{11}^* C_{22}^* + 2C_{11}^* C_{23}^* - 4C_{12}^{*2})(C_{22}^* - 2C_{23}^* + 2C_{44}^*)}{3C_{11}^* C_{22}^* + C_{11}^* C_{23}^* + 2C_{11}^* C_{44}^* - 4C_{12}^{*2}} \quad (3.2)$$

$$G_{in-plane} = C_{66}^* \quad (3.3)$$

$$G_{out-of-plane} = \frac{C_{22}^*}{4} - \frac{C_{23}^*}{4} + \frac{C_{44}^*}{2} = \frac{E_{out-of-plane}}{2(1 - \nu_{out-of-plane})} \quad (3.4)$$

$$\nu_{in-plane} = \frac{C_{12}^*}{C_{22}^* + C_{23}^*} \quad (3.5)$$

$$\nu_{out-of-plane} = \frac{C_{11}^* C_{22}^* + 3C_{11}^* C_{23}^* - 2C_{11}^* C_{44}^* - 4C_{12}^{*2}}{3C_{11}^* C_{22}^* + C_{11}^* C_{23}^* + 2C_{11}^* C_{44}^* - 4C_{12}^{*2}} \quad (3.6)$$

In equations 3.1-3.6, E stands for the Elastic Modulus, G for the Shear Modulus and ν for the Poisson ratio. The terms C_{ij}^* correspond to the positions $i-j$ of the stiffness matrix determined using an approach based on the periodic microstructure supposition.

Mechanical design efforts are focused on the avoidance of localized high stress areas and zones prone to localized leakage such as vessel connection ports [21]. As strength requirements are mainly imposed by a hydrostatic

pressure load case, low anisotropy is desired in the material configuration. For low pressure applications, a short fibre reinforced thermoset matrix such as mat or similar can be considered for the construction of the section with the most important structural load. For high pressure applications, a reinforcing strategy can be used consisting in the placement of extra, more structural resistant, material, such as multi-axial fabrics, in order to create localized reinforcement and avoid stress concentration problems. Limitations and suitability of this technique will be determined by the shape, service position and location of connection ports and any joints in the vessel wall. An evaluation of pressure limits as the critical design parameter is summarized in Table 3.1, as a function of manufacturing techniques and its typical applications.

Technique	Reference pressure	Typical applications
Hand Lay-up	10 bar	Storage tanks, Water deposits
Spray-up	10 bar	Grain silos, Septic tanks
RTM	200 bar	Immersion bottle, Food industry
RIFT	100 bar	Water storage , Underground tank
Compression moulding	50 bar	Industrial supply, Air storage
Pre-preg layup	700 bar	Aerospace tank , Fuel tank (high-end)
Filament winding	700 bar	Hydrogen storage, Truck transport
Roll wrapping	50 bar	Motorsport , Underwater tank
Adv. fibre placement	700 bar	Cryogenic, Aeronautical

Table 3.1: *Typical applications and reference pressures for different manufacturing techniques.*

For large vessels, weight and position also become important variables to include in the assessment of material selection and manufacturing process. Vessel position while in service is of great importance for static-placed products. Weight must be included as an additional key load in the design, so if the central axis is placed vertically, one lid must be reinforced to support the internal pressure and the weight of the vessel. Should the vessel be placed horizontally, central reinforcements (rings) must be placed on the long edge to ensure mechanical strength. In safety critical applications such as vessels used to store gas or liquid aboard a transport vehicle, pressure (including neg-

ative pressure for vacuum service tanks) but also storage and environmental temperature will influence the structural design [22].

In conclusion, by carefully selecting a combination of resin, fibres, additives, design approach and manufacturing technique, the manufacturer can create a part that meets the desired design specifications and manufacturing standards for a specific industrial application. Different authors such as Srinivasan et al. [23] or Gascons et al. [24] now work on analytical procedures and strategies to obtain an efficient virtual design and manufacturing tool that merges all of the selection and decision making.

The development of simulation tools to support the selection of the most adequate technique has notably increased in the past years. Simulation is able to forecast final results with little investment, which is of great attraction to industries. Simulation tools invite and accelerate further research into manufacturing techniques and have already resulted in notable improvements, leading to evolved processes and the breaking of traditional working limits and operational barriers. As manufacturing techniques are extremely varied and also often consist of different stages, several software tools are used for the simulation of different activities in different stages of the process. Among them, closed mould processes are dominated by resin flow simulation codes such as PAM-RTM (ESI Group, Paris, France [25] or LIMS (University of Delaware, Newark, DE, USA) [26], and the winding family can be covered with CADWIND (Material, Brussels, Belgium) [27] or CADFIL (Crescent Consultants Ltd, Derby, UK) [28]. The latest state-of-the-art robotised techniques are equipped with bespoke control and automation software. Finally, FEA analysis remains the standard for structural evaluation and for assessment of the manufacturing process itself on the performance of the final part (e.g. induced distortions or residual stresses).

But as different approaches can lead to similar results, there is still no real consensus on the ideal pathway for the determination of an optimal design and manufacturing technique for a given application. In what follows, the most relevant techniques for FRP composite vessel manufacturing are reviewed. The evolution of change is described from the first basic manufacturing process to the current automated, shaped-based accurate and high-tech processes.

3.2 Early beginnings

The fundamentals of FRP composite manufacturing include the correct mixture of the two constituents (matrix and reinforcement), and the subsequent consolidation of the matrix by means of an exothermic reaction that changes the matrix state from liquid to solid (this work targets thermoset composite applications). The selection of different manufacturing processes described here represents a range of different strategies to achieve these two conceptual steps (i.e. the constituent mixture and the consolidation). Limitations of a specific manufacturing process originate not only from the technique or tooling itself but also from the product design specification (i.e. level of quality, precision, finish,...) and processing regulations (environmental, health and safety). Craftsman hand laminating techniques were used at the beginning, which soon were improved via the introduction of automation, such as spray up, settling the initial milestones of a long development path.

3.2.1 Hand laminating

The first technique used in the manufacturing of FRP composite vessels was hand laminating. Also known as hand lay-up, the technique is still in use nowadays to produce low cost composite parts. The process, represented in Figure 3.1, is operator intensive, and consists of pouring resin over a dry fibre fabric or mat, spreading the resin with hand rollers, and letting it cure in an open mould setup (although it can be combined with closed mould techniques). In the hand lay-up process, the quality of the final part is closely related to the ability of the operator. Several studies, such as the analytical work conducted by the Polymer Composites Group of the University of Nottingham by Long et al. [29] and Rudd et al. [30] or Hancock et al. [31] in the University of Bristol, address the importance of the placing and draping of the dry preform to ensure best fitting of the fabric inside the mould cavity. The increase of material compaction with a roller hand tool is the only way to reduce void spots and air bubbles, creating a better mixture between components. Also, excess of resin can be removed with the roller, which will increase the low level of fibre volume of the process, and consequently, achieve better final material

properties. A major disadvantage of hand lay-up is the hefty health and safety implications in the workshop to protect the workers from the harmful styrene emissions produced by the crosslinking of the resin during curing.

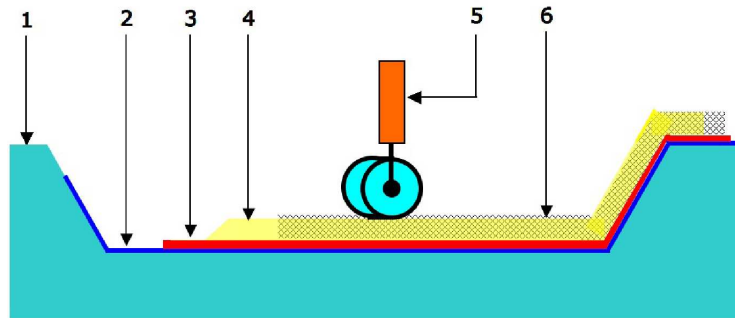


Figure 3.1: *Hand lamination scheme [33]. 1 Mould. 2 Release agent. 3 Gel-coat. 4 Resin layer previously poured. 5 Rolling. (removing air for good fibre wetting). 6 Fabric layer.*

Widely used for storage tanks or for water treatment vessels [32], hand lamination is usually associated with E-glass mat and Polyester, but various physical properties can be enhanced by selection of a different resin and reinforcement type. Considered a relatively inexpensive method for vessel manufacturing due to its low equipment and tooling cost, its main limitation is not being able to achieve high repeatability in mechanical and accuracy requirements due to its high dependence on operator skills.

3.2.2 Spray up

A first improvement, mainly related to multi-directional fabrics, consists on introducing stacked layers or plies of woven roving fabric where the resin has already been poured over in a previous stage [34]. Squeegees, rollers and brushes are used to impregnate these various textile layers. Additional resin is then applied to the outside of the stack until there is a clean surface finish without air bubbles or other deformities. This manufacturing process still needs a high degree of skill from the operator to obtain a part that extracts maximum strength from the fibre architecture. However, having the layers wetted before stack enhances the mixture of the two components. Imperfections, such as dry zones into the thickness of the wall, decreases and the

distribution of resin over the fabric becomes more homogeneous, reducing also the number of undesirable poor resin zones.

The spray-up process is a second improvement and the first automation step for the hand lay-up process. A spray-gun, which can be operated manually or by a robotic arm as shown in Figure 3.2, sprays fibre and resin over the mould.

The spray-gun is one of the key elements of the process, as it handles the fibres, mixes them with the resin and projects the compound mixture into the mould. Although the cost of the spray-up equipment is relatively low compared to the raw material, labour and overhead cost, correct equipment selection is still vital to ensure that chopping and mixing of the components is effective. Different kinds of guns can be used for this task [35, 36], such as airless internal mixing, turbulent mixing or distributive mixing. After projection into the mould, consolidation is achieved using a roller to ensure the compaction of the mixture.

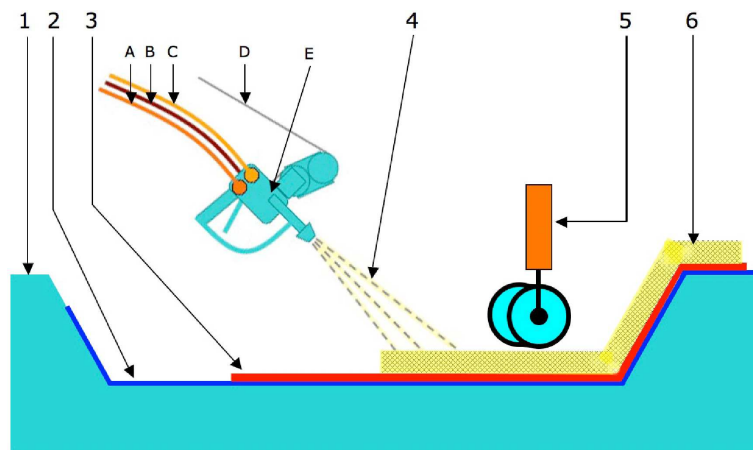


Figure 3.2: Schematics of spray-up process [37]. 1 Mould. 2 Release agent. 3 Gelcoat. 4 Deposit fibre resin mixture. 5 Rolling. (removing air for good fibre wetting). 6 Trimming. A Supply resin (A component). B Supply resin (B component). C Supply air pressure. D Supply fibre. E Spray-up / Chopper gun.

The spray-up process [38] is much faster than the hand lay-up process and is also a less expensive alternative, because it starts from a raw, low processed material such as fibre reels, which represent a cheaper reinforcement

constituent than carefully constructed reinforcement layers. After the mixing process, the compound produced with spray-up is very close to a chopped strand mat composite, but presents more flexibility in terms of fibre-to-resin ratio as well as better malleability to the curvatures of the mould (the reinforcement is built up immediately in the mould and does not need draping).

While spray-up does not solve the styrene emission problem, it is a cleaner technique than the manual wet lay-up. Indeed, the interaction between composite constituents and operator is highly reduced due to the material charge being carried by the chop gun. Regarding mechanical strength, part properties can be enhanced and part-to-part differences reduced by controlling the spray-gun with a robotic arm that is programmed with the exact spray sequence prior to the process initiation.

Typical applications of the spray-up process are the production of big surfaces for parts that do not have high mechanical strength requirements, such as storage silos, water or waste tanks [39]. The spray-up technique is considered one of the most economical processes to produce large to middle-size tanks, with diameters between half a meter to several meters.

Low investment in moulds and tooling, the relative simplicity of the process and the delivery of cheap parts were the main drivers for the initial success of the hand lay-up and spray-up processes. However, with the hazardous emission of volatiles from resin curing still remaining, a different fundamental technical approach was needed.

3.3 The impact of regulation

Worker's unions and health organizations widen the repercussion of research about the effects on workers of the volatile organic compounds (VOC) and fibreglass handling. Studies such as the ones of Minamoto et al. [40] and Dement [41] lead to restrictive environmental regulations from governments [42–44], forcing companies to invest heavily in process modifications so as to comply with new regulations and face the pressures of interest groups. The change to a more stringent regulated manufacturing landscape triggered an increase in research to improve the manufacturing techniques, not only by

reducing waste material via recycling methods [45], but also by adapting to market requirements through variability reduction in part-to-part quality [46]. Therefore, the spray-up process, though versatile and low-cost, was soon replaced with a closed mould preform infusion technique. Preform infusion consists of injecting resin into a fibre sheet reinforcement with a shape close to the final part [47]. After creation of the preform reinforcement, the subsequent infusion process can be achieved with a closed mould technique. There is a large list of nomenclatures for different closed mould techniques. Resin transfer moulding (RTM), vacuum assisted resin transfer moulding (VARTM), vacuum bagging moulding (VBM), Resin Film Infusion (RFI), Seeman Composite Resin Infusion Process (SCRIMP) or RTM-light, are techniques that can be classified depending on whether they have one or two rigid mould halves. The techniques enumerated can be considered natural evolutionary variations of the RTM or VBM process, described next, and therefore present slight differences that can be further explored in manufacturing handbooks [48].

All resin infusion processes have in common that a pressure difference is maintained over the mould, usually via a pump on the inlet, a vacuum pump on the vent or a combination of both. The propagation of injected resin into the dry fabric can be estimated by Darcy's Law. (Equation 3.7).

$$q = K/\mu \cdot \nabla P \quad (3.7)$$

In Equation 3.7, μ stands for resin viscosity, K represents the permeability tensor inherent to the preform, and ∇P is the pressure gradient inside the mould cavity. For more information on resin modelling, it is suggested to consult the work by Rudd et al. [29] or Simacek et al. [26].

3.3.1 Preform making

The infusion preform can be obtained by projecting roving fibre with a binder (e.g. unsaturated polyester) over a perforated mould, which is under a negative pressure (vacuum). As shown in Figure 3.3, this method is popular for applications involving small-to-medium dimensions with a relatively uniform reinforcement cross section, e.g. filter deposits for water or chemical prod-

ucts [49].

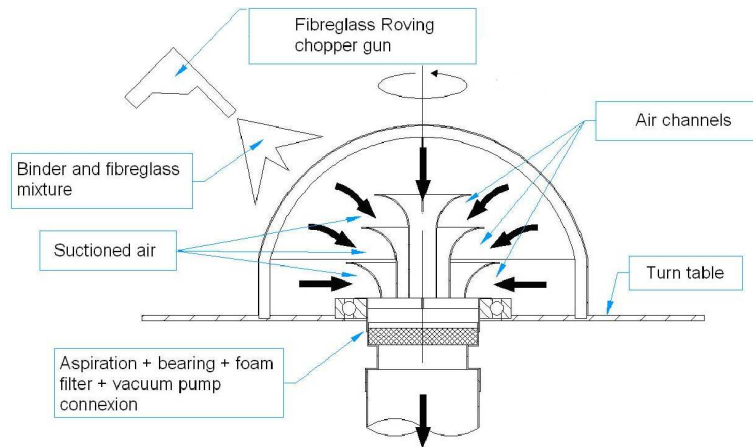


Figure 3.3: *Scheme of the production process for a preform.*

The process of preform creation can be instrumented to achieve a high level of automation with the implementation of robotics, giving the possibility to control the fibre angle and the fibre content on every zone of the part. Such a preform production system allows the creation of locally reinforced areas, such as ribs. The capability to deliver more complex composite parts under highly controlled conditions allowed meeting tougher market demands such as from the aeronautical and aerospace sector where sizeable composite parts with high mechanical performance became an important target. As an example, a subsidiary of Owens Corning Fibreglass developed a sophisticated preform production system, the Applicator P4 [50], for an automotive composite consortium. Large series of parts have to be produced to recover the investment cost, which is why such automated tooling is currently only in use by companies aiming at very large product series or by companies sharing manufacturing capabilities.

3.3.2 Double-sided closed mould infusion systems

Resin transfer moulding (RTM) is a widely implemented manufacturing process [51] that consists of manually placing dry preforms, mat or fabrics in a rigid double-sided mould, which is closed by clamping the two mould parts firmly together. The catalysed resin is then pumped into the mould cavity via

dispensing tooling equipment. Typical injection pressures are kept within 1 to 10 bar. The relatively low injection pressure allows a slow liquid impregnation, which results in better part quality but at the expense of a longer production time. Faster filling times can be achieved through single or multiple injection ports, allowing a better resin impregnation of the reinforcement placed inside the mould. Once filling is completed, an exothermic curing reaction is initiated that causes the solidification of the impregnated composite part. Heat can be applied to the mould to shorten the cure-time after curing initiation. After curing, the part is removed from the mould.

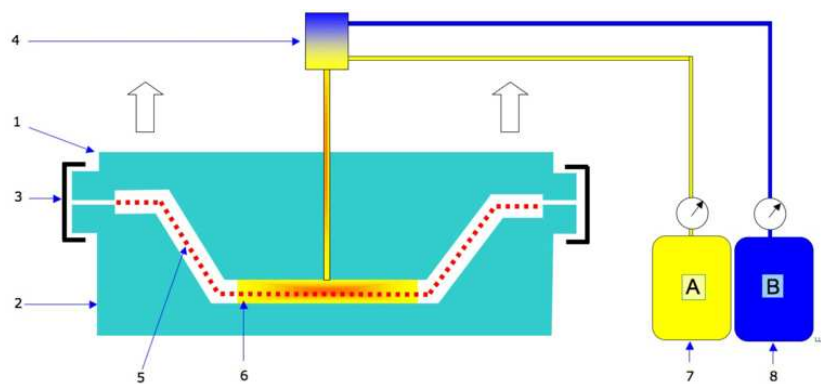


Figure 3.4: Scheme of resin transfer moulding processes. 1 Upper mould. 2 Lower Mould. 3 Clamp. 4 Pump. 5 Fibre reinforcement. 6 Mixed resin. 7 Base Resin. 8 Hardener. [52].

Structural parts that need a surface finish on both sides can be obtained with this method, unlike with the open mould processes as described before. RTM offers production of cost-effective structural vessels in medium-to-high volume series using relatively low-cost tooling and with an increase of fibre volume levels as compared to open mould techniques, allowing also the control of fibre directions. The capability of using continuous fibre fabrics and the increase of the fibre volume fraction offers improved mechanical properties over already presented techniques.

Further development of the RTM technique has been inhibited by the lack of efficient and cost-effective preforming technology and too long cycle times (infusion is a slow process). The introduction of heat during the infusion stage is a common industrial strategy. Heat reduces viscosity and results in a better

and faster resin propagation. In the following Table 3.2, reference temperature ranges for most used resins can be observed.

Resin type	Process temperature [°C]
Polyester	20-80
Vinylester	20-80
Epoxy	20-150
Phenolic	20-100
BMI	100-180

Table 3.2: *Temperature ranges of operability for major thermoset resin systems.*

Research institutions affiliated to the University of Delaware, Nottingham, Delft or Auckland, in collaboration with leading companies such as Magnum Venus Plastech or Quickstep, work on improvements that are focused on an injection mixing head technology and lay-up automation. Also PLC-based hardware and software are being developed to better control the injection parameters, such as pressure or resin flow rate, and thus providing control to avoid so-called washing effects (undesired fibre movement due to resin injection), dry zones or simply unnecessary extra filling.

3.3.3 One-sided closed mould infusion systems

The tooling cost associated with the RTM infusion stage can be reduced by moving away from the double sided mould and introducing a vacuum bagging film in place of one of the mould halves (VBM). A dry-laminate is then placed over a mould with some ancillary material that must be included to facilitate the infusion process, and the mould cavity is closed by sealing it with a plastic bagging film. The ancillary material consists of a flow enhancement sheet to help the resin flow through the preform, a bleeder cloth to absorb the excess of resin from the fibre laminate and also to ensure that vacuum pressure is distributed evenly and uniformly over the part, and a release film to help remove all from the final part. After sealing and the insertion of vacuum pressure, the

whole set-up can be introduced into an oven or an autoclave for temperature and pressure curing.

The lack of a rigid mould half results in a mould cavity that is affected by suction, causing a variation in thickness that should be taken into account when analysing the infusion process. After the work conducted at the Laboratory for Manufacturing and Productivity of the Massachusetts Institute of Technology, Gutowski et al. [53], suggest the expression to evaluate this thickness variation:

$$\frac{\partial h}{\partial t} = \frac{1}{u} \left[\left(K \frac{dh}{dP} + h \frac{dK}{dP} \right) \left(\frac{\partial P}{\partial x} \right)^2 + hK \left(\frac{\partial^2 P}{\partial x^2} \right) \right] \quad (3.8)$$

In Equation 3.8, h is the thickness of the mould cavity, x is the flow front distance, K is the permeability and P is the compaction pressure. The expression can be implemented by means of an iterative finite element method to compute the pressure field, from which flow front progression can be determined using Darcy's law (Equation 3.7).

In the case of oven curing, consolidation time is reduced with the introduction of heat. Standard composite ovens operate in a typical range from room temperature up to 250°C, in cycle times of 2 to 24 hours. The main issues regard the appropriate distribution of temperature in the oven to ensure uniformity of the curing process and avoid residual stresses. Gascons et al. [24] are working in advanced analytical models that reproduce thermal evolution inside the mould cavity.

Comparing to open mould techniques, the advantages of vacuum bagging are similar to those that RTM can offer (quality increase, reduced emissions, etc). Though Vacuum Bagging Moulding (VBM) has a significantly lower tooling cost than RTM, some attention in infusion set-up preparation is needed if VBM is to challenge the quality and structural strength obtained via double-sided rigid mould techniques. The positive effect of compression on part quality during infusion and curing cycle is clearly recognized, and as there is far less pressure build-up being achieved with VBM than with RTM, the consolidation of constituents is one of the main issues that needs attention in the vacuum bagging manufacturing process. Indeed, studies as made by Palardy

et al. [54] underline the notable increase in quality and mechanical strength from the part when interchanging the flexible tooling bag with a rigid tool in selected manufacturing processes.

However, many applications do not have strength and surface finish as the most critical design needs. For example, the manufacturing of two-half vessels can take profit of the more cost-effective vacuum bagging technique as the internal vessel sides have no surface finish quality requirements. True, VBM does imply a greater waste in ancillary material, which can not be reused. However, silicon or rubber bags can sometimes provide a solution if there is a need to re-use the same bagging material more than once.

3.4 A need for volume

Environmental regulations effectuated a first substantial change in manufacturing methods (i.e. from manual or semi-automated open mould techniques to closed mould techniques). Closed mould techniques are indeed more environmentally friendly and healthier for the operators but still have an inherent limitation to high volume manufacturing due to the nature of the (slow) injection process. Therefore, a second wave of change was related to the need for higher manufacturing rates and was characterized by the introduction of fundamentally different processing techniques.

3.4.1 Compression moulding systems

A good example away from classic injection is the creation of the compression moulding technique [55]. Compression moulding is a manufacturing method in which the moulding material, commonly referred to as moulding compound, is placed in an open, heated and matched metal mould cavity. The mould is typically made from machined steel that will ensure a long service life. The compound consists on a mixture of fibre and resin prepared beforehand in the exact proportion and amount to satisfy the material needs of the part. In the compression moulding process, the mould is closed with extreme pressure to force the fibre and resin compound into contact with all areas of the

mould. Heat and pressure are maintained until the compound material has cured. A representative compression moulding cycles uses clamping forces up to 30 tones and temperatures in range of 100°C to 300°C. The process employs thermosetting resins with short or long chopped fibres, such as random mat and/or preforms, but a similar process has been developed for the use of thermoplastic resins.

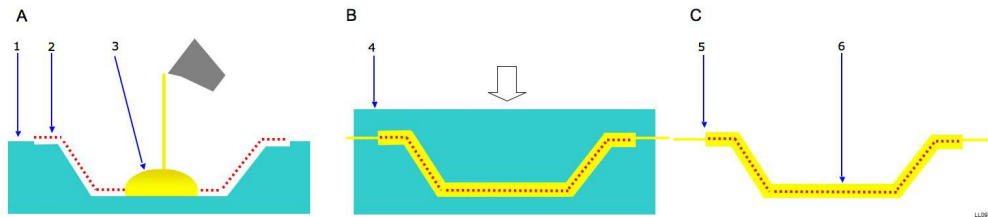


Figure 3.5: *Compression moulding processes scheme in three steps (A,B,C). 1 Lower Mould. 2 Reinforcement fibres. 3 Resin 4 Upper Mould. 5 Area to trim. 6 Final Part [56].*

Compression moulding is a high-volume, high-pressure method suitable for manufacturing complex fibre reinforced components. A distinctive advantage of compression moulding is its ability to mould small to large intricate parts with features such as holes that would otherwise have to be post-machined with other workshop processes. Compression moulding produces fewer knit lines and less fibre-length degradation than injection moulding. Carbon, aramid and fibreglass are suitable fibres for this composite manufacturing process. The technique negatively affects the mechanical strength of the vessel when compared to RTM or vacuum bagged products, so it is usually related to low requirements-high volume series applications as for example atmospheric pressure vessels.

3.5 A drive for quality

The difficulty of controlling resin diffusion through a dry fibre architecture is one of the predominant causes of rejecting parts in a quality control process. To avoid the need of resin flow through the reinforcement fabric, a production process using previously impregnated (pre-pregs) fabrics was developed.

3.5.1 Pre-preg lay-up systems

Pre-preg layers are a combination of fibres and an uncured resin that only needs temperature to be activated (which is why pre-preg laminates have to be stored in a cold and controlled environment). In the pre-preg lay-up process, the readily impregnated layers are cut and laid down in an open mould, in the desired fibre orientation, and then vacuum bagged. After vacuum bagging, the composite with the mould is put inside an oven or autoclave where heat and/or pressure are applied for curing and consolidation of the part. The cure cycle is strongly determined by the resin typology. A typical autoclave cycle comprises a 2 to 48h period, with temperatures between 25°C to 250°C and pressures up to 7 bar. Ramps and dwells are planned during the cycle in order to reduce the residual stresses and improve the consolidation process. Figure 3.6 represents a classic two dwell curing process for an epoxy pre-preg.

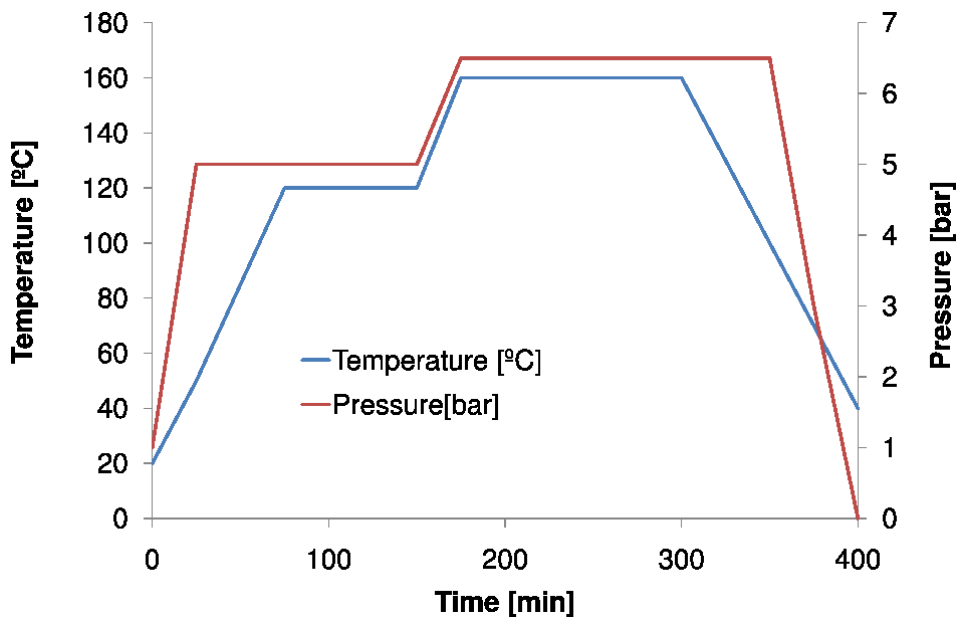


Figure 3.6: *Example of an autoclave curing cycle for an epoxy resin part.*

Although pre-peg lay-up is a very labour-intensive process, the supreme final quality of the part makes it a worthy investment for low series, high-performance products. Pre-preg lay-up facilitated the introduction of FRP tanks in the aerospace industry, where complex shapes and high mechanical strength requirements (associated with high fibre volumes) are mandatory.

The curing process causing matrix consolidation has been clearly improved in the last years by reformulating the composition and by using cure activation techniques such as UV-lights or ultrasound [57] to eliminate VOC emission and to increase part repeatability and quality. The introduction of further process control technology and new manufacturing philosophies (including continuous fibre position control) will drive future innovation in the pre-preg lay-up process. At present, new pre-preg materials are being developed by major producing companies such as Cytec, Gurit, Hexcel or Toray in order to avoid the need of autoclave curing without reducing the final quality of the part. Room temperature curing will make pre-preg technology more accessible for other markets that currently cannot invest in expensive autoclave equipment.

3.6 A push for automation

A final step towards cutting-edge manufacturing processes for FRP composite vessels includes taking profit of the specific vessel geometry. Control strategies and robotic applications, like filament winding, were introduced to substitute human intervention in the manufacturing process, ensuring best quality of each part as well as high repeatability.

3.6.1 Filament winding

The filament winding technique has been strongly developed after the initial work of Rosato and Grove [58] in 1963. In this process, a bundle of resin-impregnated fibres [59] are wound at a desired angle over a rotating mandrel, as shown in Figure 3.7. A carriage unit moves forward and backwards as the mandrel rotates, generating a relative, time-dependent, position and angle between carriage and mandrel. Numerical expressions, such as the one developed in the Production Technology section of the Delft University (Equation 3.9) can be used to analytically track this position [60].

$$G \{E_3\} + \lambda \Delta G \{E_3\} = p \{E_0\} \quad (3.9)$$

In the Equation, G is the fibre position vector, λ is the length of the free

hanging fibre, ΔG is the orientation of the tangent vector and $p\{E_0\}$ is the position of the delivery eye. Hereby is $\{E_0\}$ the general coordinate system, and $\{E_3\}$ the local (part) coordinate system.

The control of the winding speed (between 60 to 90 metres/minute) as well as the relative motion angle between parts allows the definition of the fibre angle at each point. The technique has a high capability of determination of the exact position of the reinforcement at any point on the part. Filament winding is the preferred method for high-performance vessels such as rocket vessels or accumulators [4, 61] and can be run with a high level of automation. Restrictions to this technique are the difficulty to achieve low fibre angles in reference to the longitudinal axis of the part (0° to 15°), which can be a problem for certain geometries such as elongated bodies with small cross-sectional diameters.



Figure 3.7: *Filament winding tanks and its production technique.*

In the filament winding process, fibre roving is pulled from large spools through a resin bath, such as epoxy, and wound upon specially designed mandrels. The mandrel itself is often a template and remaining part of the final vessel, as it can serve as a waterproof internal liner. While the mandrel is wound, a carriage containing the fibre spools and resin matrix travels back and forth down the length of the mandrel and the epoxy fibre matrix is applied at a precise rate to ensure proper winding. The process is automated

and monitored by specifically designed computer-controlled filament winding programs. These software ensure that the composite filament substance, now a series of laminate plies, is applied accurately with regards to fibre orientation and precise fibre-to-resin volume, which is usually around 60 % with this method [62]. Once the composite filaments are applied, a special non-stick plastic film is wrapped under tension around the part to provide additional compaction to the composite, and is easily removed after the curing process. The mandrel is subsequently placed in a computer-controlled oven in which targeted heating profiles harden the polymeric resin, solidifying the composite material. If necessary, the mandrel is then pulled from the composite part using an extracting machine. In this case, a release agent must be applied to mandrels prior to winding to aid the extraction process. The part can then be machined, finished, and painted into its final form as per customer specification.

Various patents are applicable to the filament winding method for vessel manufacturing, such as [63–65], so as to ensure protection of the industrial benefits of the adaption of a general purpose winding process to the specifics of the vessel geometry. The vessel filament winding process was mainly developed to manufacture vessels with tensed (glass) fibres [66] oriented to bear the combination of the hoop and axial force. Filament winding with a dual angle configuration can be used to obtain layers of fibre in a near axial orientation and is used to obtain high-pressurized vessels [67], such as the pressure tanks manufactured by EDO Fibre Science [68].

3.7 The impact of innovation

With growing technological innovation, the vessel manufacturing processes continue to progress. Refinements are introduced and techniques naturally evolve to deliver ever better composite parts. The higher described filament winding technique is for example evolving into a controlled fibre or tow placement process. Cross-over also occurs as existing techniques are combined to extract and merge the best properties into a new manufacturing system. An example of this evolution is the creation of the roll wrapping process.

3.7.1 Fibre placement

Fibre (or tow) placement was developed in 1970 by Hercules Aerospace Co. (now Alliant Techsystems). The process consists on heating and compacting resin pre-impregnated non-metallic fibres on typically complex tooling mandrels. The process is comparable to some extent with filament winding [69], although clear differences can be observed. Meanwhile in filament winding the fibre comes in circular tows, in fibre placement the fibre usually comes in a tape shape consisting in aligned tows of fibres impregnated with epoxy resin. Fibre placement machines (FPM) generally have a capacity of 12 to 32 tows, which are fed to a heater and compaction roller on the FPM head and through robotised machine movements, which are placed in courses across a tool surface. Some machines can control each bundle independently, so more complex surface or laminate types can be achieved. Courses are generally placed in orientations of 0° , $+45^\circ$, -45° and 90° to build up plies which in combination, have good properties in all directions. This system, showed in Figure 3.8, combines high fibre volumes with the accuracy on placement of the filament winding process, which is very suitable for the production of double-curved domes of the ends of some vessels. Also some wider lines can be obtained with a variation of the technique called Tape Placement, where several bundles are placed together at the same time.



Figure 3.8: *Mtorres Fibre placement machine.*

Advanced fibre placement machines [70] are used for the manufacturing

of large-scale, complex shaped, high-performance composite vessels and are mainly developed by and for the aerospace and aeronautical industry, where absolute control and accuracy in the manufacturing process is crucial. Still, the technique had to face with batch production limitations.

3.7.2 Roll wrapping

The mostly cylindrical vessel shape has also allowed for the creation of the roll-wrapping technique. Roll wrapping [48] is born from a combination of pre-preg lay-up and fibre placement, widely used for manufacturing pipes and sport goods. In this process, the pre-preg laminate is rolled over a removable mandrel and covered with a shrink tape, which is wrapped for consolidation. The entire assembly is then cured for solidification, assisted by the pressure applied via the shrink tape. Suitable for manufacturing the main body of cylindrical vessels, roll wrapping is a more simple and lower cost alternative to filament winding. It is applicable to recover internal linings, offering aesthetics and structural protection. Vessel extremities can be manufactured separately from the main vessel body and glued together in a later step.

3.8 Discussion

In most common tank applications, fibre reinforced thermosets were originally not considered as a first choice material, but as an alternative to other more traditional materials, such as the metals family, which is still used as a reference. However, the introduction of fibre reinforced thermosets over the past decades in multiple industrial fields has consolidated their great potential, and it is now common to see them substituting original design materials, as they have proven their advantages in durability, cost and weight. The higher specific strength of FRPs definitely positions them in front of their alternatives. However, the more complicated composite manufacturing process is still impeding wide-scale infiltration into some markets. In Table 3.3 a ranking is established between properties of fibre reinforced thermoset vessels versus properties of vessels made with alternative materials.

	Metallic	Plastic	Concrete	Fibre reinforced
Weight	M to H	M	H	L
Cost	M	L to M	M	L to H
Durability	M	M to H	M	H
Ease of Manufacture	H	H	M	M to H
L=Low M=Medium H=High				

Table 3.3: *Comparison of different evaluative parameters for vessels materials decision.*

On manufacturing cost terms, plastic and metal tanks will still be costless options due to its more optimized production process. Concrete option is a candidate for extra-large tanks where weight is not an issue and there are no compatibility problems between the tank and the stored product.

As this document states, a vast range of techniques exist that can be used for the production of thermoset resin reinforced vessels. This does compromise the definition of general characteristics for the entire materials family and one would have to perform in-depth analysis into each of them in order to better understand and classify their properties. In any case, the final performance of the product is highly dependent on its manufacturing technique.

One can now evaluate the performance capability of a manufacturing technique by analysing the typical fibre content and void fraction associated with it. In Table 3.4, typical ranges for both parameters can be observed. With this, one can position manufacturing techniques in terms of which is more suitable from a structural performance point of view.

The technical evaluation of a candidate production process for a vessel has then to be contrasted with its economical viability. A compromise solution between both performance and cost will enable or restrict the application of a production method for a predetermined design brief or market requirement. In addition, one should consider whether other restrictions such as size limitations or surface requirements can be satisfied by the process. Table 3.5 deploys key cost factors and typical restrictions as a function of the different production techniques presented. It provides a comprehensive overview of

Manufacturing technique	Fibre volume typical range	Void fraction typical ranges	Mechanical performance
Hand Lay-up	15% to 30%	5% to 10%	Low
Spray-up	15% to 30%	5% to 10%	Low
RTM	50% to 60%	< 2%	High
RIFT	40% to 60%	1% to 3%	High
Compression moulding	30% to 40%	< 3%	Medium
Pre-preg Lay-up	50% to 65%	< 2%	Top
Filament winding	50% to 70%	1% to 10%	High
Adv. Fibre placement	50% to 65%	< 2%	Top
Roll wrapping	45% to 55%	3% to 5%	Medium

Table 3.4: *Evaluation of typical indicatives of mechanical performance for each manufacturing technique.*

the cost associated to processes as well as possible limitations and final part appearance.

Manufacturing technique	Labour cost	Tooling cost[\$]	Equipment cost[\$]	Unit cost	Shape & size limitations	Surface finish
Hand Lay-up	H	< 25k to 50k	5k to 25k	H	Mould	1. Fair to good
Spray-up	M	50k	100k to 200k	H	Mould	1. Fair to good
RTM	M	100k to 250k	100k to 200k	M to H	Mould and inj. pump	2. Good to excellent
RIFT	M	50k	25k to 50k	M	Mould	1. Good to excellent
Compression moulding	L	100k to 250k	100k to 250k	M to L	Press rate and size	2. Good to excellent
Pre-preg Lay-up	H	< 250k	250k	H	Mould and autoclave	1. Good to excellent
Filament winding	L	100k	100k	M to H	Machine size	2. Medium to good
Adv. Fibre placement	L	< 250k	250k	H	Machine size	2. Good to excellent
Roll wrapping	L	50k to 100k	50k to 100k	M	Machine size	1. Good to excellent

L=Low M=Medium H=High

Table 3.5: *Key cost parameters for the selection of a manufacturing technique for composite vessels.*

Another constraint to be included to determinate the economic viability

of the candidate technique will be its production rate capability. Vessels for applications requiring large series will necessarily have to be manufactured by compression moulding or roll wrapping technique while short series, usually referred to prototyping or high-end applications, should be obtained with hand-layup or fibre placement techniques. In the following Figure 3.9 one can observe suggested techniques depending on the required production rate.

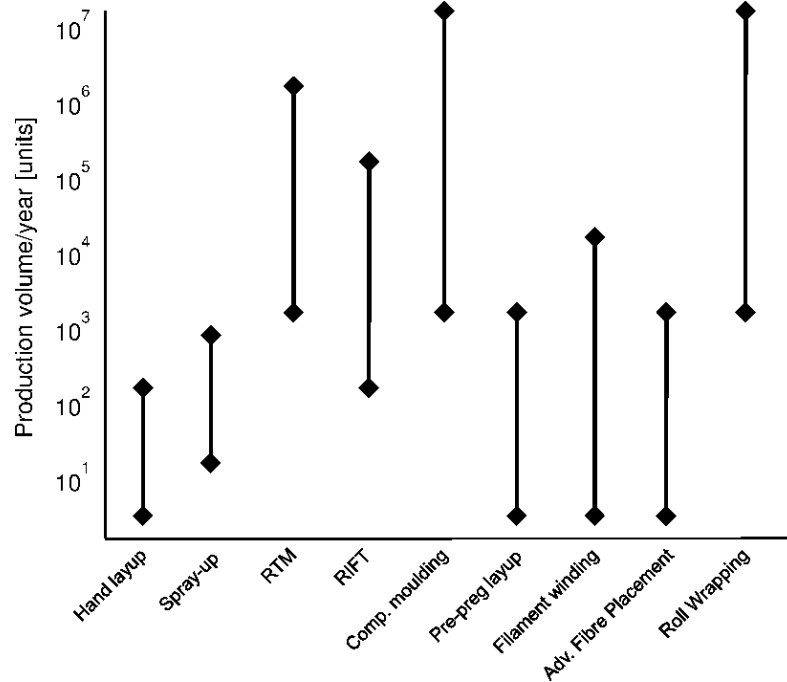


Figure 3.9: Suggested techniques for production of composite tanks depending on the produced volumes.

Different analytical evaluations can be used to determine the best manufacturing process depending on different constraints, although the industrial sector mainly defines structural [71] or cost [72] optimizations. An interesting procedure is presented by Bader ([73]), where base material and process are defined as interdependent, and expressions for selection strategies based on scale of production, tooling, part size, automation level or structural performance can be found.

Bader defines a feedstock cost C_f (Equation 3.10), and a process cost subdivided into tooling C_T , labour C_L and operations C_P (Equations 3.11 to 3.13 respectively).

$$C_F = 100mP_F/u \quad (3.10)$$

$$C_T = P_T/N_T \quad (3.11)$$

$$C_L = t_h P_L/60 \quad (3.12)$$

$$C_P = t_p P_p(1/w + i)/(W) + P_0 \quad (3.13)$$

Where m stands for mass, P_F is the raw material cost per kilo and u is the percentage of feedstock utilization. P_T is the tooling cost and N_T is the total number of parts to be produced. t_h is the operator labour time (in minutes) and P_L corresponds to its hourly economic retribution. In the last equation, t_p is the operating time, P_p is the capital value, w is the return period, i stands for global interest rates, W stands yearly working hours and P_0 is the cost related to power, maintenance, etc. of the installation.

This should be used together with an evaluation of the desired performance. For this aspect, and coincident with Ashby [74], a value function (Equation 3.14) where $E^{\$}$ represents an exchange constant that relates mass m and the cost C of the part is used. In the same manner, the expression can be shifted to include specific strength or other performance evaluators.

$$V_i = E^{\$} \cdot m - C \quad (3.14)$$

The careful consideration of the enumerated constraints has led to today's success of many fibre reinforced thermoset vessel products. As an example of a high-end application, the optimization of filament winding and fibre placement machines has led to the successful implementation of storage vessels in transport vehicles, e.g. as used in hydrogen cars. In this application, carbon fibre reinforced epoxy tanks have surpassed alternative materials due to their high strength and low weight properties, while having solved issues with damage propagation. For fibre reinforced thermoset vessel products, this has resulted into an attractive position in the transportation market, which is forecasted to become a key area for growth for vessels in the future.

Simulation techniques have helped both research centres and industry solving particular processing limitations and extend their range of application. Tanks produced via an RTM technique are used in off-shore applications, with significant cost reductions when compared to wound products, and achieving larger diameters and sizes. The flexibility of the fibre placement process also allows the development of newly optimized geometries that can better handle cryogenic temperatures or match complex fitting structures as commonly found in aerospace applications.

3.9 Summary

Since the initial introduction of the hand laminating techniques, it is clear that a great deal of technological advancement has filtered into the manufacturing process for FRP composite vessels. Following shy attempts to semi-automatize the labour-intensive hand laminating, it was really the introduction of environmental regulations that effectuated a major drive for change and brought closed mould infusion techniques onto the scene.

The possibility of more process control and the directly related higher repeatability ensured the successful spread of the closed mould techniques. At the same time, more high-performance applications in expanding markets such as aerospace were developing. This increased the amount of companies and industries that became interested in acquiring the then state-of-the-art manufacturing technology, causing an exponential growth of composites vessel manufacturing throughout.

Soon however, the need for higher volume manufacturing started challenging the further development of closed-mould resin infusion techniques, and alternatives such as compression moulding were sought and found. A need for high-quality, controlled resin impregnation also brought about the pre-preg lay-up process, another move away from infusion methods.

Further automation and innovation led to advanced processes (filament winding) and the combination of techniques (fibre placement and roll wrapping). These advanced techniques are now experiencing a clear evolution in terms of consumer markets, moving from initially high-end aerospace and

aeronautical applications to more and more generic and cost-restricted consumer products.

Despite the inspiring evolution from simple hand methods to fully-automated processes over the last fifty years, it appears that due to the variety of design needs that are to be satisfied a place for many of the here described processes will remain. The array of different vessel sizes, shapes and applications is vast, and it seems unlikely that a one-fits-all manufacturing process will come about any time soon. Perhaps we should not be worried or confused about this. In fact, we are better to embrace the very co-existence of different technologies in various stages of automation and innovation, as it provides the perfect feeding ground for further technological change and innovation in composites design and manufacturing.

Bibliography

- [1] J. M. Starbuck, Low cost manufacturing for composite natural gas vehicle (NGV) fuel tanks (1997).
- [2] D. Jones, FRP improves design of sewage treatment equipment, Reinforced Plastics 42 (8) (1998) 44–46.
- [3] T. Messenger, M. Pyrz, B. Gineste, P. Chauchot, Optimal laminations of thin underwater composite cylindrical vessels, Composite Structures 1 (58) (2002) 529–537.
- [4] O. O. Ochoa, M. Salama, Offshore composites: Transition barriers to an enabling technology, Composites science and technology 1 (65) (2005) 2588–2596.
- [5] J. C. Williams, E. S. Starke Jr., Progress in structural materials for aerospace systems, Acta materialia 1 (51) (2003) 5775–5799.
- [6] ASTM, D 4097-88 Contact-moulded glass-fibre-reinforced thermoset resin chemical-resistant tanks. American Society for Testing and Materials (1998).
- [7] ASTM, D 3299-88 Filament-wound glass-fibre-reinforced thermoset resin chemical-resistant tanks. American Society for Testing and Materials (1988).
- [8] ASME, Rpt-1 Reinforced thermoset plastic corrosion resistant equipment. American Society of Mechanical Engineers (1989).
- [9] STI, Act-100 Specification for external corrosion protection of FRP composite underground storage tanks (2001).

- [10] AWWA, D120-84 Thermosetting fibreglass-reinforced plastic tanks. American Water Works Association (1984).
- [11] E. Comitte, Directive 97/23/EC of the European parliament and of the council of 29 May 1997 on the approximation of the laws of the member states concerning pressure equipment (1997).
- [12] M. Hojjati, V. S. Ardebili, S. V. Hoa, Design of domes for polymeric composite pressure-vessels, *Composites Engineering* 5 (5) (1995) 51–59.
- [13] C. C. Liang, H. Chen, C. Wang, Optimum design of dome contour for filament-wound composite pressure vessel based on a shape factor, *Composite Structures* 58 (4) (2002) 469–482.
- [14] A. Newbery, P. Gunung, World's largest FRP acid storage tanks, *Reinforced Plastics* 49 (10) (2005) 26–29.
- [15] A. Newbery, Large diameter FRP tanks mark progress in Mexico, *Reinforced Plastics* 45 (11) (2001) 40–42.
- [16] A. Kootsookos, P. Burchill, The effect of the degree of cure on the corrosion resistance of vinyl ester/glass fibre composites, *Composites Part A: Applied Science and Manufacturing* 1 (35) (2004) 501–508.
- [17] M. Farshad, A. Necola, Strain corrosion of glass fibre-reinforced plastic pipes, *Polymer testing* 1 (23) (2004) 517–521.
- [18] R. Mohan, *High pressure vessel construction* (1987).
- [19] P. Levend, N. Katirci, Design of fibre-reinforced composite pressure vessels under various loading conditions, *Composite Structures* 58 (58) (2002) 83–95.
- [20] E. Barbero, *introduction to composite materials design*, Taylor and Francis, Philadelphia, PA, USA, 1999.
- [21] P. Mertiny, A. Gold, Quantification of leakage damage in high-pressure fibre-reinforced polymer composite tubular vessels, *Polymer Testing* 26 (26) (2007) 172–179.

- [22] K. Myung-Gon, K. Sang-Guk, K. Chun-Gon, Tensile response of graphite/epoxy composites at low temperatures, *Composite Structures* 79 (1) (2007) 84–89.
- [23] R. Srinivasan, H. M. Karandikar, F. Mistree, Understanding design and manufacture interaction using compromise decision support problems. 1-A formulation for composite pressure vessels, *Computers and Structures* 40 (3) (1991) 679–692.
- [24] M. Gascons, N. Blanco, K. Matthys, Mechanical and manufacturing optimization of a large vessel through simulations, in: *Proceedings Texcomp 9 Conference*, 2008, 151–164.
- [25] M. L. Skinner, New applications and approaches expand market for composites software, *Reinforced Plastics* 50 (6) (2006) 24–28.
- [26] P. Simacek, S. Advani, Desirable features in mould filling simulations for liquid composite molding processes, *Polymer Composite* 25 (4) (2004) 355–367.
- [27] Material, Cadwind (2010).
- [28] Crescent Consultants limited, Cadfil (2010).
- [29] A. C. Long, C. D. Rudd, M. Blagdon, P. Smith, Characterizing the processing and performance of aligned reinforcements during preform manufacture, *Composites Part A: Applied Science and Manufacturing* 27 (4) (1996) 247–253.
- [30] C. D. Rudd, M. R. Turner, A. C. Long, V. Middleton, Tow placement studies for liquid composite moulding, *Composites Part A: Applied Science and Manufacturing* 30 (9) (1999) 1105–1121.
- [31] S. Hancock, K.D. Potter, The use of kinematic drape modelling to inform the hand lay-up of complex composite components using woven reinforcements, *Composites Part A: Applied Science and Manufacturing* 3 (37) (2006) 413–422.

- [32] Poltank SAU, www.poltank.com (2006).
- [33] L. van Lieshout, Hand lay-up moulding. Visualization of the hand lay-up process (2007).
- [34] L. Stringer, Optimization of the wet lay-up/vacuum bag process for the fabrication of carbon fibre epoxy composites with high fibre fraction and low void content, *Composites* 5 (20) (1989) 441–452.
- [35] A. Jacob, Spray-up offers process improvements, *Reinforced Plastics* 46 (1) (2002) 32–34.
- [36] J. Bert, Plural component external mix spray gun and method (1990).
- [37] L. van Lieshout, Spray lay-up moulding (2009).
- [38] J. Mansvile, Roving designed for spray-up processing, *Reinforced Plastics* 5 (48) (2004) 21.
- [39] DSM, Automatic spray-up of GRP silos, *Composites* 1 (5) (1970) 321.
- [40] K. Minamoto, M. Nagano, T. Inaoka, T. Kitano, K. Ushijima, Y. Fukuda, M. Futatsuka, Skin problems among fibreglass reinforced plastics factory workers in japan, *Industrial Health* 40 (40) (2002) 42–50.
- [41] J. M. Dement, Environmental aspects of fibrous glass production and utilization, *Environmental Research* (9) (1975) 295–312.
- [42] E. Parliament, Directive 2004/42/ce of the European parliament and of the council of 21 April 2004 on the limitation of emissions of volatile organic compounds due to the use of organic solvents in certain paints and varnishes and vehicle refinishing products and amending directive 1999/13/ec (April 2004).
- [43] Department of Enviromental Quality, State of Oregon, Fibreglass manufacturing and the environment (2010).
- [44] Division of pollution prevention, Environmental assistance, Fibreglass and Composite Manufacturing (2010).

- [45] S. Wilkinson, Research into using recycled mixed plastics-fibreglass to produce coil carriers for the steel industry, Techinal Report PLA0007-11, WRAP (2002).
- [46] J.Keim, Crude awakening: rising resin costs have driven up fibreglass pool prices. What are builders and manufacturers doing to soften the blow, Pool and Spa News retrieved .
- [47] R. Crutchlow, Changing from open to closed moulding, Reinforced Plastics 48 (8) (2004) 40–41.
- [48] S.Mazumdar, Composites Manufacturing: Materials, Product, and Process Engineering, CRC Press, Boca Raton, FL (USA), 2002.
- [49] Pentair INC., Triton series of pentair inc. (2009).
- [50] Applicator System AB, www.applicator.se (2010).
- [51] J.Li, C.Zhang, R.Liang, B.Wang, Statistical characterization and robust design of RTM processes, Composites Part A: Applied Science and Manufacturing 36 (5) (2005) 564–580.
- [52] L. van Lieshout, Resin transfer moulding (2006).
- [53] T. G. Gutowski, G. Dillon, The elastic-deformation of lubricated carbon-fibre bundles - comparison of theory and experiments, Journal of Composite Materials 26 (16) (1992) 2330–2347.
- [54] G. Palardy, P. Hubert, M. Haider, L. Lessard, Optimization of RTM processing parameters for class a surface finish, Composites Part B: Engineering 39 (7-8) (2008) 1280–1286.
- [55] C. Rudd, A. Long, K. Kendall, C. Mangin, Liquid Moulding Technologies, Woodhead Publishing Limited, Cambridge (UK), 1997.
- [56] L. van Lieshout, Wet compression moulding (2009).
- [57] F. Guasti, E. Rosi, Pressure vessels: A possible application of low energy e-beam curing, SAMPE Journal 36 (36) (2000) 25–30.

- [58] D. Rosato, C. Grove, Filament winding: Its development, manufacture, application and design (1964).
- [59] F. C. Shen, A filament-wound structure technology overview, *Materials Chemistry and Physics* 42 (2) (1995) 96–100.
- [60] S. Koussios, O. K. Bergsma, A. Beukers, Filament winding. Part 2: generic kinematic model and its solutions, *Composites Part A: Applied Science and Manufacturing* 35 (1) (2004) 197–212.
- [61] V. Vasiliev, A. Krikanov, A. Razin, New generation of filament-wound composite pressure vessels for commercial applications, *Composite Structures* 62 (3-4) (2003) 449–459.
- [62] D. Cohen, S. Mantell, L. Zhao, The effect of fibre volume fraction on filament wound composite pressure vessel strength, *Composites Part B-Engineering* 32 (5) (2001) 411–427.
- [63] W. Goldsworthy, G. Korzeniowski, C. Carter, Method for fabricating composite pressure vessels (2003).
- [64] B. Avni, L. Lukov, Y. Liberman, O. Bachmutsky, Methods for manufacture of reinforced composite vessel (2000).
- [65] J. Marks, Process for lining composite vessels (1986).
- [66] T. Hwang, C. Hong, C. Kim, Size effect on the fibre strength of composite pressure vessels, *Composite Structures* 59 (4) (2003) 489–498.
- [67] S. Peters, Improvements in FEA of composite overwrapped pressure vessels, in: *Proceedings of the 41st ISTC, 2003*, pp. 44–48.
- [68] E. F. Corporation, <http://www.edocorp.com/edofiberscience.htm> (2009).
- [69] S. Beckwith, Filament winding vs. fibre placement manufacturing technologies, *SAMPE Journal* 44 (44) (2008) 54–55.
- [70] B. Shirinzadeh, G. Alici, C. W. Foong, G. Cassidy, Fabrication process of open surfaces by robotic fibre placement, *Robotics and Computer-Integrated Manufacturing* 20 (1) (2004) 17–28.

-
- [71] C. Monroy, A. Skordos, M. Sutcliffe, Design selection methodology for composite structures, *Materials and Design* 29 (2) (2008) 418–426.
- [72] K. Wang, D. Kely, S. Dutton, Multi-objective optimisation of composite aerospace structures, *Composite Structures* 57 (1-4) (2002) 141–148.
- [73] M. Bader, Selection of composite materials and manufacturing routes for cost-effective performance, *Composites Part A: Applied Science and Manufacturing* 33 (7) (2002) 913–934.
- [74] M. F. Ashby, Multi-objective optimization in material design and selection, *Acta Materialia* 48 (1) (2000) 349–369.

Chapter 4

A strategy to support design processes for fibre reinforced thermoset composite materials

M. Gascons, N. Blanco, J.A. Mayugo, K. Matthys, A strategy to support design processes for fibre reinforced thermoset composite materials, Applied Composite Materials. Accepted 20 April 2011.

DOI 10.1080/0740817X.2011.590177

4.1 Introduction

Fibre reinforced thermoset polymers (FRP) are a type of composite materials that are adopted more and more in a variety of industries and markets. FRP materials offer great design flexibility and enviable mechanical strength properties. However, these materials are also challenging from a manufacturing point of view, mainly due to the complexity of mixing two or more components together under specific manufacturing conditions. It is thus vital to *design* the manufacturing process in parallel with the component itself, making the conceptual development of a new composite part one of the most important stages of the entire process. It is a crucial step where a wide range of decisions need to be taken in a short amount of time. Time and resource limitations usually do not allow to experimentally test every potential design-to-manufacturing solution. Virtual design and manufacturing tools have thus become more appealing to industry [1–4], as they offer valuable (virtual) test or prototyping information in a short lead time and for a relatively low investment.

Responding to the industrial need, highly specialized codes have been developed over time that can cover almost every single step of the design process. Software packages such as Esacomp [5] or Cadec [6] provide micromechanical models that can give virtual design support in the selection of constituent materials and configuration of the composite architecture. Part geometry can be designed via advanced CAD programs such as CATIA, ProE, Inventor, SolidWorks, NX, to name but the most widely used. Subsequent simulations of structural behaviour can be conducted using finite element analysis (FEA) software such as MSC.MARC [7], ABAQUS [8], etc. Following, the part model can be passed to simulation software for the manufacturing process.

Manufacturing process simulations of fibre reinforced composite parts are focused on techniques that make use of a resin infusion process. Simulations

are used to localize gates and vents, avoid dry spots and optimize the process parameters such as filling time, flow front propagation, mould temperature, etc. Virtual manufacturing software tools for composites are less established than CAD or FEA structural analysis software, but some commercial packages exist [9] and some research codes are also available [10].

A final virtual design step can be conducted using enterprise resource planning software, which allows for e.g. material requirements planning [11] and manufacturing resource planning [12]. Currently available software packages for resource planning are highly configurable to the size and business objectives of the company and can be provided by e.g. SAP, SAGE, NAVISION, etc.

Although there are several software codes to assist each design step, industrial practice confirms that insufficient integration exists between the different virtual design tools, even from the same provider. This makes it a laborious task to work through an optimized solution that covers the entire process. Indeed, one can immediately envisage many difficulties in acquiring a multitude of different software platforms, and subsequently maintaining the infrastructure and operating across it.

Attempts have been made to create multi-platform packages that are able to support the design process via integration of two or more design steps, and some even tackle the complete process from material selection to manufacturing. However, such integrated packages mainly focus on improving exchange of information (e.g. file formats, data types, ...) between subsequent design steps and hardly offer a solution for iterative optimization across the design process. A linear path is followed that enables the sequential evaluation of changes in each step of the design. However, such a linear progression path quickly becomes limited. Designers first need to work through all the steps in order to get a complete picture (i.e. shape, strength, cost,..) of a first estimate solution. Subsequent changes then imply that the design process has to be reconsidered in a series of sequential (rather than simultaneous) re-design efforts, making the whole process tedious and impractical. There is currently no software commercially available that is able to conduct a truly integrated and simultaneous full path analysis, and this is certainly a hot working topic for major software companies [13].

While efforts towards fully integrated environments are progressing fast, it remains of fundamental interest to develop design decision making strategies that are independent of software packages altogether. Many authors have reviewed and contributed to this problem. Several partial or more comprehensive solutions have been proposed, though no consensus exists. Some reports focus on a specific step in the design path, such as classification and definition strategies [14], material selection to structural optimization [15], or cost optimization strategies [16, 17]. Other reports cover strategies that tackle the entire design path, but are linked to a specific part geometry, such as the work presented by Srinivasan et al. [18–20].

The work proposed here aims to provide a design decision-making strategy for virtual composites design and manufacturing. It recognizes that highly specialized software is able to provide project tailored tools and better results than generic multi-platform software. Its key feature is that it attempts to move away from a sequential or linear process progression and instead links all design process steps together through an identified common control parameter. Changes to the control parameter propagate simultaneously through all the design stages, hereby making significant efficiency gains during re-design efforts. The proposed strategy has been developed as a generic design philosophy. It can be tailored to the requirements of any specific industry and made applicable to a variety of materials and manufacturing processes. For illustration purposes, a case study is added here that involves resin infusion process and FRP materials.

4.2 Methodology

Many virtual design and manufacturing efforts abide by a sequential or linear progression scheme as presented in Figure 4.1. This is rooted in conventional design theory and methodology, and sustained in practice by the use of different software packages in the different design stages.

The strategy put forward in this paper aims not to hand over results of one software package to the next along a sequential path of design steps. Instead, it promotes a parallel approach that seeks simultaneous optimization of design

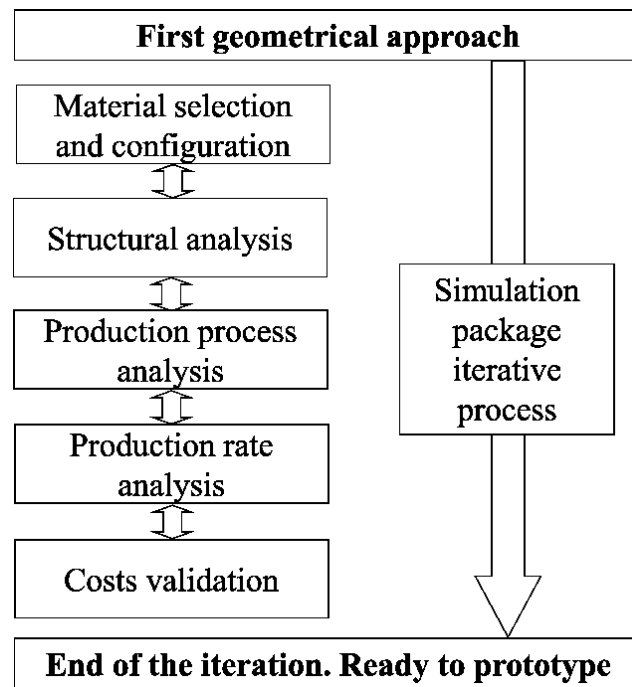


Figure 4.1: Block diagram for usual simulation-aided design process.

steps by connecting the design steps and the overall design constraints via a common control parameter.

First, the strategy identifies the different design steps or process milestones that have to be covered. The design steps usually consist of: material configuration, part geometry, structural analysis, manufacturing process analysis, production volume analysis and cost validation. Next, the necessary inputs, as well as the desired outputs for each milestone are identified. All inputs and outputs are analysed in order to identify a common control parameter whose variation impacts directly or indirectly on the results of each design step. The control parameter then becomes the pivotal for further optimization.

The scheme in Figure 4.2 represents the principle behind the proposed strategy. All the different design steps are linked together around a single control parameter. The variation of the control parameter must lead to a direct or indirect variation in the results of each of the design stages. After identification of the pivotal parameter, the next step is the definition of the working range of the control parameter for each of the steps to be covered.

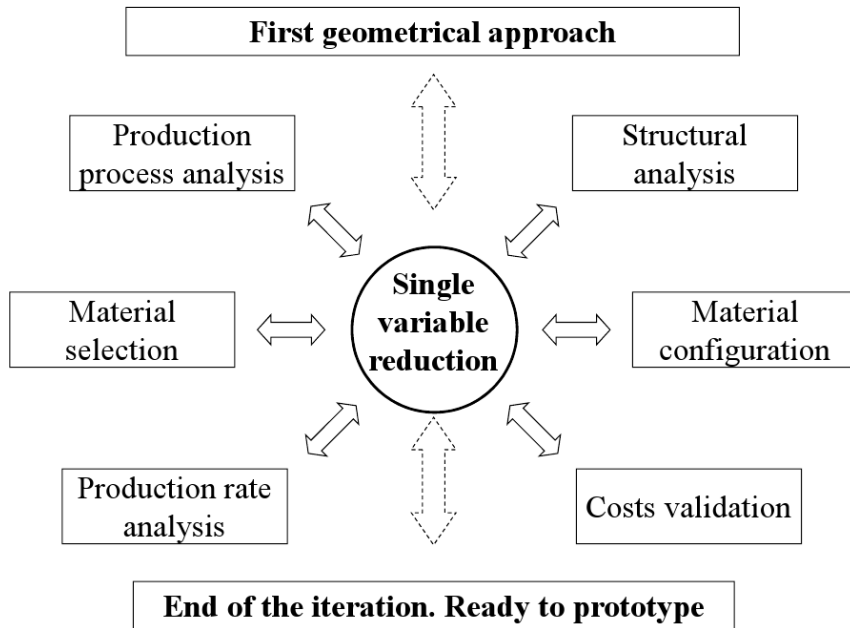


Figure 4.2: Block diagram of the background of the proposed strategy.

Each analysis is not solved for a single working point, but for a feasible range that is limited by the overall objectives or constraints of the design brief. Solving the problem for a determined range instead of a single working point does imply an initial increase of simulation time and cost, but later on, efficiency is gained in the decision making process. After obtaining simulation results in each of the different design steps separately over the identified working range of the control parameter, an output chart is created (see Figure 4.3) that can be used to easily identify an optimized design scenario. Indeed, all that is needed further is to select a value for the control parameter that is compatible with the overall design objectives or constraints and that lies in the working ranges identified per design step on the output chart. Once such a value for the control parameter is selected, the optimized design path becomes immediately clear.

In fibre reinforced polymers, volume fraction (V_f) is defined as the amount of reinforcement inside the composite. It can serve as the control parameter for a virtual composite design and manufacturing simulations, as it is a parameter that is present in all the different design steps of a composite part. Indeed, material cost and mechanical properties of a composite material are

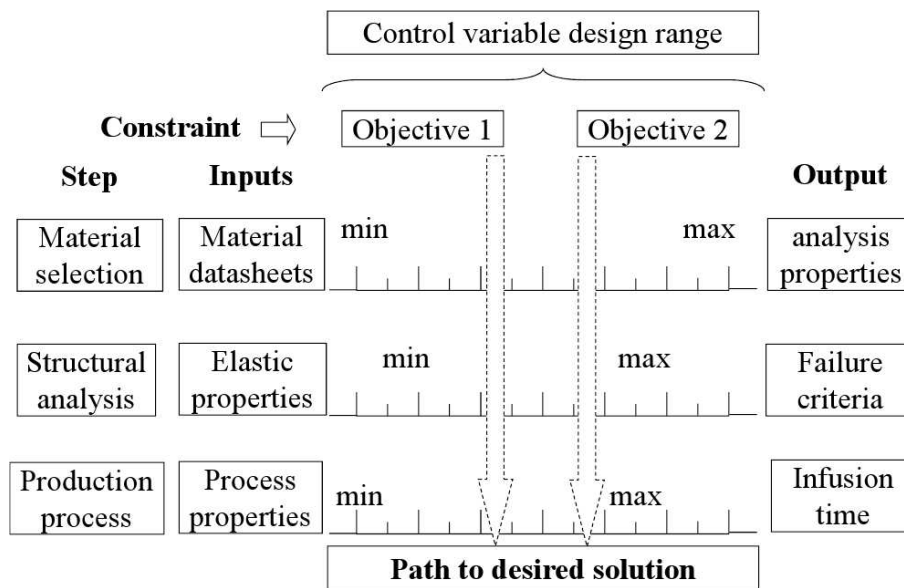


Figure 4.3: Scheme of a representative example of range analysis through a single parameter.

strongly and directly influenced by the amount of reinforcement V_f . For the manufacturing process, fibre volume fraction has a proportional relation with the reinforcement permeability value, which in its turn can be directly related to infusion time. V_f is also a key parameter in the selection of available manufacturing processes and the determination of the volume production capability. Due to the nature of composite material, not any value of V_f is suitable. Structurally, materials with extremely high fibre volume ratios will not have enough matrix to recover and ensure the consistency of the composite. From the production point of view, a mould cavity packed tight with fibres will not let the resin flow easily. On the other side, poor fibre composite will not benefit from the advantages of reinforced materials. Considering all the steps to cover in the project and references of practice in experienced industries, a fibre volume range from 25 % to 55 % is used in the following case study.

As an illustration of the potential of the presented strategy, a real case study regarding a fibre reinforced thermoset tank for industrial applications is presented next.

4.3 Case study. Supporting the decisions into the design process

The final goal of the proposed methodology is to reduce time and cut costs in the crucial stage of new products development. Cost sensitive and production driven markets (e.g. industrial supplies) have been targeted as primary objectives of the methodology. There, the application of straightforward and simplifying techniques can bring back great returns. The methodology deals with material design, overpass structural analysis, select among different candidate productive strategies and evaluate its viability through production rates and costs. Initially a set of inputs that will be used as boundary conditions through all the steps of the project are required. For instance, the customer must provide production rates and cost limits to achieve according to own capabilities and objectives. Requirements for the structural analysis are dictated by the desired application regulations.

In this case study, the design and viability analysis of manufacturing a mat fibre reinforced thermoset tank for industrial application is covered. For this type of application, Resin Transfer Moulding (RTM) [21] and Resin Infusion under Flexible Tooling (RIFT) [22] are the two main infusion techniques used. In both systems, a thermoset resin is driven through a reinforcement consisting in a mat fibrous preform. For most applications, constituents such as polyester resin and E-Glass short fibres are commonly used although vinyl ester or epoxy resins and carbon or aramid fibres can also be used to improve the quality and performance of the infused part.

4.3.1 Design step: Material selection and configuration

Elastic and mechanical properties

Different analytical and numerical techniques have been developed to obtain the elastic properties of a composite laminate, avoiding costly and time consuming experimental characterizations. Among these, different micromechanical models have been formulated, capable to derive laminate properties from standard values and configuration of the constituents. Analysing the mate-

rial configuration, composites are formed mainly by laminae of transversely-isotropic materials. Consequently, only 6 different elastic properties (5 independents + 1 dependent) need to be determined. These properties can be either obtained experimentally or determined from technical data sheets, general reference books [21], or even internal libraries of software used with that aim. A summary of used inputs in this case study is presented in Table 4.1.

Value	E_{11}	G_{12}	ν_{12}	Flexural Modulus
Unit	[MPa]	[MPa]	[-]	[MPa]
Fibreglass	72345	29649	0.22	7600
Polyester	3400	1231	0.38	13500

Value	Tensile Strength	Compressive Strength	Shear Strength	Density
Unit	[MPa]	[MPa]	[MPa]	[Kg/m ³]
Fibreglass	3450	117.2	75.9	2605
Polyester	76	200	n.a.	1120

Table 4.1: *Main mechanical properties of the material constituents [21].*

In our case study, a computing subroutine has been used to compare different micromechanical models for the six elastic properties of a transverse-isotropic layer [23, 24]. Theories developed for unidirectional or bidirectional laminates, such as the ones based on Halpin-Tsai, Rule of Mixtures, Matrix Dominated, Self-Consistent or Periodic Microstructure approaches have been compared as well as theories developed for continuous strand mats.

After the comparative analysis, the work from Luciano and Barbero [24] was found most appropriate and has been used to obtain the lamina properties of the material. Indeed, the model of Luciano and Barbero has been developed to be used for unidirectional composites. The fact that in our case study the material is a mat reinforcement with fibres randomly distributed is taken into account with the introduction of a ζ efficiency factor, which is determined as a function of the number of fibres orientated in the considered direction. The use of this reduction coefficient in the fibre-related properties reflects the sup-

position that only a percentage of the fibres is in the presupposed direction. Application of this supposition is in good agreement with experimental data available from recorded tests according to ASTM D-3039 standard [25].

As for most micromechanical models, the model used here predicts the different elastic properties in function of the degree of mixture of constituents or fibre volume fraction (V_f) or, in some cases, porosity ϕ , which is an indirect expression of the fibre volume ($\phi=1-V_f$). The fibre volume range can be determined using literature guidance to limit the improvements that can be achieved with its variation. Figure 4.4 summarises the variation of the six elastic properties of the composite material as a function of the fibre volume. It is observed that although the Poisson ratio slightly decreases, the elastic modulus and the shear modulus outline a notable improvement when fibre contents is increased.

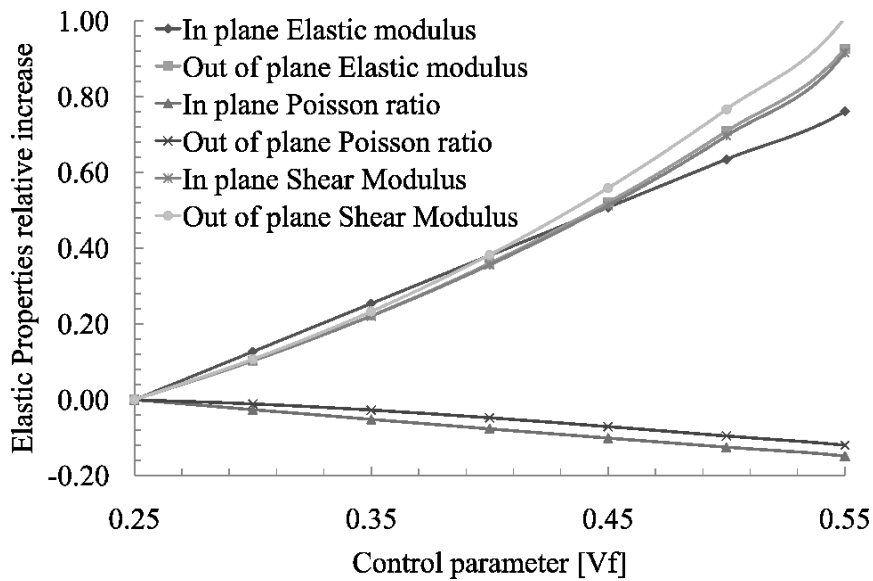


Figure 4.4: Main elastic properties variation as a function of the control parameter.

Production process properties

To obtain mat reinforcement, dry sized fibres are chopped and randomly projected over a mould to produce either dry fibre preforms for the specific part [26] or flat layers of reinforcement material that need to be patterned later.

Next, the whole laminate is closed into a mould cavity and the selected matrix is infused.

To numerically evaluate the infusion step of that production scheme, two different inputs are needed: reinforcement permeability and matrix viscosity. Permeability is related to reinforcement and is defined as the ability of the fabric to accommodate fluid penetration and propagation. This parameter is traditionally determined experimentally for each case because it is highly influenced by different parameters inherent to the fabric. Several techniques are available for its determination, such as the radial airflow proposed by Pomeroy et al. [27] or the linear flow proposed by Lee et al. [28]. However, there is no unanimity due to the lack of precision observed in all methods. For this reason, in this work the evaluation of the variation of the permeability is determined by using the analytical Kozeny-Carmann model [21], which is widely accepted and presented below in Equation 4.1. In the equation, ϕ stands for the porosity, d_g is the equivalent fibre diameter and A is the Kozeny constant which is usually determined experimentally.

$$K = \frac{\phi^3 d_g^2}{A(1 - \phi)^2} \quad (4.1)$$

For the correct simulation of non-laminated preforms, some variations with respect to the previously considered assumptions must be taken into account [29]. For instance, lower superficial density and a higher number of fibres orientated through the thickness lead to higher permeability levels than those obtained for the general case. In addition, the uniformity of the material in the through-the-thickness direction allows neglecting the through-the-thickness permeability effects and conduct 2D analysis instead.

The second parameter, related to the matrix, is viscosity. Although viscosity can be affected by temperature variations [30], it is commonly considered constant for thermoset materials. A fixed, non-temperature dependent, value of viscosity can be set depending only on the type of resin used.

For the production design step, the amount of fibre inside the cavity (V_f) can be used to establish a relation between all the necessary data to conduct the analysis. Keeping viscosity as a fixed term, a straightforward relation between the filling time and the amount of fibre in the cavity can be determined

for rigid mould setups. However, for processes with a flexible mould in one side (RIFT), the compaction effect has to be taken into account as well, as detailed later.

4.3.2 Design step: Structural analysis

The finite element method is a powerful technique that allows obtaining precise local information of the analysed part. Bidimensional representations of the geometry, using shell elements, allow versatility and agility on the design iterations; simplifying the problem with the use of a unique mesh through both the structural and production process simulations. Thickness and previously obtained material properties of each element are introduced in the pre-processor step.

In our case study, MSC software was used. MSC.Patran [31] was selected to build the mesh and MSC.MARC [7] to conduct the structural failure analysis.

The definition of correct boundary conditions is essential to conduct the analysis. For our case study, the displacements in the upper lid of the filter are restricted. The load condition considered for the analysis corresponds to the watertight test, where the tank undergoes load cycles with an internal pressure of 5 bars. Maximum strain or minimum displacement are the two more extended failure criteria in composites industry although specifically developed criteria such as Tsai Wu [32], Hashin [33], Puck [34] or LaRC [35] offer better precision. In the present case study, mechanical limits to validate the design have been extracted from international regulation codes of reference in composite analysis [36–38].

This type of analysis has as an objective the reduction of the amount of used materials, traditionally by modifying the thickness of the part wherever is possible. In our strategy we change the iteration over the thickness for iterations over the control parameter (V_f). To achieve this, a first analysis is made to set the limit thickness for a fixed base configuration of the material, creating a start point to conduct a second iteration which improves this value shifting the mixture of constituents.

Iterations over the control parameter, the fibre volume fraction, provides an opportunity for improving the efficient use of material in the vessel, as it can be observed in Figure 4.5. The variation of the thickness that can be achieved only by modifying the mixture of the constituents is plotted for the constrained range. It is observed how a fibre increase allows a reduction of the necessary material without compromising the structural resistance, relating structural improvement with the pivotal variable of the methodology.

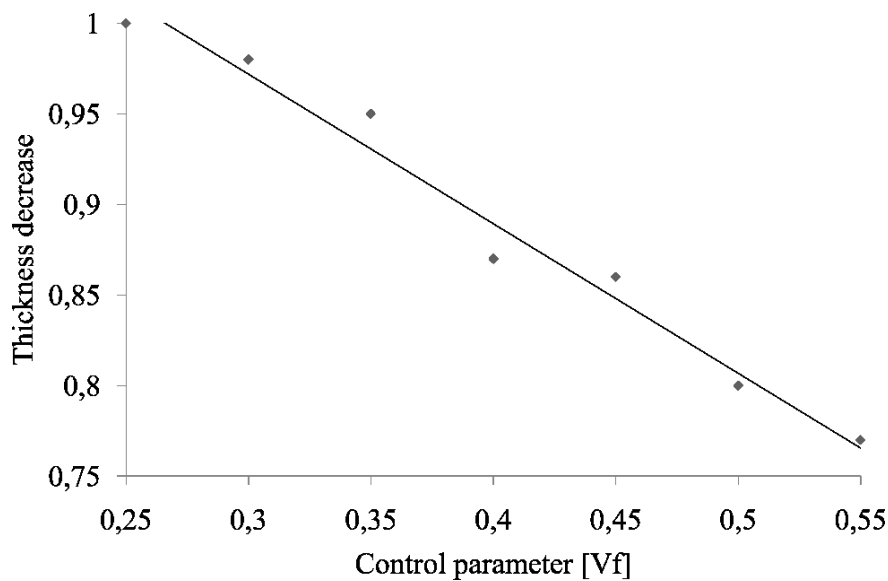


Figure 4.5: *Relative decrease of the thickness of the vessel as a function of V_f*

4.3.3 Design step: Production process

The following step to cover in the design process of a new composite part is the assessment on the selection of the right infusion technique, evaluating the gate and vent strategy, infusion time and, when necessary, the thickness variation due to the specific process.

Infusion techniques can be classified in two different families depending on the mould typology, imposing different restrictions to the design process. For rigid mould techniques, mainly known as Resin Transfer Moulding, commercially available numerical codes can provide direct solutions for the simulation of the entire process [39],[40]. For techniques using one flexible mould, such as in Resin Infusion under Flexible Tooling (RIFT), the behaviour of the flexi-

ble mould introduces a further complexity in the prediction of the production step, as different parameters must be specified affecting the obtained result. For instance, the mould cavity undergoes a compaction pressure during the process which modifies different parameters such as thickness, permeability or fibre volume, decreasing the flow front velocity [41–44].

LIMS [10], a finite element/control volume simulation code developed at the University of Delaware is used in the present case study. LIMS also includes LBASIC, a built-in script language to modify different conditions during simulations. The RTM process can be simulated directly with the user interface LIMS-UI. For RIFT, a LBASIC script is used to update the required changes and iteratively check for convergence by resolving the pressure field under the new conditions.

Compaction models based on the previously cited studies are included in the governing flow equation, to take into account the particularities of this boundary condition. Expressions are fitted to the particular part geometry and fibre volume range considered in this work. Previous studies of Robitaille et al. [45] and Kessels et al. [46], demonstrate that the variation of the thickness of the part is related to the position of the flow front, decreasing from inlet to vents. Most of the expressions used for compaction have been unified in the work of Correia et al. [47].

In order to avoid dry spots caused by incomplete filling, a correct gate and vent strategy is a key factor during the production step, as well as in the determination of the infusion time. Using the largest path along the part is a good approach to start with this iterative process. Mould geometry must be also taken into account to ensure that simulation points for gates and vents are feasible in a real setup.

For RIFT mould setups, compaction is dependent on the pressure difference and is recalculated based on the percentage of mould cavity already filled with resin. Hence, the size of the cavity and the path do not affect the thickness variation and, consequently, the permeability.

The benefits of a correct gate and vent strategy can be observed in Figure 4.6. If inlets are placed in the central areas of the part instead of towards the edge, filling time is reduced by almost two as the distance to be covered is

also halved. When the inlet is placed at the central area of the part, the flow front advance can expand in a circumferential pattern, while when located in an edge the expansion is limited in one direction.

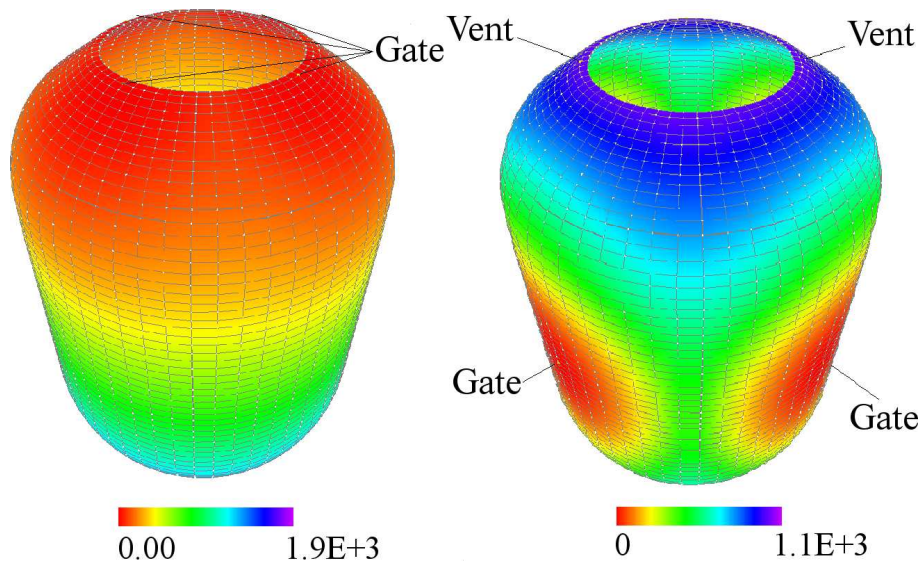


Figure 4.6: *Gate and vent placement for the two infusion strategies proposed. Time in seconds.*

In Figure 4.7, the infusion time results can be observed for the conducted simulations using different combinations of initial fibre volumes (our selected control parameter), and relative compaction models. It is observed in the figure that time is clearly affected by the compaction model used in the case of the RIFT setup. Consequently, from the production point of view, the RTM technique will always provide a faster filling alternative.

The thickness variation of the preform during the infusion process is a phenomenon associated to flexible mould setups. Figure 4.8 shows the dimensionless variation of thickness versus the flow front advance for the RTM setup and three different compaction models for the RIFT setup. As it can be observed in the figure, the thickness of the preform remains constant from gates to vents for the RTM case. However, the compaction behaviour clearly affects the final thickness of the preform as the flow front develops from the gate to the vent in the case of the RIFT setup. The compaction can result in a thickness decrement between 36 and 41% depending on the considered model. As a consequence, permeability is also affected which results in slower

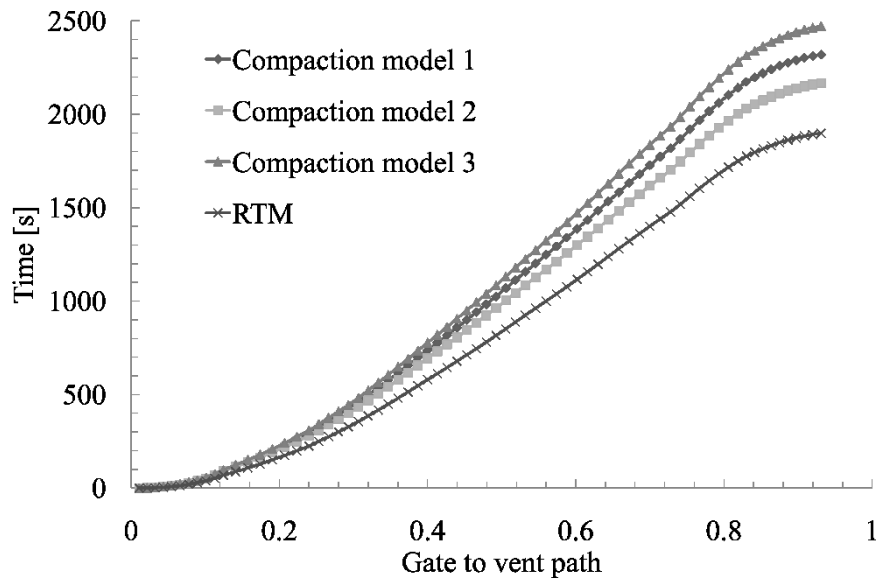


Figure 4.7: *Filling time for the different infusions considered.*

infusion processes.

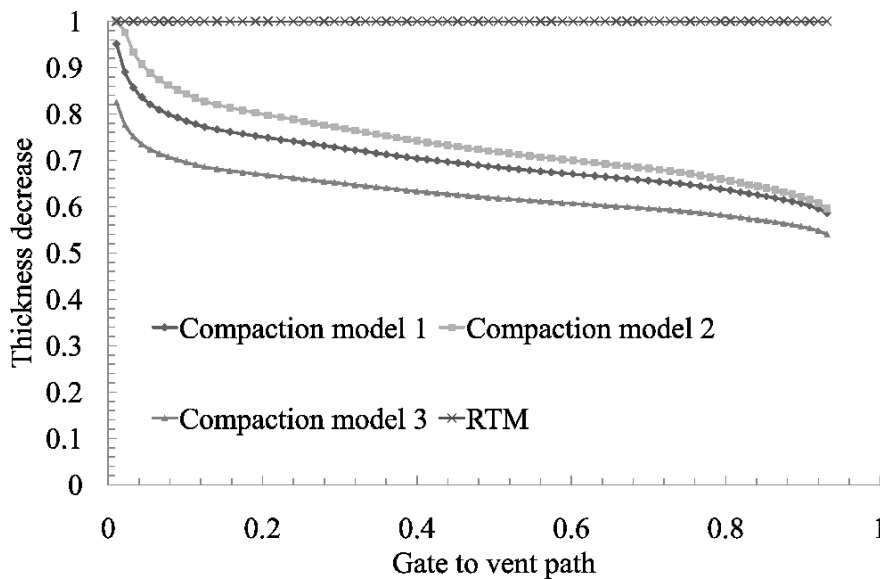


Figure 4.8: *Variation of the thickness along the filling path, 0 inlet and 1 vent.*

In conclusion, the infusion time to produce the part is linked to gate and vent configuration and to permeability, compaction and thickness decrement, which in turn are related to the pivotal variable of the analysis, fibre volume. In this way, the expected structural behaviour of the part and its production

process are linked through this control parameter.

4.3.4 Design step: Production rates and costs

Production rates and its associated costs are the main constraints considered in the project. The aim is to illustrate the methodology as clear as possible using our control parameter, fibre volume. Part viability in this preliminary stage is evaluated through two different constraints, described below, among the many possible different economic factors that one can consider.

To define this step, information about the production layout needs to be provided. Typical composite production processes differentiate two production zones. All the preform cutting and preparation is conducted in a so-called clean room zone. Afterwards, the preform is introduced into a mould, closed and infused in the infusion zone. The key aspect that defines this process is the infusion step (Figure 4.9), as usually there is only one mould and the material stays there during the infusion and most of the consolidation process.

This typical lay-out shown in Figure 4.9 is used together with the production capabilities and the desired production rates for the product to define the work plan and size up the production rate for the selected process. Rates must fit three production stages that represent the introduction, growth and mature stage of the part, setting the production time.

Material costs and its repercussion into the project are also covered in this strategy, with the objective to keep them as low as possible.

Material cost is determined through the evaluation of the price of the constituents of the final composite material, fibre and resin. In this case, as fibre preforms are obtained from fibre spools, the fibre is less expensive than the resin. As the fibre volume increases, mechanical properties of the part are improved while the resultant composite is less expensive.

The second factor used to illustrate the methodology is production time. The variation on preform cutting time, moulding and demoulding time and other related periods associated to each of the fibre volume configuration considered has to be taken into account. However, it has been found that all this time variations are of little importance when compared to infusion time. An

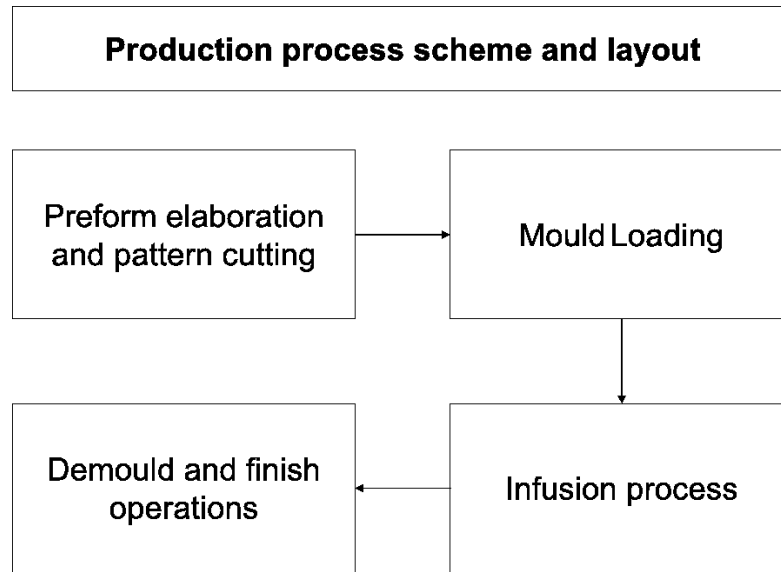


Figure 4.9: *Scheme and layout of the production process.*

increase of the fibre volume results in large infusion times for each part, which is added to the rest of process times. Three different productions scenarios that reflect the product life cycle have been considered for this application case: market introduction, growth and mature stage. These are detailed in Table 4.2 along with the available production time for each vessel considering a standard production capability of 1752 hours per year.

Production scenario	Stage	Units	Time available
Low production rate	Growth	500	210 minutes
Medium production rate	Market	2000	52 minutes
High production rate	Mature	3500	30 minutes

Table 4.2: *Production scenarios considered in the case study.*

The evolution of the material cost as well as the time increase on the infusion time as a function of our control parameter, fibre volume, for both production methods considered, RTM and RIFT, is represented in Figure 4.10, demonstrating how the pivotal variable of the analysis V_f can be used to obtain an evaluative image of the production rate and costs of the project.

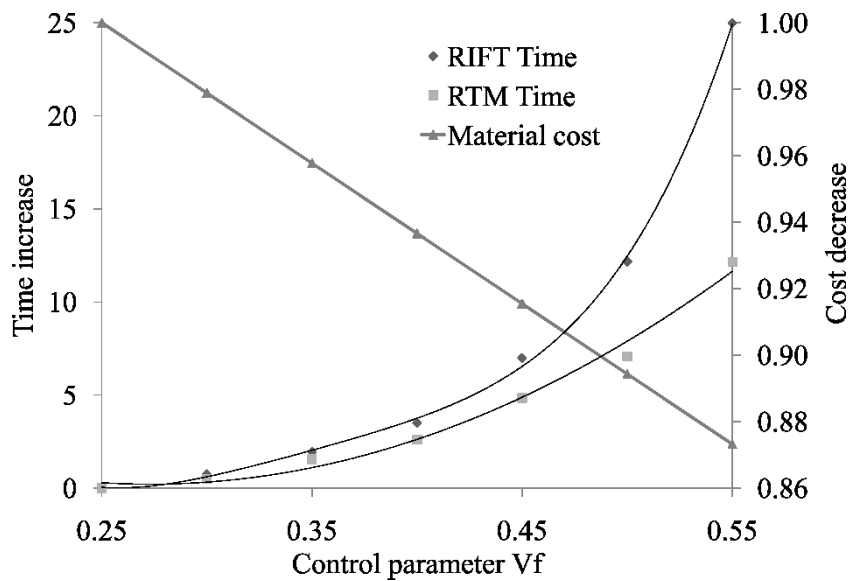


Figure 4.10: Cost and production time variation vs control parameter V_f .

4.3.5 Design step: Strategy application

The previous points provided an overview of the large amount of information that has to be handled through the entire process. However, with the proposed strategy all this information coming from different milestones is provided as a function of a single control parameter which makes simplifies its use. In Figure 4.11, this information is conceptually presented, identifying three different blocks of information.

The first block of data consists on inputs needed to conduct the numerical work in the different milestones of the project. The second block stands for the type of analysis that need to be fulfilled, representative of each step of the process. The third block contains the output obtained from each of the milestones using this strategy. The design range of the pivotal variable is covered with the help of user subroutines that automate the different analysis, running them in parallel. This allows multiplying the amount of information of the process with a slight increase in effort. This block is used to determine and validate the proposed solution according to previously selected constraints.

The deployment of the outputs (included in the right rectangle of Figure 4.11) in a clever disposition allows an easy introduction of the constraints that relate the different fields in a straightforward manner. Therefore, designers

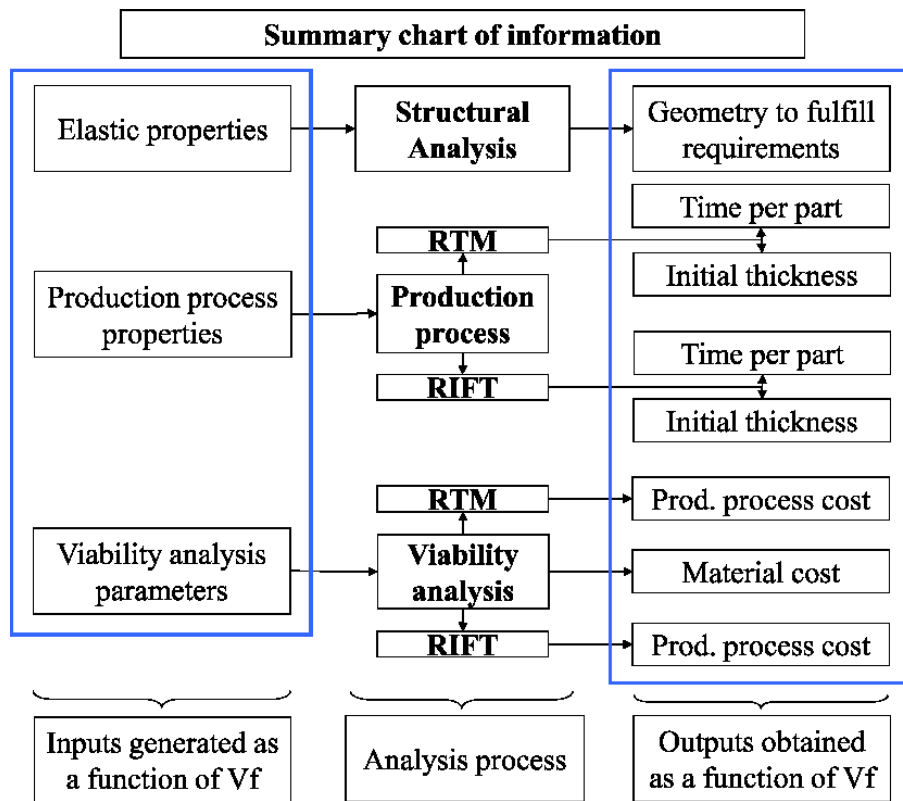


Figure 4.11: *Blocks of data handled in the proposed strategy.*

can evaluate at a glance the validity of the proposed solution, the weak points of the strategy or the possible conflicts in particular areas. The strategy is illustrated with the two different constraints presented in the previous point.

The first constraint reflects limitations on the production capabilities of the company. Therefore, the maximum allowable time to produce the part is used as a restriction (30 minutes, according to Table 4.2).

The second constraint, related to the economical point of view, is introduced to evaluate the capacity of the strategy to provide assessment in cost reduction. With the aim of simplicity, the maximum cost of all the possible configurations has been referred as the unit, and any cost reduction is presented as a percentage of it. A numerical example is deployed in Figure 4.12 for the two different constraints considered.

The selection of the optimized solution according to each constraint is presented as a path through all the different design steps in Figure 4.12 chart. For the first constraint, production time, one starts the path in the highlighted

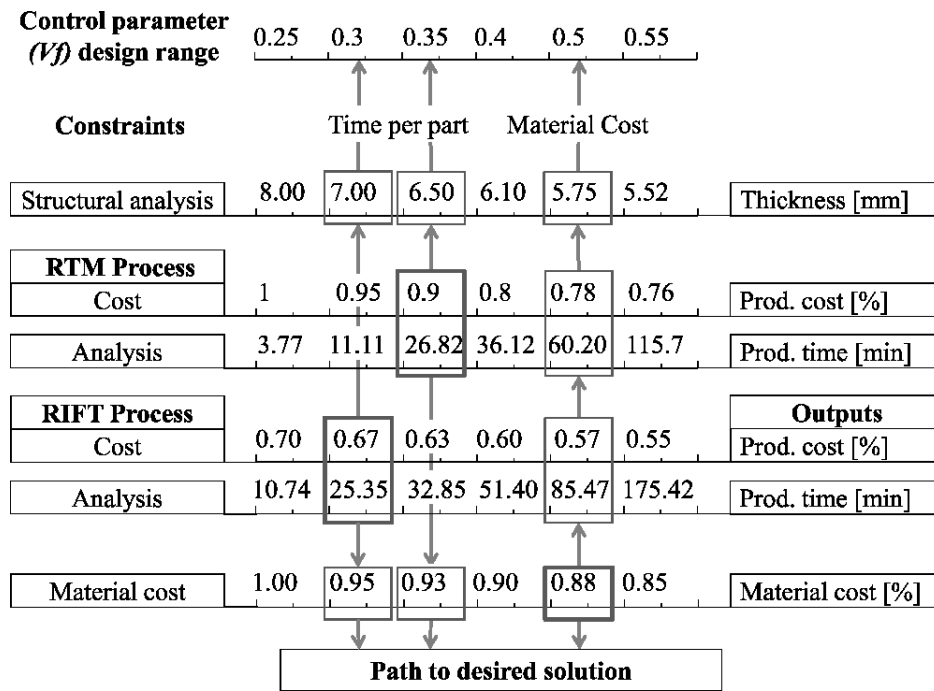


Figure 4.12: Chart illustrating the strategy for the specific case study.

time square of the specific production design step. Moving up, one can obtain the associated thickness required to meet the structural analysis requirements, and the related fibre volume ratio, depending on the production technique used. Moving down, one obtains the associated material cost.

For the material cost restriction, the starting point is highlighted in the material cost line. Here the constraint creates even a more straightforward path, as one material configuration is associated with one cost and thickness independently of the technique used. Therefore, a single straight line defines the best alternative for both options.

4.4 Discussion

With the objective to provide as much information as possible at a low investment cost, a strategy based on a common control parameter for all the stages involved in a part development process has been introduced. This strategy is set out as a tool to focus and guide the initial development stage of a product. It can be used to guide and optimize the prototyping task and reduce the

amount of effort spent in this crucial stage of the project.

The most critical point in this type of strategies is to evaluate the possible inaccuracy that exists between the numerical methods used and the real data provided by experimental trials. Errors may come from the difference of the ideal data extracted from handbooks and references and the real material used. The extensive number of tests documented for several material configurations, as well as the numerical strategies to adapt one from another offers a reasonable approach to the final solution, but not an exact one. The use of micromechanical models and numerically based models in the finite element codes are also sources of error that must be taken into account into the results, which should be understood as guide limits to conduct the experimental work to finally validate the solution.

The precision in the cost determination has been carefully treated to provide reliable information about the economical feasibility of previous milestones. As real material data can be provided from suppliers, the material cost strategy has a high level of confidence. However, the most critical discrepancies might come from the time estimation obtained in the production process simulation stage.

The proposed strategy is highly oriented to support real cases in industrial environments. It has been illustrated by a case delimited by different parameters such as one material type, two different production techniques and very concise times due to market requirements.

The rationale of this delimitation is to reflect the situation that a company faces when developing a new product. Companies know what their production alternatives and capabilities are and they need decision strategies that handle all the information and return the best possible alternative for the available resources.

Although the family of composite materials and the industrial supplies market has been selected here for the demonstration case, the strategy can be also applied to other industrial sectors and materials by selecting the correct control parameter and link all the information managed in all the involved steps.

4.5 Conclusions

A comprehensive design strategy is presented that simultaneously optimizes different design steps from material configuration, over structural analysis, to production process costs. The strategy is based on the identification of a control parameter common to all stages of a typical industrial design process.

A case study promotes the fibre volume ratio as the control parameter for the virtual design and manufacturing of resin infusion processes and FRP materials.

Nevertheless, the strategy is a generic, parallel decision-making tool, proposed as an alternative to the conventional sequential design iteration approaches found in many fields and applications.

This strategy can support and improve the efficiency and performance of design engineers that face the reality of working across several stand-alone software packages in the most expensive and time pressured stage of a product development, namely the initial conception and prototyping.

Bibliography

- [1] A. Delaplace, R. Desmorat, Discrete 3D model as complimentary numerical testing for anisotropic damage, *International Journal Fracture* 2 (148) (2007) 115–128.
- [2] B. Farahmand, K. Nikbin, Predicting fracture and fatigue crack growth properties using tensile properties. *Engineering Fracture Mechanics* 75 (8) (2008) 2144–2155
- [3] C. Gonzalez, J. Llorca, Virtual fracture testing of composites: A computational micromechanics approach, *Engineering Fracture Mechanics* 74 (7) (2007) 1126–1138.
- [4] L. Mishnaevsky, N. Lippmann, S. Schmauder, Computational modelling of crack propagation in real microstructures of steels and virtual testing of artificially designed materials, *International Journal of Fracture* 120 (4) (2003) 581–600.
- [5] D. B. Miracle, S. L. Donaldson, *ASM Handbook*, ASM International, Materials Park, OH, USA, 2001.
- [6] E. Barbero, *Computer aided design environment for composites (CADEC)* (2008).
- [7] MSC. Software, *Marc User's Guide*, Vol. *Marc Manuals*, 2007.
- [8] Dassault Systemes, *Abaqus 6.7 documentation* (2007).
- [9] M. L. Skinner, New applications and approaches expand market for composites software, *Journal of Reinforced Plastics and Composites* 50 (6) (2006) 24–28.

- [10] P. Simacek, S. Advani, Desirable features in mould filling simulations for liquid composite moulding processes, *Polymer Composites* 25 (4) (2004) 355–367.
- [11] T. Loh, S. C. L. Koh, Critical elements for a successful ERP implementation in SMEs, *International Journal of Production Research* 17 (42) (2004) 3433–3455.
- [12] E. Monk, B. Wagner, *Concepts in enterprise resource planning*, Course Technology, Cengage Learning, Boston, MA, USA, 2008.
- [13] V. McConnell, Software delivers faster time-to-part and reduced testing, *Journal of Reinforced Plastics and Composites* 8 (51) (2007) 24–28.
- [14] M. F. Ashby, Multi-objective optimization in material design and selection, *Acta Materialia* 48 (1) (2000) 349–369.
- [15] C. Monroy, A. Skordos, M. Sutcliffe, Design selection methodology for composite structures, *Materials Design* 29 (2) (2008) 418–426.
- [16] M. Bader, Selection of composite materials and manufacturing routes for cost-effective performance, *Composites Part A: Applied Science and Manufacturing* 33 (7) (2002) 913–934.
- [17] K. Wang, D. Kely, S. Dutton, Multi-objective optimisation of composite aerospace structures, *Composites and Structures* 57 (1-4) (2002) 141–148.
- [18] R. Srinivasan, H. M. Karandikar, F. Mistree, Understanding design and manufacture interaction using compromise decision support problems. 1 A formulation for composite pressure vessels, *Computers and Structures* 40 (3) (1991) 679–692.
- [19] R. Srinivasan, H. M. Karandikar, F. Mistree, Understanding design and manufacture interaction using compromise decision support problems. 2 Preliminary synthesis of composite pressure vessels, *Computers and Structures* 40 (3) (1991) 693–703.

- [20] R. Srinivasan, H. M. Karandikar, F. Mistree, Understanding design and manufacture interaction using compromise decision support problems. 3 Design for manufacture of composite pressure vessels, *Computers and Structures* 40 (3) (1991) 705–717.
- [21] C. Rudd, A. Long, K. Kendall, C. Mangin, *Liquid Moulding Technologies*, Woodhead Publishing and SAE International, Warrendale, PA, USA, 1997.
- [22] C. Williams, J. Summerscales, S. Grove, Resin infusion under flexible tooling(RIFT). A review, *Composites Part A: Applied Science and Manufacturing* 27 (7) (1996) 517–524.
- [23] E. Barbero, *introduction to composite materials design*, Taylor and Francis, Philadelphia, PA, USA, 1999.
- [24] R. Luciano, E. Barbero, Formulas for the stiffness of composites with periodic microstructure, *International Journal of Solids and Structures* 31 (21) (1994) 2933–2944.
- [25] ASTM International, D3039-D3039M standard test method for tensile properties of polymer matrix composite materials (2007).
- [26] Aplicator systems AB, www.aplicator.se (retrieved March 2010).
- [27] R. Pomeroy, S. Grove, J. Summerscales, Y. Wang, A. Harper, Measurement of permeability of continuous filament mat glass-fibre reinforcements by saturated radial airflow, *Composites Part A: Applied Science and Manufacturing* 38 (5) (2007) 1439–1443.
- [28] Y. J. Lee, J. H. Wu, Y. Hsu, C. H. Chung, A prediction method on in-plane permeability of mat/roving fibres laminates in vacuum assisted resin transfer moulding, *Polymer Composites* 27 (6) (2006) 665–670.
- [29] K. A. Olivero, Y. K. Hamidi, L. Aktas, M. C. Altan, Effect of preform thickness and volume fraction on injection pressure and mechanical properties of resin transfer molded composites, *Journal of Composite Materials* 38 (11) (2004) 937–957.

- [30] C. J. Seeton, Viscosity temperature correlation for liquids, *Tribology Letters* 22 (1) (2006) 67–78.
- [31] MSCSoftware (2008) Patran Manuals. Patran User's Guide. Msc.Software, Santa Ana, CA, USA
- [32] S. Tsai, E. Wu, A general theory of strength for anisotropic materials, *Journal of Composite Materials* 5 (1) (1971) 58–80.
- [33] Z. Hashin, Failure criteria for unidirectional fibre composites, *Journal of Applied Mechanics* 47 (2) (1980) 329–334.
- [34] A. Puck, A. Schürmann, Failure analysis of FRP laminates by means of physically-based phenomenological models, *Composites Science and Technology* 62 (12-13) (2002) 1633–1662.
- [35] C. Davila, P. Camanho, C. Rose, Failure criteria for FRP laminates, *Journal of Composite Materials* 39 (4) (2005) 323–345.
- [36] ASME. Boiler and Pressure Vessel Committee, ASME boiler and pressure vessel code, Part 1, American Society of Mechanical Engineers (1971).
- [37] International Standard Organization, ISO 16528-1:2007 boilers and pressure vessels, Part 1: Performance requirements (2007).
- [38] G. Lloyd, Regulations for the certification of wind energy conversion system (1999).
- [39] M. Lin, H. T. Hahn, H. Huh, A finite element simulation of resin transfer moulding based on partial nodal saturation and implicit time integration, *Composites Part A: Applied Science and Manufacturing* 29 (5-6) (1998) 541–550.
- [40] J. A. Garcia, L. Gascon, F. Chinesta, A fixed mesh numerical method for modelling the flow in liquid composites moulding processes using a volume of fluid technique, *Computer Methods Applied to Mechanics* 192 (7-8) (2003) 877–893.

- [41] N. C. Correia, F. Robitaille, A. C. Long, C. D. Rudd, P. Simacek, S. G. Advani, Use of resin transfer moulding simulation to predict flow, saturation, and compaction in the VARTM process, *Journal of Fluids in Engineering-Transactions of the ASME* 126 (2) (2004) 210–215.
- [42] T. G. Gutowski, G. Dillon, The elastic-deformation of lubricated carbon-fibre bundles - comparison of theory and experiments, *Journal of Composite Materials* 26 (16) (1992) 2330–2347.
- [43] P. Simacek, S. G. Advani, A numerical model to predict fibre tow saturation during liquid composite moulding, *Composites Science and Technology* 63 (12) (2003) 1725–1736.
- [44] P. Simacek, S. G. Advani, Modeling resin flow and fiber tow saturation induced by distribution media collapse in VARTM, *Composites Science and Technology* 67 (13) (2007) 2757–2769.
- [45] F. Robitaille, R. Gauvin, Compaction of textile reinforcements for composites manufacturing 2: Compaction and relaxation of dry and H₂O-saturated woven reinforcements, *Polymer Composites* 19 (5) (1998) 543–557.
- [46] J. F. A. Kessels, A. S. Jonker, R. Akkerman, Fully 2,5 d flow modelling of resin infusion under flexible tooling using unstructured meshes and wet and dry compaction properties, *Compos Part A-Appl S* 38 (1) (2007) 51–60.
- [47] N. C. Correia, F. Robitaille, A. C. Long, C. D. Rudd, P. Simacek, S. G. Advani, Analysis of the vacuum infusion moulding process: I. analytical formulation, *Composites Part A: Applied Science and Manufacturing* 36 (12) (2005) 1645–1656.

Part II

Impact of thermal effects in virtual design manufacturing

Chapter 5

Impact of the fibre bed on resin viscosity in liquid composite moulding simulations.

M. Gascons, N. Blanco, P. Simacek, J. Peiro, S. Advani, K. Matthys, Impact of the fibre bed on resin viscosity in liquid composite moulding simulations, Applied Composite Materials. Accepted 28 June 2011.

DOI 10.1007/s10443-011-9218-7

5.1 Introduction

In Liquid Composite Moulding processes (LCM) [1–3], a dry fibre reinforcement is placed in a closed mould and a liquid thermoset resin is driven through via a pressure gradient applied between mould inlet gate and outlet vent. Though other (newer) manufacturing methods for composites are on the horizon [4, 5], a keen interest in the advancement of conventional closed mould manufacturing techniques still exists given their widespread use in key composite markets such as the aerospace, automotive, marine and defense industries.

For a composite part to consolidate, LCM processes rely on the curing and hardening capability of the infused resin. Knowledge about curing characteristics and changing resin properties during consolidation is therefore critical to the success of the moulding process.

Gel time (also known as 'pot life') [6] is defined as the time interval required for a colloidal solution to become a solid or a semi-solid gel. Within fibre reinforced thermoset moulding processes, this term denotes the working period defined between the moment that the resin starts impregnating the reinforcement and the moment when the resin initiates its polymerization process.

It is common practice in LCM process control to consider the infusion period smaller than the gel time. Under this condition, polymerization effects during infusion can be neglected and the assumption of a constant value for viscosity is a valid approach [7–9]. However, in reality, this premise cannot always be accomplished due to limitations of the LCM technique applied, or due to physical and chemical constraints of the constituent materials involved.

For one-shot infusion of large parts, the long propagation path to be covered by the resin implies a long infusion period, as propagation velocity is lim-

ited by reinforcement permeability, resin viscosity and driving pressure. This can cause the polymerization process to start before the resin reaches the end of the mould, causing a noticeable viscosity variation of the resin liquid during infusion.

The problem of early polymerization is particularly notorious in sizeable parts. More and more, very large composite parts are made by infusion and this is mostly done using the Resin Infusion under Flexible Tooling (RIFT) technique [10]. RIFT can only accommodate a limited pressure gradient over the mould section as it is based on vacuum suction. Therefore, this technique will always imply a slow resin front advance compared to other infusion processes such as closed mould Resin Transfer Moulding (RTM) [3], and the production of sizeable parts via RIFT is thus prone to run beyond the gel time.

The specific performance requirements of high-end composite markets, such as the aerospace and automotive sectors, have led to the creation of a range of resins that need heat so as to lower viscosity before becoming suitable for infusion. An example of such a resin is RTM6 [11]. For these resins, gel time is a critical issue, as the polymerization process is directly affected by the required working temperature.

Several academic research codes [12, 13] as well as commercial software packages [14] are available nowadays to describe resin infusion processes via numerical simulation. For advanced simulations, one can already implement process parameter (mainly temperature) dependent viscosity models, which should assist the simulation of processes whereby infusion time exceeds gel time. However, especially near the end of infusion, such models still do not seem to provide a very accurate prediction of flow front progression when compared to real production set-ups.

These process dependent viscosity models are thus far still based on neat (i.e. outside the mould) experimental characterizations of resin cure kinetics. The hypothesis of this investigation is that the inaccuracy of the infusion simulation may be attributed to the fact that resin properties (mainly viscosity) are measured and modelled in the absence of an enclosing fibre architecture, thereby not mimicking true viscosity behaviour as deemed present in the infusion set-up under process conditions and with the reinforcement in place in

the mould.

5.2 Background

To describe the viscosity changes of a thermoset polymer, one must study its behaviour over time at a given temperature. Such a chemoviscosity study relies on the use of Differential Scanning Calorimetry (DSC) or Dynamic Mechanical/Dielectric Analysis (DMA-DEA) in order to obtain viscosity variation and cure kinetics of neat (i.e. outside the mould and thus without the presence of fibres) resin in a controlled environment.

Figure 5.1 illustrates a typical viscosity evolution under isothermal conditions for a pre-heated thermoset polymer resin. As can be seen in this figure, three stages can be clearly distinguished.

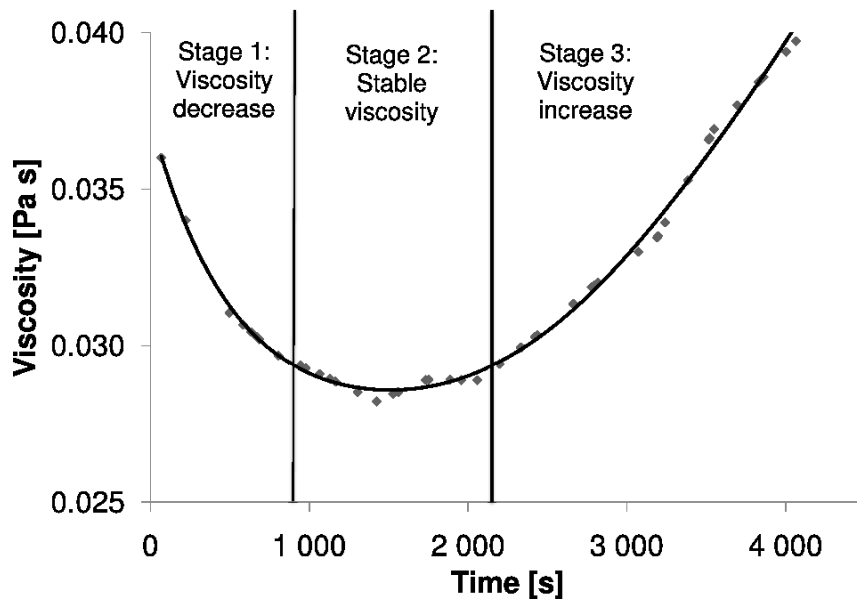


Figure 5.1: *Viscosity behaviour of an epoxy-based thermoset polymer as a function of time for a constant temperature.*

In a first stage, resin viscosity (μ_0) starts from an initial value and subsequently decreases. This is a transient effect that follows the temperature increase due to pre-heating.

During the second stage, the viscosity reduction due to heating is compensated by the formation of a cross-linked network in the resin polymer. The

viscosity value remains relatively stable over time, pointing out this period as the target time window for using the resin polymer in an infusion moulding process.

The third and last identifiable stage is marked by the start of the curing phase, in which viscosity increases dramatically. A macroscopic 'lump' with gel-like features can be observed in-situ as the liquid resin starts its rapid conversion into a solid substance. In the beginning of this last stage, the gel point, or more commonly, the *gel time* or *pot life* (t_{gel}) is defined. From this moment onward, viscosity tends to infinity; the resin loses its flow capabilities and becomes a solid.

The described viscosity evolution over time can be influenced by external parameters and it is a topic in literature that has been concisely reviewed by many authors in the field of thermoset polymers [15–18]. Pressure P , shear rate γ , temperature T , time t , and the presence of additives and fillers in the resin are parameters identified as having significant influence on viscosity.

The application of heat when processing thermoset polymers has become common practice across the composite moulding industry [19]. Heating the resin polymer up to a certain temperature has the most direct influence on viscosity. Several mathematical expressions have been validated in the literature to express the general non-linear variation of viscosity with temperature for different thermoset materials and processing conditions [20–22]. A selection of basic expressions commonly used is summarized in Table 5.1. All expressions model the viscosity change using an exponential law. In the first example (Table 5.1, Empirical), the exponential law is built around temperature and a model parameter b fitted by an empirical process. Other authors [23] related the variation of viscosity with time using its dependence on the chemical reaction and activation energy through the Arrhenius relationship (Table 5.1, Arrhenius) or the Williams-Landel-Ferry expression (Table 5.1, WLF).

The increase of high performance applications and the development of new materials have emphasized the need for highly application specific analytical expressions to characterize the viscosity evolution. Several studies have therefore adapted or modified the basic expressions with other factors, such as the presence of fillers, sizings, additives or even specific processing

Non-linear viscosity expressions	
Model	Expression
Empirical	$\mu(T) = \mu_0 e^{(-bT)}$
Arrhenius	$\mu(T) = \mu_0 e^{\left(\frac{E}{RT}\right)}$
WLF	$\mu(T) = \mu_0 e^{\left(\frac{-C_1(T-T_r)}{C_2+T-T_r}\right)}$

Table 5.1: *Basic non-linear viscosity expressions used in simulation codes (WLF stands for William-Landel-Ferry). μ_0 stands for the initial viscosity at the considered reference temperature, b is an empirically derived coefficient, T stands for temperature, E is the activation energy, R is the universal gas constant and C_1 , C_2 and T_r , are independent empirical parameters. For further information the reader is referred to the work by Halley and Mackay, 1996 [16]*

conditions. This has led to the development of more empirical fittings [24], probability and molecular based models [25], gelation models [26], advanced Arrhenius models and detailed models based on free volume analysis [27]. A list of representative advanced expressions is provided in Table 5.2.

Advanced non-linear viscosity expressions	
Model	Expression
Molecular	$\mu_c = A e^{(D/RT)} (M/M_0)^{(C/RT+S)}$
Empirical	$\ln \mu_c = \ln \mu_v + E_v/RT + k\alpha + k\alpha$
Gel Model	$\frac{\mu_c}{\mu^0} = \left(\frac{1+kT}{1-T/T^*} \right)$
Modified WLF	$\ln \frac{\mu_c(T)}{\mu_c(T_g)} = \frac{C_1(\alpha)[T-T_g(\alpha)]}{C_2(\alpha)+T-T_g(\alpha)}$

Table 5.2: *Advanced non-linear viscosity expressions. In the equations, parameters μ_0 , b , T , E , R , C_1 , C_2 and T_r are as in Table 5.1. Additional parameters stand for gelation temperature (T_g), viscosities (μ_c , μ_v , μ^0), degree of cure (α), viscous activation energy (E_v), molecular weights (M , M_0), and model constants (k , A , D , C , S). For further information, the reader is referred to the work by Halley and Mackay, 1996 [16].*

All these viscosity expressions have in common that they are adjusted through parameters associated with the specific constituent materials or the constraints of the infusion process. Initial resin parameter information is obtained via experimental characterization of neat resin samples. Using this technique, also the inclusion of resin fillers and additives can be covered [28], obtaining detailed information about the rheokinetics of the thermoset resin polymer.

Although such non-linear viscosity expressions have certainly increased the accuracy of mould filling simulations, they tend to lose predictive power as the flow front reaches the end of the mould. The fact that resin characterization cannot take into account the influence of the reinforcement in the actual moulding process might be a possible cause for this (so-called 'fibre bed effect').

Apart from the fibre bed effect, another element relating to the fibre reinforcement is worthy of further consideration. Special material coatings (referred to as 'sizing') are applied to the fibre reinforcement in order to safeguard the quality of the dry textile and also to promote bonding between resin and fibre during the moulding process. Though resin system compatibility is normally taken into account during sizing formulation, it is possible for resin properties to be affected when sizing dissolves into the resin, potentially triggering a change in resin cure kinetics.

This work aims to present a novel investigation regarding the effect of the fibre bed and fibre sizing on thermoset polymer resin viscosity characterisation for the purpose of improving accuracy of infusion moulding simulations. This investigation is of special interest for design of infusion processes whereby filling time gets close to or becomes equal to the resin gel time. A new simulation method is presented next that allows to obtain an effective viscosity expression for liquid composite moulding processes that apply thermoset resins and make use of long fibre bed preforms.

5.3 Methodology

5.3.1 Analytical model

The proposed analytical model aims to describe the propagation of resin flow through a fibre bed under realistic moulding process conditions. Nevertheless, some assumptions are to be made. First, the model assumes an one-dimensional flow behaviour and neglects through-the-thickness flow. This simplification implies a mould configuration whereby cavity height size is an order of magnitude smaller than width and length dimensions, and whereby the inlet gate design is such that an in-plane flow profile can be generated. It is thus ensured that the assumption of a homogeneous flow front propagation is justified and no transversal flow movement has to be considered. Second, the model is using a constant pressure inlet boundary condition. These set-up constraints are not stringent and enclose a wide range of current infusion applications.

Under the above conditions, one can apply Darcy's law [29] as described in Equation 5.1.

$$q(t) = \frac{K}{\mu} \frac{dP}{dx} = \frac{K}{\mu} \frac{\Delta P}{x(t) - x(0)} \quad (5.1)$$

Equation 5.1 relates the instantaneous Darcy velocity of the resin $q(t)$ to the fabric permeability K , resin viscosity μ , infusion driving pressure difference ΔP and flow front position $x(t)$ at time t .

In Equation 5.2, Darcy velocity $q(t)$ is also related to seepage velocity dx/dt through the use of porosity ϕ . Porosity is an indirect measurement of the fibre volume ratio V_f of the composite part and is defined as $\phi = 1 - V_f$.

$$q(t) = \phi \frac{dx}{dt} \quad (5.2)$$

Assume an initial condition of $x = 0$ for $t = 0$ (the mould filling process begins at the inlet gate position), and substitute Equation 5.2 in Equation 5.1. Integrating x over time, one finally obtains Equation 5.3.

$$x(t) = \sqrt{2 \frac{K \Delta P}{\phi \mu} t} \quad (5.3)$$

Equation 5.3 describes the flow front propagation $x(t)$ as a function of time t , constituent material properties (resin viscosity μ , preform permeability K , porosity ϕ) and specific process parameters (driving pressure difference ΔP).

Step 1 - Model initialisation.

One defines a period of time when the effect of the initial resin cross-linking and fibre sizing can still be considered negligible. As a rule of thumb, a quarter of the gel time of the employed resin can be used as a conservative estimate. Over the chosen time window, the flow process can be treated as a basic isothermal infusion, which is accurately reproduced by currently available simulation codes based on Darcy's law (Equation 5.1). For this initializing simulation step, one can implement constant model parameters (ΔP , ϕ , K and μ). The value of ΔP is controlled by the process operator and ϕ can be derived from mould dimensions and lay-up thickness information. Model input parameters ΔP and ϕ can thus readily be obtained from the design of the process that is to be simulated. Further, a permeability value needs to be determined. Numerical techniques described in literature [30, 31] can be used to determine the permeability of the fabric. However, the high dependence of permeability on material parameters such as reinforcement architecture, lay-up sequence, etc., results in considerable variation when evaluating this parameter through analytical or numerical methods. As an alternative, the strategy proposed here is to simply describe permeability as a function of viscosity using the model applied for the analysis of the flow front propagation. Given an ideal one-dimensional infusion trial, a valid assumption within the initial time window as described above, the isolation of permeability results from Darcy's law as in Equation 5.4.

$$K = \frac{q\mu L}{\Delta P} \quad (5.4)$$

Hereby is q defined as the quotient of flow rate and mould cavity cross-sectional area (Q/A) and L is the distance travelled by the flow front from the start. A constant viscosity estimate can be obtained from the resin supplier data sheets, which then allows to perform an initialisation run with constant parameters, based on Darcy's law and valid for the chosen time window.

Step 2 - Viscosity expression

The next step in the model is the adoption of a non-linear description for the resin viscosity evolution over time. As can be seen from Table 5.1 and Table 5.2 in Section 5.2, all models used to reproduce non-linear viscosity expressions are based on power laws, albeit each with different levels of sophistication and based on a variety of different process parameters. For our purpose, setting forward an exponential law to express viscosity as a function of time is therefore an appropriate start.

In fact, we propose to apply the empirical model from Table 5.1 but with viscosity as a function of time, represented in Equation 5.5, where μ_0 is the viscosity at the initial stage of the injection process for the considered temperature and b is the time constant to be empirically fitted.

$$\mu(t) = \mu_0 e^{bt} \quad (5.5)$$

Substitution of Equation 5.5 in Equation 5.3 and the posterior integration of x over time, results in Equation 5.6, which represents the change of the flow front position through the mould cavity.

$$x = \sqrt{2 \frac{K \Delta P}{\phi} \left(-\frac{1}{\mu_0 b} (e^{-bt} - 1) \right)} \quad (5.6)$$

One can now describe the flow front propagation as a function of the parameters stated in Equation 5.6 and the viscosity time constant b . The present work aims to use two different approaches to determine a value for b .

The first approach is based on a neat resin characterization outside the mould without the presence of fibres. The initial viscosity μ_0 can be extracted from supplier datasheets, and parameter b can be determined using an isothermal time-viscosity chart.

The second approach consists of the determination of parameter b through an empirical fitting based on a time-flow front propagation diagram extracted from an experimental trial, that should be set up to be representative of the real injection moulding process.

Using this last approach, one obtains a value for b that takes into account the real situation in the mould cavity, including the presence of a fibre bed

architecture and a coating on the fibre reinforcement (sizing).

Model implementation

The two-step analytical model has been implemented as a numerical routine in the Liquid Injection Moulding Simulation (LIMS) software [12, 13], a finite element/control volume simulation code with thermal and cure prediction capabilities developed by the Center for Composite Materials at the University of Delaware. Having obtained Equation 5.6, one might try to directly implement this function into LIMS using a user subroutine. But, considering viscosity as a function of time, in LIMS one must recalculate the entire matrix system of the numerical algorithm at each time-step to do so [13]. In order to obtain a more efficient simulation tool with low computational cost (i.e. avoiding heavy matrix recalculations), a different approach was considered here. Though the implementation is rather LIMS specific, the thought process behind the approach is generic and is therefore included here. Reviewing the governing equations of flow through porous media (Equation 5.1), one observes that permeability K and viscosity μ always appear as a ratio. One can use this ratio to transpose the viscosity change over time to an artificial change in fabric permeability as in Equation 5.7.

$$\frac{K}{\mu(t)} = \frac{K}{\mu_0 e^{bt}} = \frac{K(t)}{\mu_0} \quad (5.7)$$

Applying this method to Equation 5.6, one can keep the viscosity constant to its initial value μ_0 and reset the permeability value K for each time step instead. In LIMS, the additional numerical cost of this approach is - unlike changing viscosity per time step - without significant impact on the system solution, as the modification of permeability can be easily inserted via a user routine and entire matrix recalculations are not necessary.

Further, in order to determine the empirical parameter b for the analytical model as expressed in Equation 5.5, an infusion process of a flat composite panel has been considered in this investigation as an example (details are described in the next section). For the numerical implementation, the panel was represented via a rectangular mesh formed by 200 nodes and 171 shell type

elements. Figure 5.2 depicts an image of the used mesh and the placement of the infusion gates, considered to be constant pressure inlet gates that combine together to form a line gate along the short panel side, thus ensuring a homogeneous and one-dimensional flow front propagation.

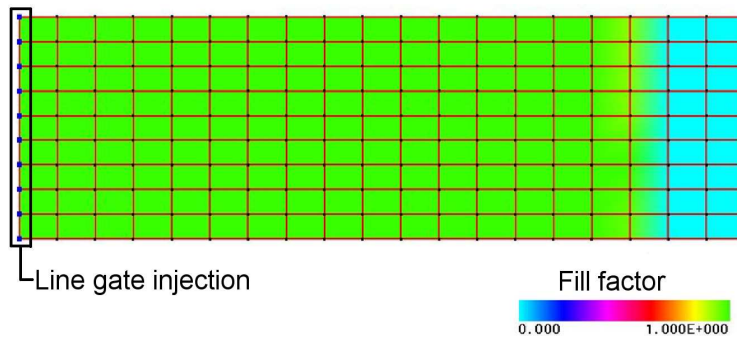


Figure 5.2: *Representative plot of the two-dimensional mesh used for the numerical implementation*

5.3.2 Experimental work

Experimental trial data for the determination of model parameter b was obtained with assistance of aerospace industry partners. As described in Step 2 of the analytical model, two approaches are needed for b determination, so as to allow comparison between modelling techniques based on resin characterisation outside the mould with the proposed model based on in-situ resin characterisation. So, a neat characterization of a monocomponent, epoxy based resin was conducted first, and a controlled infusion with the same resin was performed after. The infusion set-up selected was for a two-dimensional rectangular composite panel made out of a non-crimp carbon fibre fabric. However, the selection of resin, part shape and fabric materials were merely made for reasons of availability and relevance to real part applications of assisting industrial partners, and the specific set-up properties of the experimental trial do not influence the general nature of the study findings.

Neat resin characterization

Neat resin characterisation data was obtained for Hexflow RTM6 [11] from supplier Hexcel (Hexcel, Cambridge, UK). Characterization tests were performed of the RTM6 resin to obtain a viscosity chart under isothermal curing conditions. The results of these tests are shown in Figure 5.3. They provide the time-dependent viscosity behaviour over a discrete range of curing temperatures (100°C to 180°C) and up to the point that the resin cross-linking starts and the conversion into a solid substance takes place. Figure 5.3 confirms, as can be expected, that resin viscosity increase over time is accelerated at higher temperatures due to the earlier activation of the exothermic reaction.

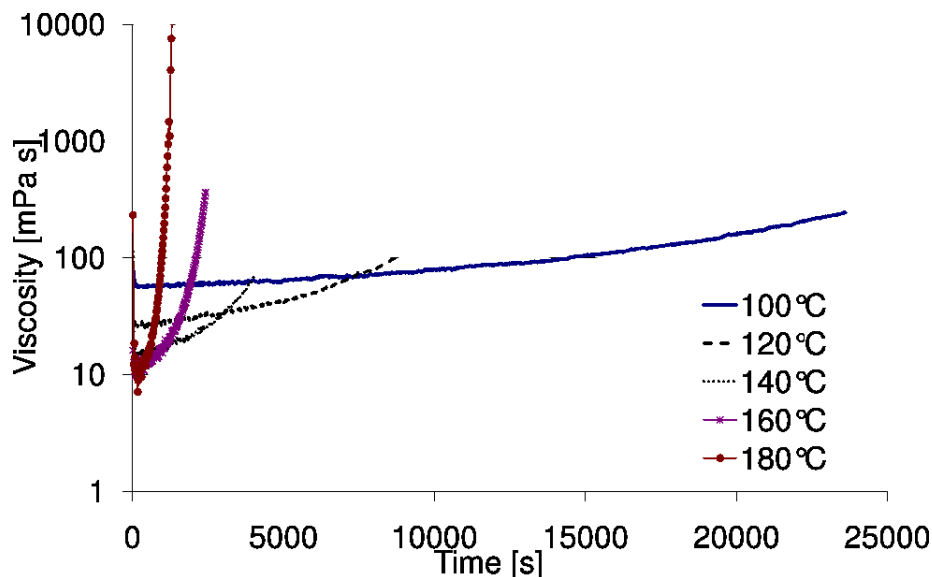


Figure 5.3: *RTM6 isothermal time-dependent viscosity behaviour over a temperature range of 100-180°C (Courtesy of resin supplier Hexcel)*

Experimental trial

Long, flat panel samples were subjected to an isothermal, one-dimensional flow infusion setup (RIFT). Aluminium mould tooling was used with controlled electric heating capability. The fibre reinforcement preform for the samples consisted of 8 layers of multi-axial carbon fabric, creating a quasi-isotropic laminate lay-up. The monocomponent, epoxy based Hexflow RTM6 resin, as

characterised before, was used to consolidate the fibre architecture. Details about panel dimensions and used materials are given in Table 5.3.

Sample information summary			
Panel dimensions			
Dimensions	Length	Width	Thickness
	2060 mm	590 mm	2.9±0.1 mm
Constituent materials			
Fabric	Hexcel G0926 Carbon Fabric 5 harness, 6k (370 g/m ²) lay-up (0, 90, ±45, ±45, 0, 90) _s		
Resin	Hexflow RTM6 Monocomponent Aerospace qualified		

Table 5.3: *Main panel dimensions and description of constituent materials as used in the experimental infusion trial[11, 32]*

Resin was injected via a line gate from the short left side of the panel. A line vent was used on the short right side of the panel to establish a vacuum in the mould and have the possibility to extract exceeding resin. Infusion pressure was set to 552 kPa and vacuum level prior to infusion was approximately 0.4 kPa.

The acquisition system used in the tests recorded pressure throughout the filling stage, and amount of resin transferred into the mould was registered using a weighting scale on the resin supply. To track the position of the flow front, pressure sensors were embedded in the mould tooling. A pressure reading step change occurred when resin passed over the sensor location.

Tooling temperature was held constant at 120°C during infusion. Due to the low thickness of the panel, the transversal temperature gradient was considered negligible, and the set-up considered as isothermal. The resin pot temperature was kept constant at 80°C during infusion. On first contact with the mould, a resin temperature variation occurs due to the difference in resin

pot and tooling temperature. However, this initial resin temperature adjustment is a transient effect that only exists over a very short period of time. As this investigation focuses on the end of infusion when resin polymerisation is likely to occur, the small transient effect at the start of infusion can safely be neglected. Note that, in line with these considerations, the analytical models in this study also do not have a transient effect for resin temperature coming out of a resin pot embedded, though it has been implemented that resin initially starts from the average temperature between pot and tooling at mould entry.

In Figure 5.4, the evolution of the flow front position during the infusion process can be observed. It highlights the decrease of flow front propagation as the process reaches the later stages of infusion. The length of the time interval between consecutive data points was gradually increased from approximately 3 minutes to 6, 12 and finally 24 minutes. The infusion trial reached a final flow front position of 1.98 m after 10020 seconds (167 minutes).

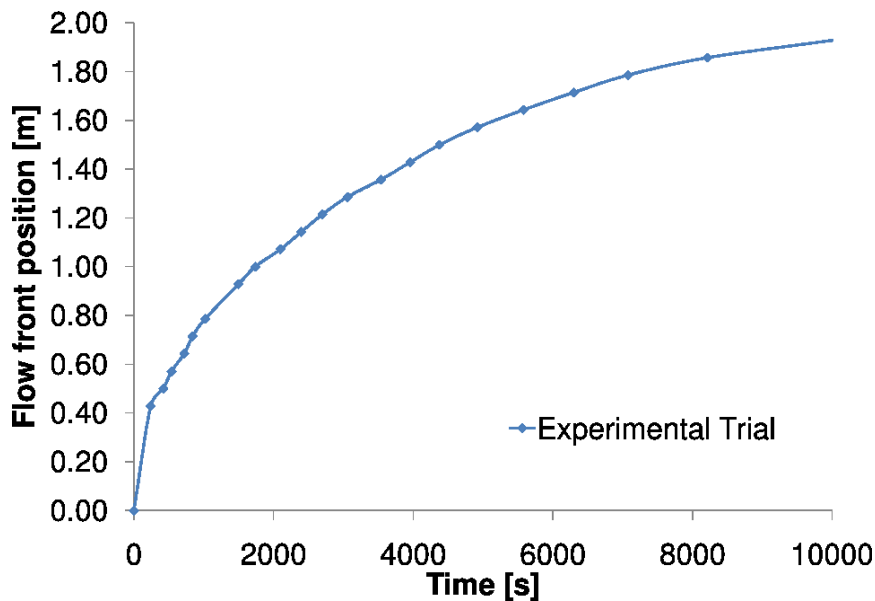


Figure 5.4: Resin flow front position vs. infusion time as derived from the experimental trial

Information on fibre volume fraction V_f was additionally extracted from the experiment. To obtain V_f , discrete thickness measurements on the dry preform and the infused final part were conducted. In Figure 5.5, the position

of the control points and their thickness values are displayed. From these thickness measurements the fibre volume fraction V_f was obtained, giving an average V_f value of 58.14% throughout the entire mould cavity.

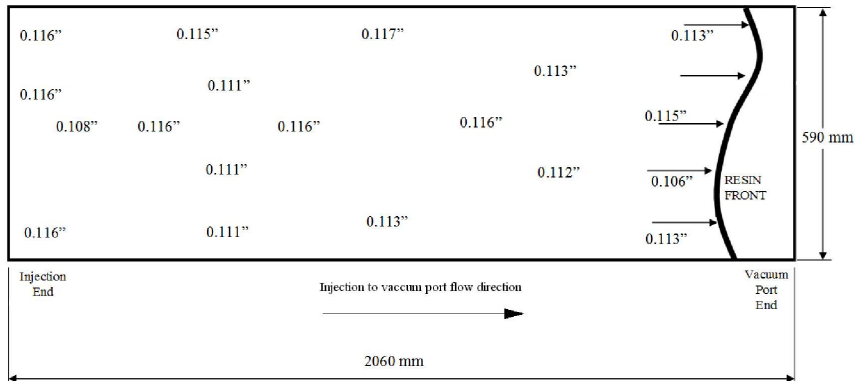


Figure 5.5: Schematic of the infused flat panel. Results of discrete thickness measurements are presented (in inches)

5.3.3 Experiment vs. simulation

The flow front propagation as derived in the experimental trial (section 5.3.2) was compared against numerical predictions (section 5.3.1). Apart from performing a simulation using a constant viscosity parameter to provide a baseline numerical prediction, two further simulations were made. These simulations made use of a non-linear viscosity expression based on neat resin characterisation data and in-situ resin characterisation from flow front propagation data respectively.

Based on the experimental trial, empirical and process-related parameters for the simulation are derived. In order to set the initial simulation working point (see section 5.3.1), one assumes constant values for all parameters involved in the infusion process (ϕ , ΔP , K and μ). The acquisition and control system used in the experimental rig can derive porosity ϕ and driving pressure ΔP , but not fabric permeability K and resin viscosity μ .

An initial value for viscosity μ can be obtained from the neat resin characterisation curves. As resin pot temperature was kept at 80°C and the tooling at 120°C, an initial value of 0.057 Pa·s was determined from isothermal curves of Figure 5.3.

An estimation for permeability K can be obtained from the one-dimensional description of Darcy's law, as stated in Equation 5.4. Parameters involved are: permeability K [m^2], viscosity μ [$\text{Pa}\cdot\text{s}$], sample length L [m], pressure P [Pa] and specific discharge or Darcy velocity q [m/s], which consists of flow Q [m^3/s] through area A [m^2]. Darcy velocity can be obtained from the experimental trial data. A value of $0.3 \text{ mm}/\text{s}$ was estimated from the time vs. flow front position data displayed in Figure 5.4. Substituting this value into Equation 5.4, one obtains a permeability value of $1.31 \cdot 10^{-11} \text{ m}^2$, for the initial period of infusion time. This value is consistent with consulted material data sheets of the same fibre fabric and similar lay-up [33], and can be applied to the entire infusion plane due to the quasi-isotropic state of the prepared laminate. As the permeability property is inherent to the fabric and should not change throughout the infusion, the value of the obtained permeability K is kept for the entire filling simulation.

With permeability addressed, only the changing behaviour of viscosity over the duration of the simulation needs to be determined. The approach as described in section 5.3.1 can now be considered and simulations based on different viscosity expressions compared: (i) the first case is a simulation with a time-independent or constant viscosity value throughout, (ii) the second case is a simulation with a time-dependent viscosity expression based on neat resin characterisation data and (iii) the third case is a simulation with a time-dependent viscosity expression based on in-situ resin characterisation via flow front propagation data.

In the first simulation case, the value of resin viscosity is considered constant during the entire process and is set equal to $0.057 \text{ Pa}\cdot\text{s}$, the initial value interpolated earlier from the neat resin characterisation curves (Figure 5.3).

In the second simulation case, a time-dependent viscosity expression (Equation 5.5) is used. Unknown parameter μ_0 could be extracted from resin supplier datasheets, but is here given the interpolated value as derived in the first simulation case. Unknown parameter b can be derived from fitting Equation 5.5 onto the curves of the neat resin characterisation experiment available in Figure 5.3. Table 5.4 lists the values of parameters μ_0 and b , together with an R^2 precision value for the fitting.

In the third simulation case, the initial viscosity value μ_0 is again maintained but now the flow front propagation data of the experimental trial are used to establish empirical parameter b for the time-dependent viscosity expression in the form of Equation 5.5. Empirical parameter b can be derived by matching the flow front position of the numerical prediction (Equation 5.6) with the experimental trial data for all control time intervals using optimization techniques and sensibility analysis [34]. The derived viscosity expression parameter values are again given in Table 5.4.

Parameter	Neat resin fit	Flow front fit
μ_0 [mPa·s]	57.4	57.4
b [-]	$0.6 \cdot 10^{-4}$	$8.2 \cdot 10^{-5}$
R^2	0.985	0.985

Table 5.4: *Expression parameters and R^2 fitting precision values for the time-dependent viscosity given by Equation 5.5, based on neat resin characterisation data fitting and on in-situ resin characterisation using flow front propagation data fitting from the experimental trial*

5.4 Results

Figure 5.6 summarises the flow front propagation over time as observed during the experimental trial, together with three numerical predictions, each based on a different approach to incorporate resin viscosity into the simulation.

One can observe in Figure 5.6 that the consideration of a constant viscosity value leads to inaccurate predictions of the flow front propagation after the first stages of infusion. Although initially the numerical prediction with constant viscosity is excellent and matches well the experimental results, as the infusion advances, the resin ends its 'gel time' and viscosity starts increasing its value to the point that a constant parameter assumption can no longer be upheld. This is when the flow front prediction starts to deviate from the exper-

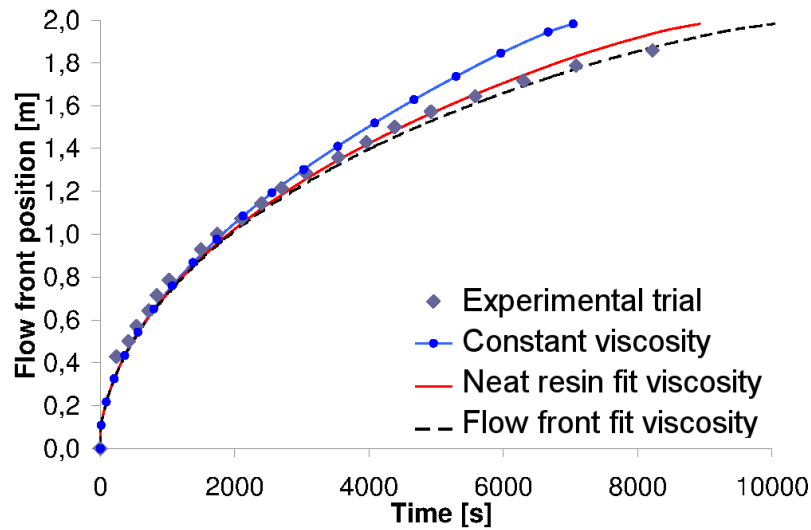


Figure 5.6: *Experimental flow front position vs. time and numerical predictions obtained with three different viscosity models*

imental trend, which shows a clear propagation slow-down as time advances that is not reproduced in the numerical result with constant viscosity.

It can be seen that a clear improvement is achieved in the numerical prediction when the time-dependent viscosity model based on neat resin characterisation data is used instead of the constant viscosity model. However, the improvement still does not match the experimental trend to the very end of the infusion period.

Finally, the numerical prediction obtained with the time-dependent viscosity model based on flow front propagation data does reach the end of the filling stage in excellent agreement with the experimental trial. This is because with this model one can reproduce in the simulation an in-situ resin viscosity characterisation that incorporates the effect of having a fibre reinforcement present in the mould, with its specific fibre sizing and fibre bed architecture, which cannot be taken into account using neat resin characterization data.

5.5 Discussion

So far, this study has looked at changes over time of process or material parameters. However, some parameters, such as fibre volume fraction (V_f), can

display a spatial variability over the sample investigated. As V_f is related to permeability [35], and permeability is an input parameter for Darcy's law upon which the proposed analytical model is based, it is worth investigating whether the spatial variability of V_f has any impact on the presented findings.

In the presented simulations, fibre volume fraction (V_f) was set for all elements to an average value of 58.14%, extracted from various thickness measurements across the sample before and after infusion. The collected data presented a standard deviation of 1.56%. Though the small variations in V_f were not expected to have any significant effect on the final simulation results, this has nevertheless been verified by comparing results for a specific sample preform using detailed V_f values assigned to each element in the mesh with results based on having an average value assigned for all the elements in the mesh.

The spatial distribution of V_f was derived from discrete thickness measurements, as can be seen in Figure 5.2. The mapping of the distribution to the mesh elements is provided in Figure 5.7. Mesh elements that could not benefit from direct V_f measurement mapping were assigned an interpolated V_f value based on values of adjacent elements.

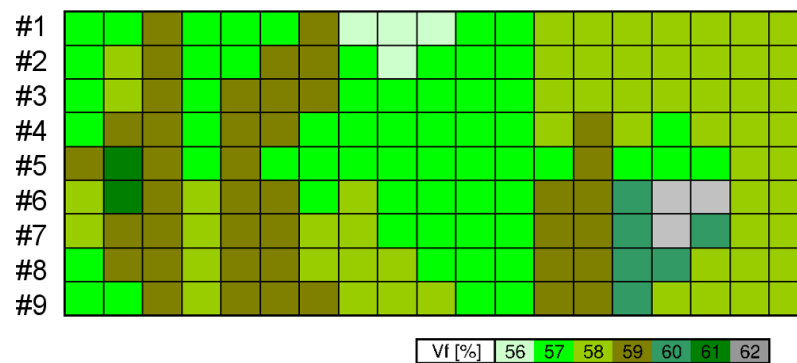


Figure 5.7: Mesh element distribution of fibre volume fraction V_f based on experimental thickness measurements and interpolation. Paths used for the fibre volume variability analysis are indicated with row numbers

Flow front propagation has been calculated separately for each of the 9 horizontal rows in the mesh using the flow front fitted viscosity model, allowing for investigation of 9 different scenarios. Results have been compared with the simulation based on a mesh with averaged V_f value as well as with

the experimental injection trial. It is clear from Figure 5.8 that the influence of spatial V_f variation, within a range that can realistically occur due to e.g. lay-up inconsistencies, is negligible.

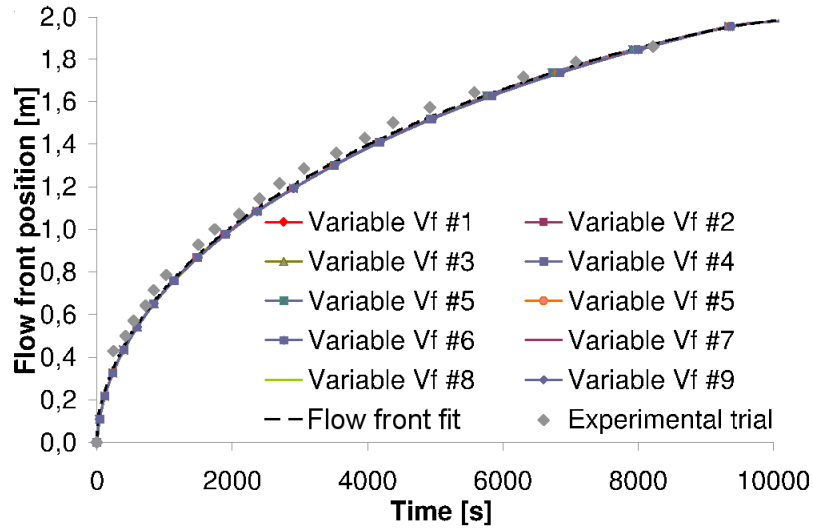


Figure 5.8: Comparison of the experimental flow front propagation with predictions based on the flow front fitted time-dependent viscosity model. Nine different scenarios of V_f variation are evaluated along the horizontal rows in the mesh, and compared to the simulation with averaged V_f value

Another issue in the prediction of the flow front propagation in resin infusion processes is the possible mismatch between the initial permeability determination and its actual value during infusion. Indeed, common simulation practice is to start with permeability values as found in the literature for similar materials, rather than performing an experimental determination of K with fabric samples under planned infusion process conditions. For the type of materials and fibre bed architecture considered in this work, the permeability value and variation range reported by [30, 31, 33, 36] can be considered. Thus, based on these studies, the lower bound for a suitable permeability value could be set to $K = 6.7 \cdot 10^{-12} \text{ m}^2$, while an upper bound could be considered as $K = 3.1 \cdot 10^{-11} \text{ m}^2$.

One can now simulate flow front propagation using the proposed permeability values. Figure 5.9 shows the results of this simulation test for three different values of permeability: upper and lower bounds as taken from liter-

ature, as well as the permeability value derived from the actual experimental trial (see section 5.3.3). While the simulation result obtained with the experimentally determined permeability value aligns well with the experimental trial result for the complete infusion process, the predictions obtained with the upper and lower permeability bounds as taken from literature only agree with the experimental data at the very beginning of the process, but further display poor agreement with the experimental curve throughout. The poor predictions based on the upper and lower permeability bounds indicate that though permeability value estimates can usually be obtained from literature for similar materials and similar fibre architectures, the simulation results are sensitive to variations of K and high accuracy simulations do require the in-situ experimental determination of permeability under actual process parameters.

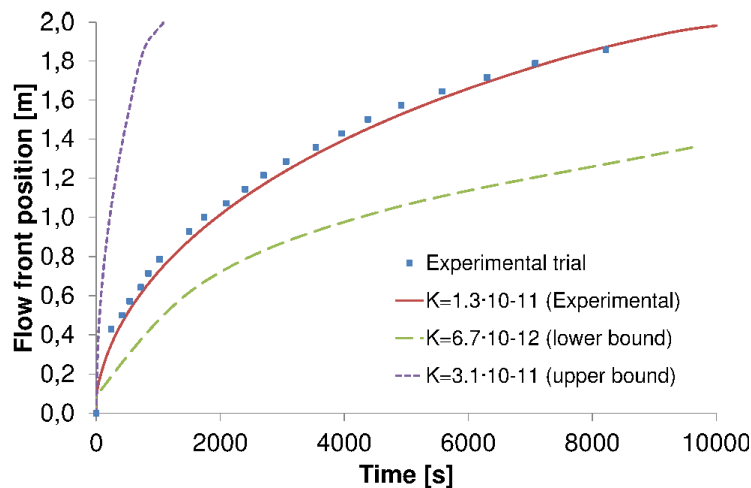


Figure 5.9: *Effect of permeability determination on accuracy of numerical predictions for flow front propagation. Permeability values in m^2*

5.6 Case Study

To underline the industrial relevance of the presented simulation methodology based on flow front fitted time-dependent viscosity, a case study is given here. The simulation was used to assist the manufacturing process design of three different sizes of a cylindrical, flat lid ended vessel. The vessels are to be used

for water treatment in industrial environments. A vessel is composed of two symmetrical parts held together by means of a metallic clamp. Figure 5.10 depicts the vessel half geometry considered for the analysis.

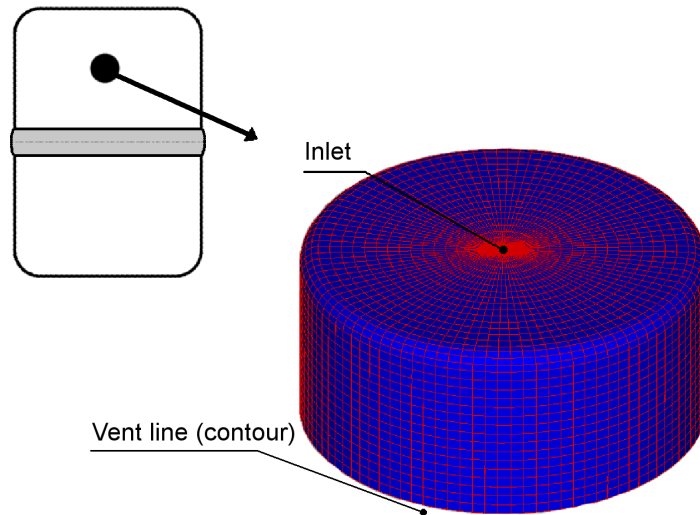


Figure 5.10: *Representative mesh of a vessel half geometry as used in the case study*

The boundary conditions of the vessel infusion scheme are consistent with the experimental trial on long, flat panels described earlier in this study. The resin gate is placed in the middle of the top of the lid, creating a circumferential but homogeneous flow pattern. A line vent is placed at the end contour of the cylindrical vessel half. Considered vessel diameters are 1000, 1200 and 1400 mm, respectively. Constituent materials match in type and lay-up with the fibre fabric used in the experimental flat panel trial, of which details are given in Table 5.3.

Filling simulations with three different viscosity models have been conducted for each size, using a constant viscosity, a time-dependent neat resin characterisation based viscosity and a time-dependent flow front based viscosity expression. Table 5.5 summarizes the final filling times for each scenario.

Results show noticeable differences between the predictions made by the different models. The predictions also become more disparate as the size of the geometry grows, which underlines the rationale for this work (i.e. that infusion simulation inaccuracies are more dominant with large parts working close to the end of the resin *gel time*).

Diameter	1000	1200	1400	[mm]
Constant viscosity	6067	8800	13007	[s]
Neat resin fit	6181	9877	18245	[s]
Flow front fit	6731	11552	28719	[s]

Table 5.5: *Filling times for three different vessel sizes and three different viscosity models*

Time-dependent viscosity based predictions are clearly differentiated from constant viscosity predictions, which is in line with expectations, but results also point to a clear distinction between the two time-dependent models, which is further discussed through the analysis of the filling isochrones as shown in Figure 5.11.

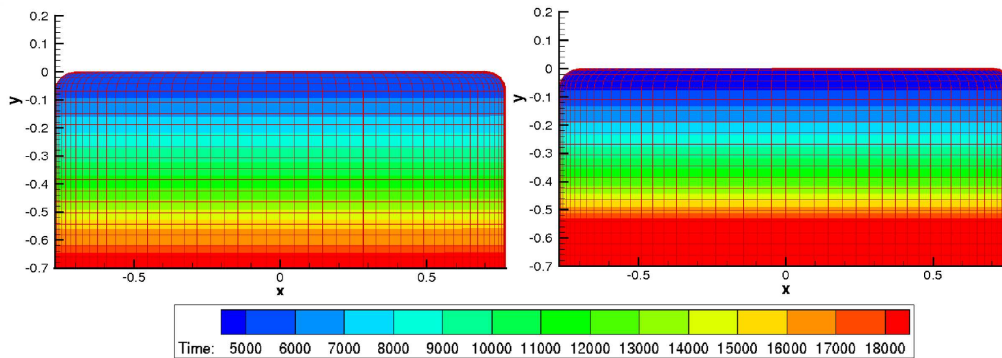


Figure 5.11: *Filling isochrones [s] for the 1400 mm vessel using different time-dependent viscosity models.*

Figure 5.11 depicts a lateral view of the 1400 mm vessel half geometry as well as isochrones of the resin filling process, calculated with the viscosity time-dependent models based on neat resin characterisation (left), and based on flow front propagation, (right). The 1400 mm vessel has been selected for this comparison as it represents the critical case of the three sizes (see also Table 5.5 demonstrating the most disparate values for the 1400 mm diameter).

The difference in flow front propagation prediction is particularly noticeable in the later stages of the infusion, when the resin reaches the end of its *gel time*. Both models indeed exhibit a similar propagation pattern until the vessel's bottom half section. However, the model based on neat resin

characterisation demonstrates a significant slow down in flow front propagation only from the lower quarter of the vessel geometry, whereas for the flow front propagation based model the flow front velocity is already dramatically reduced when still one third of the vessel remains to be infused.

The sudden increase of viscosity, occurring during the initial cross-linking, almost stops the resin flow front propagation, resulting in a high risk of voids and dry spots for the last section of the part. The flow front propagation based time-dependent model (5.11, right) captures this effect and thus provides more conservative simulation results than the neat resin characterization time-dependent model (5.11, left), reducing the possibility of underestimating infusion time and avoiding incompletely infused parts with consequent loss of material and time.

5.7 Conclusions

A keen interest in liquid composite moulding processes still exists in strategic markets such as the aerospace, automotive and defence industries. More and more, very large one-shot infusion composite parts are attempted and their manufacturing is therefore prone to run beyond the gel time of available resin systems, hereby increasing the risk of voids, dry spots and incomplete part infusion. Current infusion simulation strategies have already started to move away from constant viscosity based models, but even advanced viscosity expressions seem to not always provide a very accurate prediction of flow front progression in real infusion processes, especially in cases where filling time reaches or extends beyond resin gel time.

This study has now proposed a two-step analytical simulation model based on Darcy's law, making use of an exponential time-dependent viscosity expression that incorporates an in-situ resin viscosity characterization. This was achieved through an empirical parameter fitting using a flow front propagation trial under actual infusion process conditions. The method incorporates the impact of the fibre reinforcement presence in the mould on resin viscosity, which cannot be taken into account by a traditional neat resin characterization test. It has been validated by comparison with an experimental

trial that the proposed model can predict flow front propagation results more accurately than methods based on neat resin characterization, especially in the later stages of large part infusion processes when resin cross-linking can drastically increase resin viscosity and hamper flow front propagation. The sensitivity to variations in process and material parameters such as fibre volume fraction and permeability were discussed. Finally, a real application case study was included, highlighting the industrial relevance of adopting the proposed model over other non-linear viscosity based infusion simulation models, by demonstrating results that gave a more conservative prediction of flow front propagation behaviour, thus avoiding potential filling time underestimation that could lead to loss of material and time in subsequent manufacturing trials.

Bibliography

- [1] R.S. Dave, A.C. Loos, Processing of Composites, Hanser Publishers, Cincinnati, OH, USA, (1999).
- [2] F. Campbell Jr., Manufacturing Processes for Advanced Composites, Elsevier Science, Amsterdam, NL, (2003).
- [3] S. Mazumdar, Composites Manufacturing. Materials, Product and Process Engineering, CRC Press, Boca Raton, FL, USA, (1997).
- [4] B. Shirinzadeh, G. Alici, C. Foong, G. Cassidy, Fabrication process of open surfaces by robotic fibre placement, Robotics and Computer-Integrated Manufacturing 20 (1) (2004) 17–28.
- [5] G. Newell, R. Buckingham, K.Khodabandehloo, The automated manufacture of prepreg broadgoods components. A review of literature, Composites Part A: Applied Science and Manufacturing 27 (3) (1996) 211–217.
- [6] P. W. Schuessler, W. J. Dobbin, Gel time measurement of resins, Analytical Chemistry 53 (-) (1981) 2380–2381.
- [7] S. Advani, E. Murat Sozer, Process Modelling in Composites Manufacturing, Marcel Dekker Inc., Taylor and Francis, UK, (2003).
- [8] C. Tucker III, Fundamentals of Computer Modelling for Polymer Processing, Hanser Publishers, New York, NJ, USA, (1989).
- [9] M. Bruschke, S. Advani, A finite element/control volume approach to mould filling in anisotropic porous media, Polymer Composites 11 (6) (1990) 398–405.

- [10] C. Williams, J. Summerscales, S. Grove, Resin infusion under flexible tooling (RIFT). A review, *Composites Part A: Applied Science and Manufacturing* 27 (7) (1996) 517–524.
- [11] Hexcel Composites, HexFlow RTM6 Datasheet, Publication ITA 065e, Hexcel Composites, Stanford, CO, USA, (2009).
- [12] P. Simacek, S. Advani, Desirable features in mould filling simulations for liquid composite moulding processes, *Polymer Composite* 25 (4) (2004) 355–367.
- [13] S. Advani, P. Simacek, Programming in LBasic. Lims 5.0.4 Software Documentation, Center for Composite Materials, UDel, Newark, DE, USA, (2003).
- [14] M. L. Skinner, New applications and approaches expand market for composites software, *Reinforced Plastics* 50 (6) (2006) 24–28.
- [15] J. Bear, *Dynamics of Fluids in Porous Media*, Dover Books, New York, NJ, USA, (1989).
- [16] P. Halley, M. E. Mackay, Chemorheology of thermosets-an overview, *Polymer Engineering and Science* 36 (5) (1996) 593–609.
- [17] N. Kiuna, C. Lawrence, Q. Fontana, P. Lee, T. Selerland, P. Spelt, A model for resin viscosity during cure in the resin transfer moulding process, *Composites Part A-Applied Science and Manufacturing* 33 (11) (2002) 1497–1503.
- [18] Q. Fontana, Viscosity: thermal history treatment in resin transfer moulding process modelling, *Composites Part A-Applied Science and Manufacturing* 29 (1-2) (1998) 153–158.
- [19] C. Seeton, Viscosity temperature correlation for liquids, *Tribology Letters* 22 (1) (2006) 67–78.
- [20] A. Malkin, S. G. Kulichikhin, *Rheokinetics of curing*, Springer Berlin/Heidelberg, Berlin, DE, (1991).

- [21] M. Kamal, S. Sourur, Kinetics and thermal characterization of thermoset cure, *Polymer Engineering and Science* 13 (1) (1973) 59–64.
- [22] F. Mussati, C. Macosko, Rheology of network forming systems, *Polymer Engineering and Science* 13 (3) (1973) 236–240.
- [23] M. L. Williams, R. F. Landel, J. Ferry, The temperature dependence of relaxation mechanism in amorphous polymers and other glass-forming liquids, *Journal of American Chemical Society* 77 (1955) 3701–3707.
- [24] A. M. Stolin, A. G. Merzhanov, A. Y. Malkin, Non-isothermal phenomena in polymer engineering and science: A review. part I: Non-isothermal polymerization, *Polymer Engineering and Science* 19 (15) (1979) 1065–1073.
- [25] S. D. Lipshitz, C. W. Macosko, Kinetics and energetics of a fast polyurethane cure, *Journal of Applied Polymer Science* 21 (8) (1976) 2029–2039.
- [26] J. Mijovi, C. H. Lee, A comparison of chemorheological models for thermoset cure, *Journal of Applied Polymer Science* 38 (12) (1989) 2155–2170.
- [27] P. L. Chiou, A. Letton, Modelling the chemorheology of an epoxy resin system exhibiting complex curing behaviour, *Polymer* 33 (18) (1992) 3925–3931.
- [28] J. Martin, J. Laza, M. Morras, M. Rodriguez, L. Leon, Study of the curing process of a vinyl ester resin by means of TSR and DMTA, *Polymer* 41 (11) (2000) 4203–4211.
- [29] S. Advani, M. Bruschke, R. Parnas, Resin Transfer moulding flow phenomena in polymeric composites. In *Flow and Rheology in Polymer Composites Manufacturing*, S.G. Advani, Amsterdam, NE, (1994).
- [30] E. Heardman, C. Lekakou, M. Bader, Flow monitoring and permeability measurement under constant and transient flow conditions, *Composites Science and Technology* 64 (9) (2004) 1239–1249.

- [31] C. Wong, A. Long, M. Sherburn, F. Robitaille, P. Harrison, C. Rudd, Comparisons of novel and efficient approaches for permeability prediction based on the fabric architecture, *Composites Part A-Applied Science and Manufacturing* 37 (6) (2006) 847–857.
- [32] Hexcel Composites, G0926 Carbon Fabric Product Data, Hexcel Composites, Stamford, CO, USA,(2009).
- [33] A. Endruweit, K. S. Matthys, J. Peiro, A. C. Long, Effect of differential compression on in-plane permeability tensor of heterogeneous multi-layer carbon fibre preforms, *Plastics, Rubber and Composites* 38 (1) (2009) 1–9.
- [34] B. J. Henz, K. Tamma, R. Kanapady, N. Ngo, P. Chung, Process Modeling of Composites by Resin Transfer Moulding: Sensitivity Analysis for Isothermal Considerations ARL-TR-2686, Army Research Laboratory (ARL), University of Minnesota, MN, USA, 2002.
- [35] H. C. Stadtfeld, M. Erninger, S. Bickerton, S. G. Advani, An experimental method to continuously measure permeability of fiber preforms as a function of fiber volume fraction, *Journal of Reinforced Plastics and Composites* 21 (10) (2002) 879–899.
- [36] E. Heardman, C. Lekakou, M. Bader, In-plane permeability of sheared fabrics, *Composites Part A-Applied Science and Manufacturing* 32 (7) (2001) 933–940.

Chapter 6

Numerical implementation and experimental validation of a through-the-thickness temperature model for non-isothermal vacuum bagging infusion.

M. Gascons, N. Blanco, J. Vives, K. Matthys, Numerical implementation and experimental validation of a through-the-thickness temperature model for non-isothermal vacuum bagging infusion, Journal of Reinforced Plastics and Composites. Accepted 17 Aug 2011.

DOI 10.1177/0731684411423321

6.1 Introduction

In performance driven applications as found in the aerospace and high-end automotive sector, autoclaving techniques with prepreg composite materials are an established code of practice. Liquid moulding techniques are however increasingly considered as a lower-cost alternative, especially with demand for thicker monolithic composite parts rapidly rising. Liquid Composite Moulding (LCM) can be divided into two categories defined by mould typology, as represented in Figure 6.1. The first category is that of Resin Transfer Moulding (RTM) [1], whereby the mould cavity is formed between two rigid mould halves. The second category is defined as Resin Infusion under Flexible Tooling (RIFT) [2], also known as Vacuum Bagging Moulding (VBM), whereby one of the rigid mould halves is replaced by a layer of flexible 'bagging' material. RIFT techniques are gaining importance over RTM [3], mainly due to the lower tooling investment needed, which is of particular importance for the manufacturing of large or thick composite parts.

As many variations exist on the RTM and RIFT processes, different nomenclature can be found, such as Resin Film Infusion (RFI), Vacuum Assisted RTM (VARTM), Liquid Resin Infusion (LRI), Seeman Composite Resin Infusion Process (SCRIMP) and RTM-Light. The essence of all LCM processes is however that resin in liquid form is driven through the dry fibre preform by means of a pressure difference between an inlet and an outlet or vent gate. The pressure difference is maintained via a pump on the inlet, a vacuum pump on the vent or a combination of both, and it drives the resin flow front propagation and impacts part filling and impregnation time. Following impregnation, resin curing starts and the part is consolidated.

The introduction of a heat source in the infusion process is a common tech-

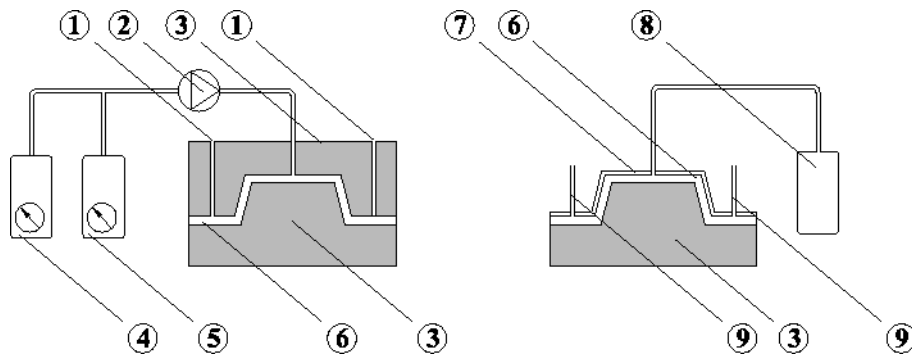


Figure 6.1: *Schematic representation of the RTM (left) and RIFT (right) infusion techniques. 1:Vents, 2:Mixing pump, 3:Rigid tool, 4:Resin pressurized pot, 5:Catalyst pressurized pot, 6: Mould cavity, 7:Vacuum Bag, 8:Resin non-pressurized pot, 9:Vacuum pump connection.*

nique to reduce resin viscosity and enhance resin propagation. For sizeable parts the resin itself is heated rather than applying mould temperature control. Thermal interventions are important and often vital for the manufacturing of thick parts. Even with the evolution of low or non-reactive resins into the market, thermal gradients caused by the external heat supply are still generated as the resin advances. This can lead to inhomogeneous cure of the part, which is a potential source of residual stresses or deformation [4–6].

Heat transfer management in LCM is a complex topic of study due to the interaction of many physical phenomena. As resin flows through the mould, it exchanges heat with the dry preform and the mould by conduction but also transports the heat inside the mould cavity by convection. In addition, changes in resin flow propagation due to temperature dependence of the resin viscosity are to be considered.

Heat transfer phenomena have been thoroughly described in literature for double sided rigid mould infusion techniques, as found in RTM [7–10], but are still less explored for single sided rigid mould infusions, as found in RIFT techniques. The nature of RIFT techniques implies that one side of the mould is closed with an element of little thermal inertia (bag) onto which the external temperature will have more influence.

In the case of autoclave processing of vacuum bagged composites, the assumption of a constant temperature boundary condition for the entire system

is appropriate, due to the forced air convection in the autoclave environment. However, in the case of infusion by means of non-isothermal out-of-autoclave vacuum bagging, forced air circulation is lacking and the constant temperature boundary assumption cannot be maintained. Instead, to resolve this, a heat transfer coefficient might be used to reproduce the passive carry of heat by natural convection phenomena. The accuracy of such simplification will be discussed further.

Regarding thickness, in thin composite plates the temperature gradient through-the-thickness can be neglected, but the difference of temperature in a thick part, object of this study, can rise up to several degrees. For heated resin set-ups, the preform can provide insulation to the entering heat, leaving the inside of the part hotter than the edges. For the heated mould set-up, heat propagates from the source at the bottom (mould side) to the top of the specimen (bag side). Temperature will decrease accordingly from bottom to top of the specimen.

In the absence, to our knowledge, of an adequate analytical thermal model for RIFT manufacturing, it is suggested here to draw from thermal models that were originally designed for RTM.

An experimental protocol has been developed to validate the fitness of purpose of such RTM models for the prediction of temperature distribution and evolution during the filling stage of thick monolithic shell parts produced in a RIFT set-up. In order to single out the effect of external thermal interventions, low-reactive epoxy resin has been used, but this is still representing a considerable range of the available thermosets resin used in industrial environments.

The analytical model is based on an estimated through-the-thickness temperature profile, this allows the reduction of the fully three-dimensional problem to a two-dimensional one. Under this supposition, one can solve first a two-dimensional discretization in the plane of the flow, currently available in simulation codes, and later apply the desired profile. Extruding the two-dimensional plane under the guidance of this profile provides the temperature gradient in all directions for the real geometry. This supposition significantly improves the computational efficiency in the process and avoids the difficulty

of gathering all necessary parameters to run the full three-dimensional analysis, a key point in infusion simulations of large structures.

In what follows, the analytical background of the RTM modelling work is explained, the implementation of the models for a RIFT set-up is clarified and the experimental validation protocol is presented. It will be shown that the analytical solution is approximate but of practical use for RIFT applications.

6.2 Methods

6.2.1 Analytical background

A detailed overview of non-isothermal LCM modelling can be found in reviews by e. g. Advani et al. [11] or Tucker and Dessenberger [12]. For RTM processes, two different heat transfer models are commonly used [13]. The first one is the Non Local Thermal Equilibrium (NLTE) model, also known as the two equations model (Equation 6.1 and Equation 6.2). In this model the energy balance is considered independently for the two components present in the mould cavity, the fluid (resin) and the solid (fibre). In the following equations the subscripts f and s refer to the fluid and the solid respectively.

$$\begin{aligned} \phi(\rho C_p)_f \frac{\partial \langle T_f \rangle}{\partial t} + (\rho C_p)_f \nabla \cdot (\langle v_f \rangle \langle T_f \rangle) = \\ = \nabla \cdot (K_f \bullet \nabla \langle T_f \rangle) + H(T_f - T_s) + \phi \dot{s} \end{aligned} \quad (6.1)$$

$$(1 - \phi)(\rho C_p)_s \frac{\partial \langle T_s \rangle}{\partial t} = \nabla \cdot (K_s \bullet \nabla \langle T_s \rangle) - \alpha_{fs} h_{fs} (T_f - T_s) \quad (6.2)$$

In both equations, ρ , C_p , $\langle v_f \rangle$, T , K , H , ϕ , \dot{s} and h_{fs} are the density, the heat capacity of the materials, the local averaged velocity of fluid, the temperature, the heat conductivity tensor, the heat exchange parameter, the porosity, the curing reaction heat and the heat exchange coefficient between fluid and solid respectively. α_{fs} is the specific area representing the laminate architecture at tow scale and is defined in Equation 6.3.

$$\alpha_{fs} = \frac{4}{d_p} \frac{\epsilon}{1 - \epsilon} \quad (6.3)$$

In Equation 6.3, d_p corresponds to the diameter of a fibre tow and ϵ to the bed or fabric porosity.

Difficulties appear when all the necessary data to use these equations needs to be gathered experimentally. The necessity of fully characterizing both resin and fibre independently, in addition to the complex set-ups needed to obtain particular data, such as the heat exchange coefficients or the conductivity tensor, makes the NLTE model impractical for industrial use.

An alternative and simplified method is the Local Thermal Equilibrium (LTE) or one equation model (Equation 6.4).

$$\begin{aligned} (\phi(\rho C_p)_f + (1 - \phi)(\rho C_p)_s) \frac{\partial \langle T \rangle}{\partial t} + (\rho C_p)_f \langle v_f \rangle \cdot \nabla \langle T \rangle = \\ = \nabla \cdot ((\phi K_f + (1 - \phi)K_s) \cdot \nabla \langle T \rangle) + \phi \dot{s} \end{aligned} \quad (6.4)$$

The LTE model is obtained under the assumption that local temperatures of resin and fibre become equal as soon as resin and fibre come into contact with each other. In the resulting equation, each term stands for a phenomena occurring in the heat transfer process.

The first term represents the internal energy term (heating of the resin), followed by the convection term (heat transport due to moving resin). This equals to the heat generation (due to dissipation and chemical reaction) and the conduction/dispersion term (due to diffusion of heat from the mould walls into the resin and the microscopic resin motion not taken into account in the convection term).

The simplification of the NLTE model into the LTE model is not always valid, as it is constrained by certain assumptions regarding e.g. the fluid velocity. However, computing cost can be reduced with LTE.

Regarding the velocity of the fluid going through the mould cavity, one can evaluate the effect of filling speed through the Graetz number [14]. It defines a dimensionless relation between the convection in the flow direction and the transverse conduction.

A small Graetz number corresponds to a filling speed that is slow compared to heat conduction. The conduction terms are then large compared to the convection term, so they dominate the energy equation. For infusion processes

with Graetz number much larger than one ($Gz \gg 1$), the LTE model becomes imprecise [13, 15, 16], and is thus only suitable for low speed infusion manufacturing. RIFT processes utilize vacuum suction to pull the resin through the mould. Resin velocities achieved by pressure gradients from vacuum suction are limited; therefore the Graetz number for RIFT processes is always small, and the LTE model is applicable.

Regarding computing cost, some authors [9, 17, 18] developed fully three-dimensional models for non-isothermal infusion processes. Many others have dealt with the extensive computational cost issue and have tested and validated the feasibility of applying many simplifications in the three-dimensional model to obtain the so called "two and a half" dimensional models [19] or even two-dimensional models that explain the full evolution of the flow.

The last option has been commonly used in industrial environments, as most of the composite parts produced can be defined as shell parts (a thickness to in-plane ratio less than 1/100). However the need from companies to produce thicker parts reopens the necessity to obtain an accurate prediction of temperature gradients and its evolution in the through-the-thickness direction at a reasonable computational cost.

6.2.2 Implementation

The proposed method here has been implemented using the thermal module of the Liquid Injection Moulding Simulation (LIMS) software (version 4.2) [20], a finite element/control volume code with thermal and cure prediction capabilities developed by the Center for Composite Materials of the University of Delaware.

As a core solver, LIMS deals with the resin flow front advance using Darcy's law (Equation 6.5).

$$\langle V_f \rangle = \frac{\mathbf{K}}{\eta} \nabla \langle p_f \rangle \quad (6.5)$$

In the previous equation, \mathbf{K} stands for the permeability of the fabric, η is the resin viscosity and p_f is the fluid volume-averaged pressure. Using Equation 6.5 in the mass conservation equation, it results in the Laplacean equation for

the fluid pressure (Equation 6.6), which will be used together with the energy equation (Equation 6.4) to solve the temperature during filling stage.

$$\nabla \cdot \left(\frac{\mathbf{K}}{\eta} \nabla \langle p_f \rangle \right) = 0 \quad (6.6)$$

The particular production technique focus of this work, RIFT, presents specific peculiarities when modelling flow front advance. A flexible mould half supposes an uncontrolled mould cavity, as thickness is affected by compaction, caused by the driving suction.

Compaction of the fibre bed inside the mould cavity causes a thickness variation that influences fibre volume and consequently the permeability of the fabric. Different approaches and models are available in literature [21–23] to implement compaction into Darcy's law. In the present work, the compaction effect has been evaluated and introduced into the system by shifting the value of permeability used in the analytical models. However, advanced models were not considered in the present work due to the low thickness variation detected in the tested samples, keeping the main focus on the macro evolution of temperature during the filling stage. In this manner, dry compaction and wet unloading are considered, but not the post-filling compaction.

In addition, this technique allows the determination, beforehand, of some parameters in the general LTE equation (Equation 6.4). The low resin flow propagation velocity into the mould allows neglecting the in-plane conduction and dispersion term. The pressure and the velocity profile can be assumed uniform through-the-thickness, and the variation of the viscosity once the working temperature is achieved is not strongly dependent on temperature, which is acceptable for most of the thermoset formulated resins.

Regarding the thermal boundary conditions, in the rigid mould side one can consider that the heat transfer between elements occurs mainly by conductivity and a fixed temperature can be supposed.

On the other side of the mould, where the vacuum bag is used, convection needs to be taken into account in addition to the thermal conduction. Convection effects can be expressed as $h_{conv} \cdot (T - T_{out})$ where h_{conv} is the coefficient of convection and T_{out} the temperature of the external media. Conduction can be expressed as $-k \cdot (dT/dz)$, where T is the temperature inside the mould, z the

through-the-thickness direction (perpendicular to the surface of the mould) and k the thermal conductivity coefficient of the material. To achieve equilibrium, both expressions are handled together leading to Equation 6.7. If the temperature in the mould surface (T) and the surrounding temperature (T_{out}) are the same, it can be considered that k and h_{conv} are the only parameters that determine the heat transfer.

$$(T - T_{out}) = \frac{-k}{h_{conv}} \frac{dT}{dz} \quad (6.7)$$

Previous statements are used into a first iteration using a two-dimensional representation of the geometry. The temperature at midplane of the equivalent thickness is obtained by means of the previously presented LTE equation (Equation 6.4). Midplane temperature is determined mainly as a function of diffusivity and conductivity of the preform and the resin.

Boundary conditions at top and bottom of the mould will determine the temperatures at each side, depending on the set-up and the prevailing heat transfer phenomena. In Figure 6.2, a dimensionless plot of the temperature gradient (T^*) is represented against a dimensionless representation of the thickness of the mould cavity (h^*). The two expected profiles for the heated mould and the heated resin configuration are represented. In the vertical axis of the graph, 0 stands for the bottom of the mould cavity (rigid mould), and 1 stands for the top of the mould (vacuum bag).

The polynomial profile used for the through-the-thickness temperature gradient is suggested in the work of Advani and Simacek [24–26] and is described by Equations 6.8, 6.9 and 6.10.

$$T(z; x, y, t) = T_1(z) \cdot T_m(x, y, t) + T_2(z) \quad (6.8)$$

$$T_1(z) = 4 \frac{z \cdot (h - z)}{h^2} \quad (6.9)$$

$$T_2(z) = 2T_0 \frac{(h - z)(h/2 - z)}{h^2} + 2T_h \frac{z(z - h/2)}{h^2} \quad (6.10)$$

x stands for the longitudinal direction (flow front advance), y for the transversal direction, defining the plane, T_m is the temperature at midplane, T_0 is the

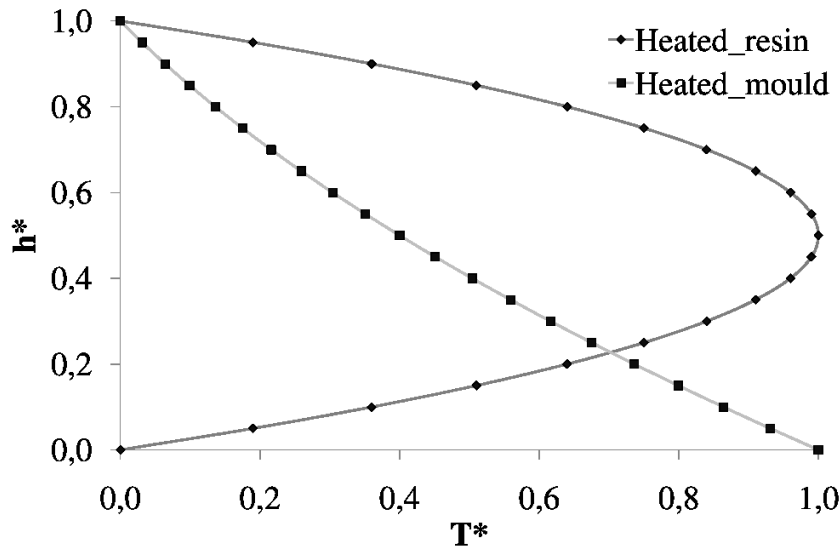


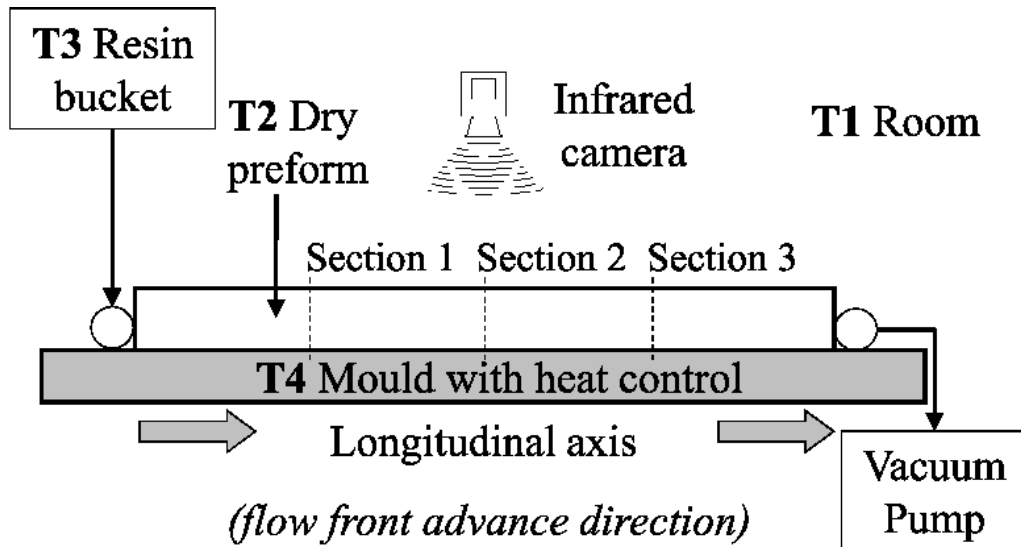
Figure 6.2: Representation of the expected temperature gradient profile (T^*) through the normalised thickness of the sample (h^*) (0 for bottom, rigid mould, 1 for top, vacuum bag).

temperature at the bottom mould and T_h is the temperature at the top of the mould. z stands for the desired point of the thickness and h stands for the mould height.

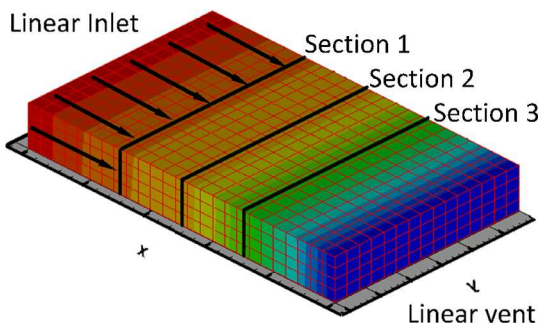
6.3 Experimental set-up

A specific experimental rig was designed to extract the necessary information to validate the proposed model. The rig used is able to reproduce two different non-isothermal set-ups, which are representative of the methods used to introduce heat into an infusion process. The first set-up allows the introduction of heat by means of a heated resin entering into the mould cavity and the second set-up allows the introduction of heat via a heat source from the mould side. A schematic view of the set-up can be observed in Figure 6.3(a) together with a real top view of the set-up (Figure 6.3(c)).

The resin is placed in an open bucket (T3) and is driven to the mould cavity, where a distribution channel creates a linear gate across the entire edge. The resin fills the mould, which consists of a thick aluminium slab on one side,



(a) Scheme of a longitudinal cut of the experimental rig. T1, T2, T3 and T4 stand for the different temperatures involved in the set-up



(b) Three-dimensional view of the sample, including filling isochrones. Control sections and direction of flow front advance highlighted



(c) Real image of the upper surface of one of the samples produced heating the resin. Linear flow front advance observed

Figure 6.3: Real set-up overview. (a) Scheme of the set-up, (b) 3D representation, and (c) top view of the real set-up

as a rigid tool, and a vacuum bag on the other side, as a flexible tool. No flow enhancement layers or other ancillary materials were used during the infusion. As the resin flow advances, the resin goes through the different control sections (Section 1, Section 2 and Section 3) and finally reaches the end of the mould cavity, connected to the vacuum pump.

Type K thermocouples were embedded in three different sections of the preform (Section 1 to 3 in Figure 6.3(b)) at different heights to monitor the evolution of temperature. The thermocouples were placed in the central areas of the sections in the width direction to avoid possible boundary effects. Thermocouples were lined up in layers corresponding to midplane, first quarter and third quarter of the thickness of the sample. Once the entire preform is assembled, the disposition of the thermocouples configures a 9 points grid. Three different control points are in the longitudinal axis for each instrumented layer and three control points are in the through-the-thickness direction for each section.

These thermocouples are used first to determine the temperature of the dry preform (T2), and later to determine the evolution of the temperature during the infusion process.

In addition, temperatures at top and bottom of the sample need to be recorded to monitor the interaction of the mould and the part. To this purpose, three thermocouples were embedded in the surface of the aluminium slab in contact with the part (T4), and an infrared camera was placed on top. This camera not only verified the evolution of the temperature on the analysed top layer but was also useful to monitor flow front advance and temperature on the entire sample surface. Linear advance of the resin through the sample was controlled visually, as shown in Figure 6.3(c).

Two extra thermocouples were used to monitor the room temperature (T1) and the temperature of the resin at the inlet point (T3) during the infusion stage. A detailed transversal view of a control section (Section 1 in Figure 6.3(a)), can be observed in Figure 6.4, where the position of each control point in the section and its nomenclature is detailed.

All signals of the tests are handled through a data acquisition device. An acquisition GUI was developed in-house using a Labview environment. Tem-

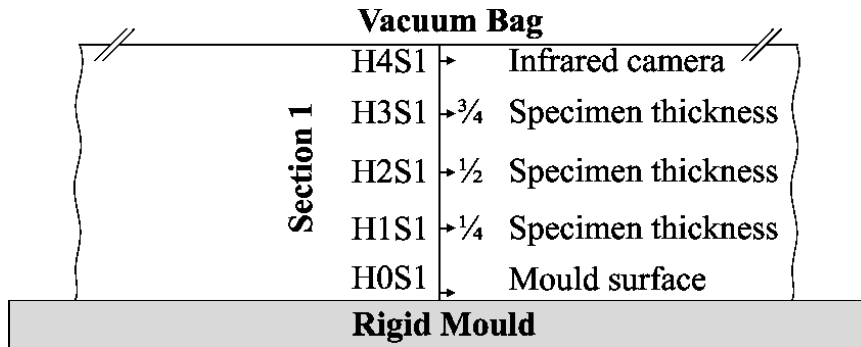


Figure 6.4: Representative (not scaled) detail of the transversal section of the sample with position and nomenclature of the recorded points.

perature was recorded in real time at 1Hz frequency. Synchronized with the thermocouple measurement, the amount of resin transferred to the mould cavity was controlled placing the resin bucket over a precision weighing scale to obtain the exact flow rate and flow front velocity at any time of the test. A description of the material used during the infusion of the glass fibre reinforced epoxy rectangular plates is provided in Table 6.1.

Materials properties (Multi axial fibreglass + Epoxy resin)			
	SP Gurit (QE1174)	Epolam 5020 (amine hardener)	
Conductivity	1.05	0.25	W/mK
Specific heat	344	1800	KJ/KgK
Density	2550	1275	Kg/ m^3
Superficial density	1273	-	g/ m^2
Fibre volume	48	-	%
Permeability(dry)	1.5^{-10}	-	m^2
Number of layers	40	-	
Hardener content	-	34	%
Viscosity	-	0.225	Pa·s

Table 6.1: Properties of the materials used in the tests conducted.

Regarding the resin, a low-reactive resin (Epolam 2020) with no accelerator in the mixture was used for this purpose. Figure 6.5 show the pot life of the used resin for the available range of accelerator content. As the average

time of the infusion process for all tests performed was 15 minutes, the graph is supportive for the decision of not taking into account the heat reaction and therefore focus on the external thermal interventions.

For the first configuration tested, the resin and the catalyzer were heated up in a controlled temperature oven beforehand, and mixed into an insulated bucket. An insulated tube was used to connect the bucket with the inlet of the mould to ensure the temperature stability of the incoming resin. A thermocouple is placed at the mould cavity inlet to provide the temperature in the entrance of the system, which is needed for the analytical model. This point is chosen to avoid heat loss from the short path between the bucket and the entrance of the mould cavity. Data provided from this thermocouple confirms the supposition of a constant temperature at the entrance.

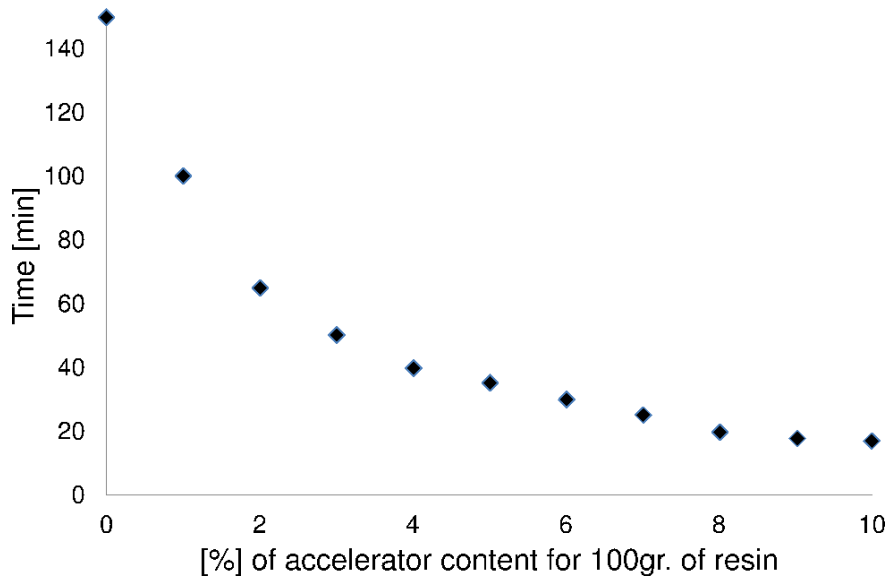


Figure 6.5: *Potlife of the resin according to accelerator content [27].*

For the second configuration, an electric heating device was attached underneath the aluminium slab with a close loop feedback calibration system to keep a constant surface temperature. As the thickness of the rigid aluminium tool used is also considerable (40 mm), the thermal inertia ensures the stability of the temperature on the contact surface. An extremely thick sample was used in order to reproduce the goal of this study, thick shells. For each configuration, six infusions were conducted following the details described in Table 6.2.

Sample dimensions and test plan			
Repetitions	Length	Width	Thickness
6	250 mm.	150 mm.	30 mm.
Heated	Mould Temp.	Fibre Temp.	Resin Temp.
Resin	<i>Room</i>	<i>Room</i>	60°C
Mould	60°C	Variable	<i>Room</i>
Details of the experimental equipment			
	Model	Work Range	Precision
Infrared camera	NEC-TH7800N	-20°C to 250°C	min[-2°C or 2%]
	Model	Work Range	Precision
Thermocouples	Type K	0°C to 200°C	min[2°C or 0.75%]

Table 6.2: *Main dimensions and experimental program information for conducted tests, both for heating the resin and for heating the mould.*

Difficulties were found when dealing with non-controlled parameters such as difference in day-to-day room temperature, which was proven to affect the final temperature profiles. To solve this problem and summarize the results, all the temperatures were normalised to filter out such factors from the presented results.

6.4 Results

6.4.1 Outputs of the numerical analysis

After the simulations, the temperature distribution in all the samples can be extracted from the previously stated Equation 6.10 for any point of the sample during the entire process. In Figure 6.6, the plot showing the temperature distribution at the end of filling stage of a mould heated configuration is shown.

In addition to the end-of-stage temperatures, the numerical analysis is also able to provide the temperature throughout all the infusion stage in any desired point. The highlighted central longitudinal cut corresponds to the plane where the tracers were placed during the experimental program.

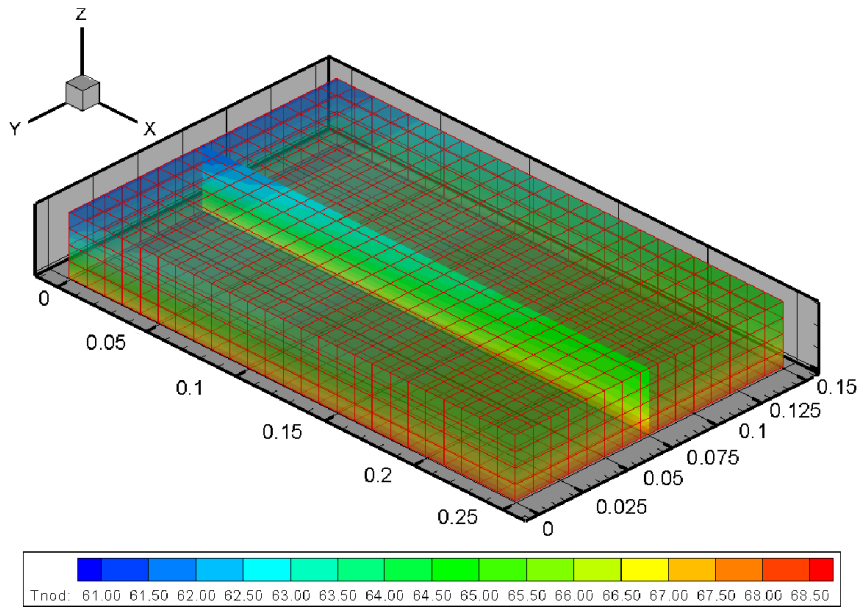


Figure 6.6: Numerical prediction of the temperature for a heated resin configuration injected from the left top edge. Highlighted, the longitudinal cut where tracers are placed. Temperature in $^{\circ}\text{C}$

6.4.2 Data treatment and post processing

The acquisition process starts with a conditioning period where the bag leakage is tested and (when necessary) the mould is heated to the desired temperature and allowed to stabilize. Later on, the complete infusion, including cure and cool-down stages, is recorded. The process stops in the instant just prior to demould, when the part is fully consolidated.

To compare the results from the experimental data and the analytical prediction, a preliminary set of inputs, such as the flow rate and the temperatures at the start point of the analysis are provided to the analytical model. Flow rate is extracted from a scale placed under the resin bucket and temperature from the thermocouples inside the system.

Once the data is introduced to the code, the analysis is executed and the implemented subroutines provide the temperature profile. The analysis considers only the temperature of the fibre until the resin reaches the tracer point; therefore, it is expected to provide a flat line and a sudden increase as soon as the resin reaches the point. This results in a mismatch in the data shown

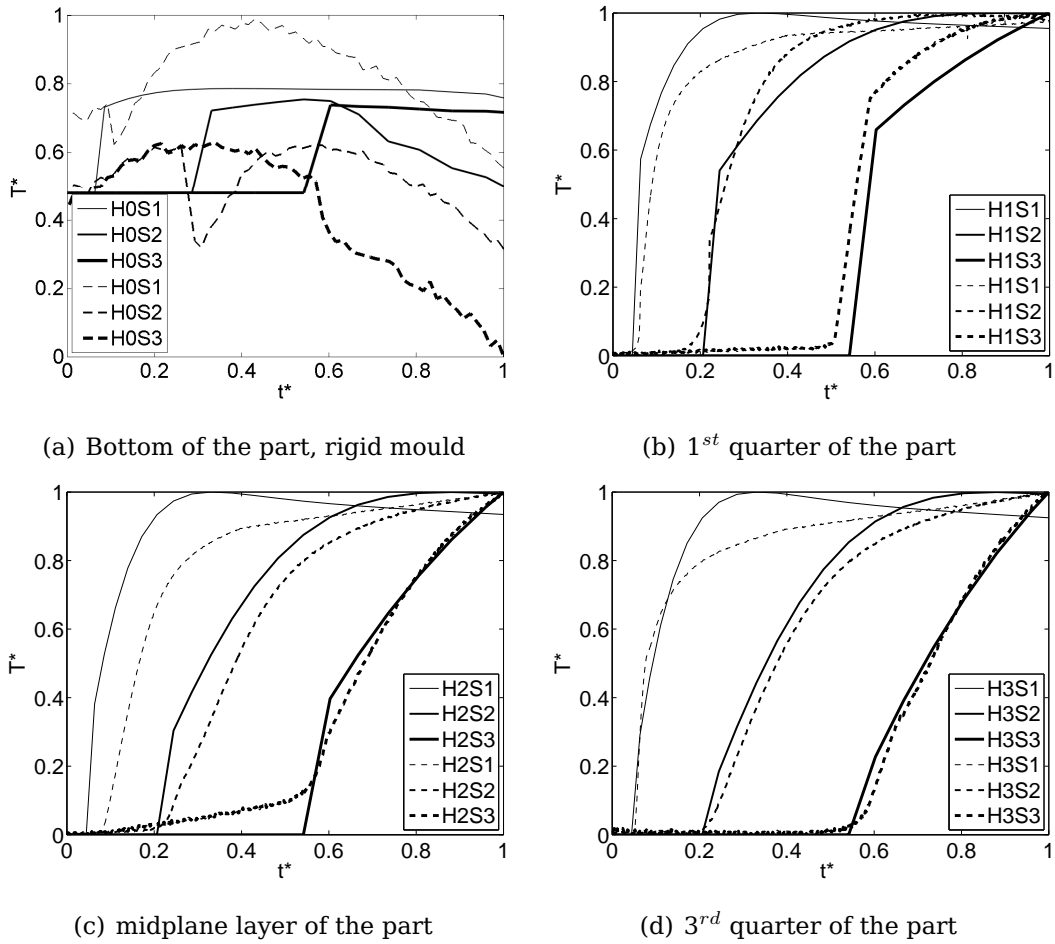


Figure 6.7: Comparison of analytical (continuous line) and experimental (dashed line) results for the resin heated configuration.

on the pictures 6.7, 6.9, 6.10 and 6.12, but is considered irrelevant as it is a limitation of the numerical formulation that does not influence the infusion period of the process, which is the real objective of this work.

For both configurations, resin or mould heated, the data is provided normalized. It presents a normalization of the temperature (T^*) against a normalization of the total filling time (t^*). The legend on the graph identifies the different tracers in the same layer, corresponding to each of the quarters in height of the sample. Continuous lines represent the numerical data, and dashed lines the experimental results. H stands for height, with zero being the mould and four the top layer, and S stands for the section, with one being the closest to the gate and three the closest to the vent.

The most critical aspect of the set-up, the flexible mould, is taken into account by the analysis of the images provided by the infrared camera. Figure 6.8 shows a representative snapshot of the test, where temperature at the external side of the bag can be observed. The image justifies the convection boundary condition instead of a fixed temperature, as temperature gradients occurring are clearly observed. Numerical information has been extracted from the camera snapshots for the control points to be compared with the values provided by the analytical model.

6.4.3 Resin heated configuration

For this configuration, the mould cavity, the rigid mould and the flexible mould stay at the same temperature. A different temperature is introduced into this isothermal system when the resin enters the cavity.

The comparison between the analytical results and the data extracted from the infusions conducted are shown in the multiple graphic of Figure 6.7.

The temperature evolution at the mould side measured by the thermocouples and predicted by the model can be observed In Figure 6.7(a). In the case of the experimental data, the recorded values present significant oscillations because the measuring accuracy of the employed thermocouples is 2 °C and the maximum variation in temperature in this case is of only 4 °C. Such a small variation of temperature during the test is due to the fact that the ther-

mal capacity of the entering hot resin is not capable of overcoming the thermal inertia of the cold mould. Therefore, the experimental curves show that the temperature increases slightly once the resin reaches each section but it decreases after a while. This is especially true for sections 1 and 2, while for section 3 the inherent precision of the thermocouple hides this tendency. Concerning the numerical predictions, the tracers are able to follow the general trend of the temperature, denoting slight increases in the first and second section and, at the latest stage, detect the cooling effect of the rigid part of the mould.

Figure 6.7(b), provides the results for the 1st quarter in thickness of the sample. The temperature trend is followed in all the tracers. Imprecision is observed in the analytical prediction of the first tracer and also in the start point of the third tracer, attributed to the variability of the permeability of the preform.

In Figure 6.7(c) the results for the midplane configuration are shown, directly extracted from the two-dimensional simulation of LIMS. The level of accuracy in this case is similar to the previous ones, increasing as the resin advances through the mould cavity.

The bottom right image, Figure 6.7(d), provides the trend for the layer of thermocouples closest to the top of the preform. Best results are shown for the prediction of the second and third tracers.

Temperatures extracted from the infrared camera (Figure 6.8) and the analytical prediction are presented in Figure 6.9. Data presented in this figure shows the same level of confidence as previous analysis for the second and third tracer but a clear mismatch for the first tracer, where the temperature is clearly over predicted.

The infrared data can also be contrasted with the real top view image, previously depicted in Figure 6.3(c), which confirms the premise of the line front advance through the complete specimen.

Comparing the four subfigures in Figure 6.7 it can be observed that the evolution of the temperature for the hot resin configuration is different depending on the considered height inside the mould, especially in the side of the rigid mould. This is an effect that the the proposed model can reproduce

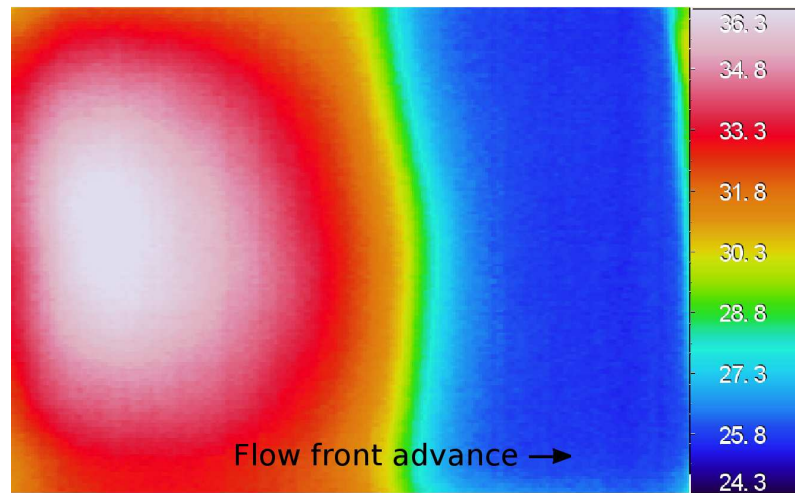


Figure 6.8: Infrared image of the upper surface of one of the samples produced heating the resin. Temperature in $^{\circ}\text{C}$

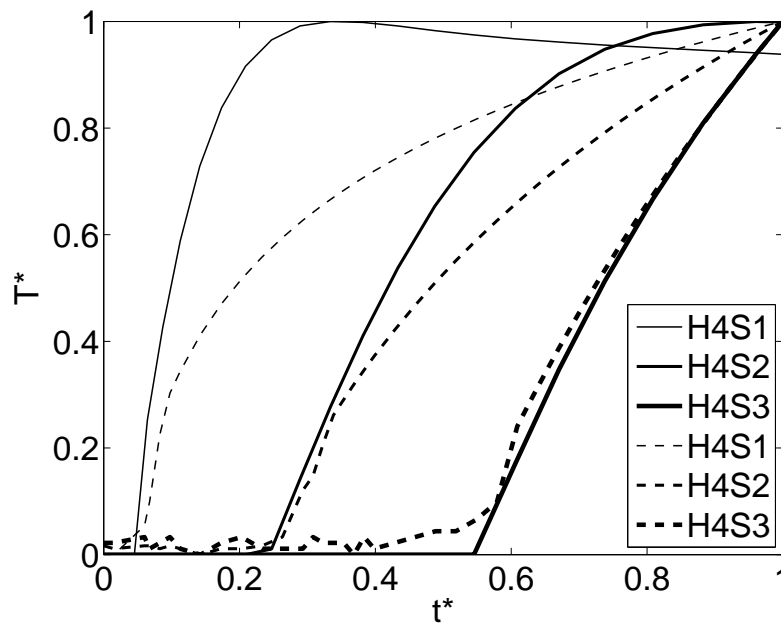


Figure 6.9: Comparison of the temperatures extracted from the infrared camera (dashed line) and the solution provided by the analytical model (continuous line) for the resin heated case.

while the so-called two and "two and a half" dimensional temperature models used in different simulation codes can not.

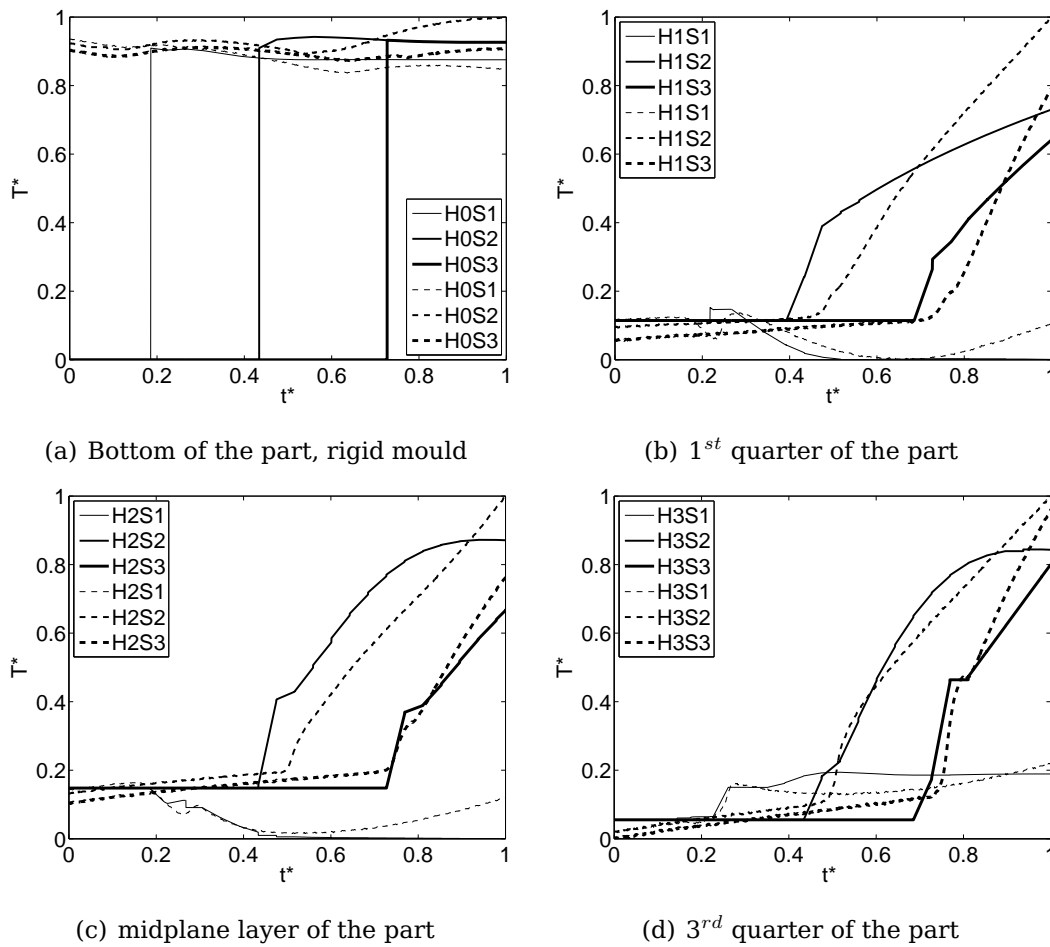


Figure 6.10: Comparison of analytical (continuous line) and experimental (dashed line) results for the mould heated configuration

6.4.4 Mould heated configuration

In the case of the heated mould, the resin is expected to absorb the temperature of the preform. The through-the-thickness temperature decreases as the height of the preform increases, which causes a difference between the temperature of the resin entering into the system (constant) and the different temperature at each height of the mould. The determination of this temperature gradient at each height has to be done beforehand and introduced as an input in the analytical model to be able to predict the full temperature evolution.

For the tracer comparison of this case, Figure 6.10, the resin temperature

causes the reference temperature increase or decrease depending on the section that is considered.

For the image of the mould tracers, Figure 6.10(a), the same tendency as in the predictions of the resin heated configuration is observed, with a clear change at the moment that the resin reaches each thermocouple section. Some disturbances are observed in the experimental trend, caused by the own thermocouple precision range.

Next two figures, corresponding to the 1st quarter (Figure 6.10(b)) and midplane (Figure 6.10(c)), show the same pattern of evolution. Temperature of the tracers decreases in the first section as the resin, which is at lower temperature than the preform, cools it down. In the next two sections, the resin advancing has lost cooling capacity, causing an increase of the temperature when the tracer is reached.

The insulating nature of fibreglass is broken as soon as it is impregnated by the resin causing a change in the heat conductivity of the mould cavity.

In the Figure corresponding to the 3rd quarter, temperature of the resin entering the mould is slightly higher than the temperature of the preform at the first tracer. It causes an increase of the temperature in this point and a latter, more pronounced increase of the temperature for the second and third tracers.

Figure 6.11 depicts one image representative of the information given by the infrared camera. A comparison between the data extracted from these images and the experimental trend is presented in Figure 6.12.

6.5 Discussion

As it is observed in (Figures 6.7(a) and 6.10(a)), the experimental data of the mould tracers present some disturbances. The finite precision of the thermocouples has been corroborated as its inherent cause. The supposition of a constant temperature in the mould side for both techniques is therefore accepted as adequate.

Analysing the other comparative images, it is observed that the accuracy tends to increase as the resin advances, being more accurate in the second

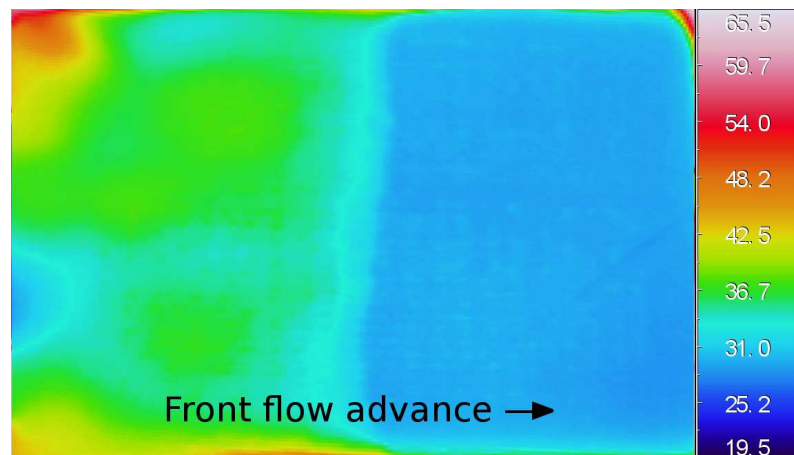


Figure 6.11: Infrared image of the upper surface of one of the samples produced heating the mould. Temperature in $^{\circ}\text{C}$

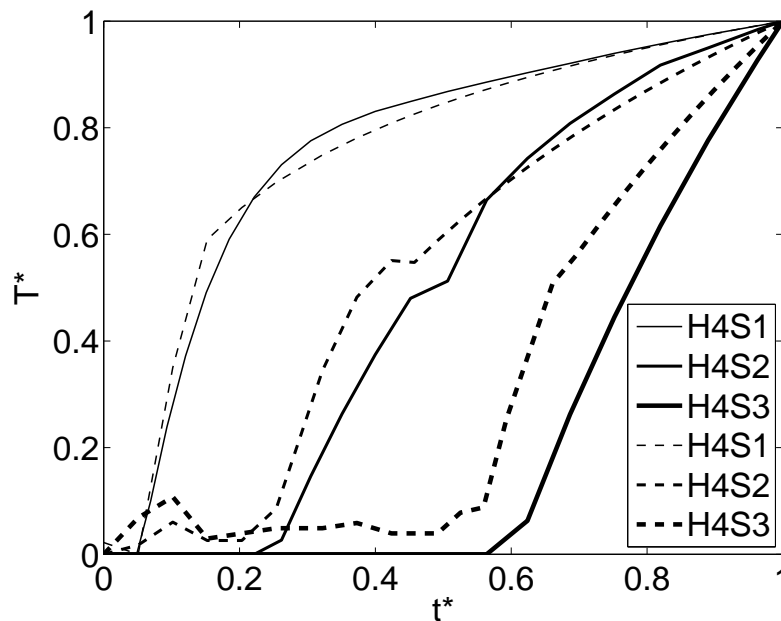


Figure 6.12: Comparison of the temperatures extracted from the infrared camera (dashed line) and the solution provided by the analytical model (continuous line) for the mould heated case.

and third tracers than in the first one. The transient to steady state process is pointed to as the cause of the under and over prediction in the results. Accuracy is achieved more properly at the end of the stage than in the beginning of the fill period, which matches with the observations of Simacek and Advani [24] in the two-dimensional validation of the method.

This can be attributed to the limitations of the LTE method, as indicated in [13]. As the process advances, the velocity of the resin slows down and the precision of the proposed method increases. As resin travels faster through the first tracer than the second and third ones, the precision in the first decreases when compared with the other two, where the trend is more accurately followed.

Regarding the analysis of the bag side, although imprecisions could be partially attributed to the fact that the analytical model and the infrared camera are providing information from different sides of the bag, the insulation effect of the bag can be neglected due to its limited thickness. Therefore, bag insulation can be discarded as the cause of differences between predicted and measured temperature evolutions in the bag side of the mould.

The difference between the trend of the first tracer in Figure 6.12 and the those observed for the first tracers in each height in Figure 6.10 points to the influence of the convection boundary condition on this side of the mould.

The general observation of the trends in the midplane and the 3rd quarter already shows a slight increase of the temperature when the resin reaches the first tracer. On the surface of the sample, the higher exchange of temperature with the room provides a different pattern, leaving the heat transported by the resin with more importance than in the other tracers.

6.6 Conclusions

The capability of an analytical model to reproduce the experimental data in non-isothermal vacuum bagged set-ups has been validated through the measurement of the spatial temperature distribution and time evolution during a sample infusion process.

Results show that the numerical implementation of the analytical model via the use of a convection boundary condition on the flexible mould side offers a good level of agreement between experiment and simulation.

Fast resin propagation in the entrance of the mould cavity is pointed to as the cause of the temperature overprediction in zones close to the resin inlet, obtained when using the LTE as a base for the calculation

It has been demonstrated that a prediction of the thermal map in space and time for a thick shell composite part infusion can be obtained with a simple analytical approach. The accuracy of the prediction is limited due to the simplifications made in the numerical formulation, but the method can be considered to give an adequate solution for industrial applications. Moreover, the work represents an opportunity for improvement of further analysis. As an example, the thermal map can be used as a more precise initial condition for the investigation of inhomogeneous cure gradients as well as for mechanical issues regarding part distortions and residual stresses.

Bibliography

- [1] C. Rudd, A. Long, K. Kendall, C. Mangin, *Liquid Moulding Technologies*, Woodhead Publishing and SAE International, Warrendale, PA, USA, 1997.
- [2] C. Williams, J. Summerscales, S. Grove, Resin infusion under flexible tooling (rift). A review, *Composites Part A: Applied Science and Manufacturing* 27 (7) (1996) 517–524.
- [3] S. Mazumdar, *Composites Manufacturing. Materials, Product and Process Engineering*, CRC Press, Boca Raton, FL, USA, 1997.
- [4] W. Schulz, D. Myers, T. Singer, P. Ifju, R. Haftka, Determination of residual stress and thermal history for im7/977-2 composite laminates, *Composites Science and Technology* 65 (13) (2005) 2104–2024.
- [5] J. Xiong, R. Shenoi, J. Gao, An analytical model to predict residual thermal stress in 2d orthogonal plain weave fabric composites, *International Journal of Solids and Structures* 46 (9) (2009) 1872–1883.
- [6] L. You, X. You, A unified numerical approach for thermal analysis of transversely isotropic fibre-reinforced composites containing inhomogeneous interphase, *Composites: Part A-Applied Science and Manufacturing* 36 (6) (2005) 728–738.
- [7] A. Abbassi, M. Shahnazari, Numerical modelling of mould filling and curing in non-isothermal RTM process, *Applied thermal engineering* 24 (16) (2004) 2453–2465.

- [8] M. Lin, M. Kang, H. Hahn, A finite element analysis of convection problems in RTM using internal nodes, *Composites Part A-Applied Science and Manufacturing* 31 (4) (2000) 373–383.
- [9] A. Shojaei, S. Ghaffarian, S. Karimian, Simulation of the three-dimensional non-isothermal mould filling process in resin transfer molding, *Composites Science and Technology* 63 (13) (2003) 1931–1948.
- [10] K. Pillai, M. Munagavalasa, Governing equations for unsaturated flow through woven fibre mats. Part 2. Non-isothermal reactive flows, *Composites Part Part A-Applied Science and Manufacturing* 35 (4) (2004) 403–415.
- [11] S. Advani, M. Brusckhe, R. Parnas, Resin Transfer molding flow phenomena in polymeric composites. In *Flow and Rheology in Polymer Composites Manufacturing*, S.G. Advani, Amsterdam, NE, 1994.
- [12] C.L. Tucker III, R. Dessenberger, Governing equations for flow and heat transfer in stationary fibre beds in *Flow and Rheology in Polymer Composites Manufacturing*, S.G. Advani, Amsterdam, NE, 1994.
- [13] M. Delèglise, C. Binètruy, P. Castaing, P. Krawczak, Use of non local equilibrium theory to predict transient temperature during non- resin flow in a fibrous medium, *International Journal of Heat and Mass Transfer* 50 (11-12) (2007) 2317–2324.
- [14] C.L.Tucker III, Heat transfer and reaction issues in liquid composite moulding, *Polymer Composites* 17 (1) (1996) 60–72.
- [15] H. Chiu, B. Yu, S. Chen, L. Lee, Heat transfer during flow and resin reaction through fibre reinforcement, *Chemical Engineering Science* 55 (17) (2000) 3365–3376.
- [16] M. Quintard, S. Whitaker, Local thermal equilibrium for transient heat conduction: theory and comparison with numerical experiments, *International Journal of Heat and Mass Transfer* 38 (15) (1995) 2779–2796.

- [17] O. Mai, A. Courniot, F. Dupret, Non-isothermal simulation of the resin transfer moulding process, *Composites Part A-Applied Science and Manufacturing* 29 (1-2) (1998) 189-198.
- [18] W. Chang, N. Kikuchi, Analysis of non-isothermal mould filling moulding and structural reaction process in resin transfer moulding (RTM) and structural reaction injection moulding (SRIM), *Computational mechanics* 16 (1) (1995) 22-35.
- [19] J. Kessels, A. Jonker, R. Akkerman, Fully 2,5 d flow modelling of resin infusion under flexible tooling using unstructured meshes and wet and dry compaction properties, *Composites Part A-Applied Science and Manufacturing* 38 (1) (2007) 51-60.
- [20] P. Simacek, S. Advani, Desirable features in mould filling simulations for liquid composite moulding processes, *Polymer Composite* 25 (4) (2004) 355-367.
- [21] B. Yenilmez and E. Murat Sozer, Compaction of e-glass fabric preforms in the Vacuum Infusion Process. A: Characterization experiments, *Composites Part A-Applied Science and Engineering* 40 (4), (2009) 499-510
- [22] Q. Govignon and S. Bickerton and P.A. Kelly, Simulation of the reinforcement compaction and resin flow during the complete resin infusion process, *Composites Part A-Applied Science and Engineering*, 41(1), (2010) 45-57.
- [23] A. Hammami and B.R. Gebart, Analysis of the Vacuum Infusion Moulding Process, *Polymer Composites*, 21(1), (2000) 28-40
- [24] P. Simacek, S. Advani, Approximate numerical method for prediction of temperature distribution in flow through narrow gaps containing porous media, *Computational Mechanics* 32 (1-2) (2003) 1-9.
- [25] P. Simacek, S. Advani, An analytic solution for the temperature distribution in flow through porous media in narrow gaps I . Linear injection, *Heat and Mass Transfer* 38 (1-2) (2001) 25-33.

- [26] P. Simacek, S. Advani, An analytic solution for the temperature distribution in flow through porous media in narrow gap II. Radial injection, *Heat and Mass Transfer* 38 (6) (2001) 497–505.
- [27] Epolam 2020 Epoxy laminating system with variable reactivity technical datasheet. Axson, UK, 2005

Chapter 7

Study of the influence of the in-plane conduction and convection term in the determination of the temperature distribution in non-isothermal setups

M.Gascons, N.Blanco, K.Matthys, Study of through-the-thickness heat conduction and dispersion in Resin Infusion under Flexible Tooling (RIFT). To be submitted to International Journal of Heat and Mass Transfer.

7.1 Introduction

Resin Infusion under Flexible Tooling (RIFT) [1], is a specific method used for the industrial production of fibre reinforced thermosets. This moulding technique makes use of a flexible "bagging" material to enclose the mould cavity as shown in Figure 7.1.

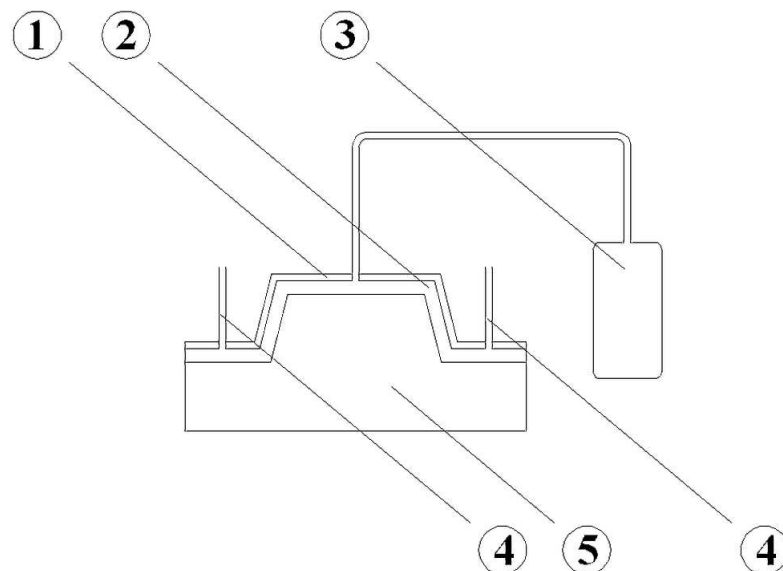


Figure 7.1: *Schematic representation of the RIFT infusion technique. 1:Vacuum bag, 2: Mould cavity, 3:Resin non-pressurized pot, 4:Vacuum pump connection 5:Rigid tool.*

Although RIFT has already been a proven technique for many years in selected industrial environments, it has been infiltrating into a broader range of applications [2]. For example, RIFT is increasingly used for the manufacturing of thick and large structural parts due to the lower cost of the flexible mould compared to the tooling price of alternative methods, but this new application also poses new technical challenges to the process.

RIFT has matured through steady evolution and continued improvement.

The physical underlying principle, i.e. the suction of a liquid matrix through a sealed mould cavity in which a reinforcement fabric is placed, has been refined by research groups and industrial users, and has led to many variations such as Vacuum assisted RTM (VARTM) or Seeman Composite Infusion Process (SCRIMP).

Inside the mould cavity, the reinforcement fibres are being compressed by the vacuum suction and the resin propagation is affected by the imposed pressure gradient, which conditions the part filling and affects impregnation time. In order to accelerate or influence the filling process, the introduction of heat is commonly used [3].

Heat is either introduced via a temperature controlled mould or heated resin. The first option is directly derived from Resin Transfer Moulding (RTM) [4], where the mould cavity is formed by two solid halves. Heating of both sides of the mould allows optimal temperature control and good thermal stability of the process.

However, with RIFT set-ups only disposing over one solid mould halve, heat is only introduced unilaterally. This one-sided heat introduction causes thermal gradients that can lead to inhomogenous cure, which is a potential source for the formation of residual stresses and distortions in the injected part [5–7]. In the case of very large parts or complex geometries it is sometimes not even practically feasible to heat the solid mould half, and for these cases, heat introduction via heated resin is the selected option.

Many physical phenomena are involved in the heat transfer inside Liquid Composite Moulding (LCM) processes. As resin flows through the mould, it exchanges heat with the dry preform and the mould by conduction but also transports the heat inside the mould cavity by convection. In addition, changes in resin flow propagation due to temperature dependence of the resin viscosity are to be considered. The thermal boundary conditions of the mould cavity also affect heat transfer during infusion [8].

Resin flow simulations codes [9, 10] do implement the non-isothermal environment using the Thermal Equilibrium equations [11]. Existing software packages can provide approximate solutions but are subjected to impractically high computing costs for more accurate simulation studies.

Published scientific works on this matter presents two different alternatives to model the heat transfer phenomena for flow through fibre beds [12]: the Non Local Thermal Equilibrium (NLTE) and the Local Thermal Equilibrium (LTE) models. The LTE model is widely used in many thermoset resin flow processes, mainly due to its simplicity. Many authors have reported its use to describe the thermal evolution in RTM processes [13–16].

However, though established for RTM, the validity of the LTE model still needs to be checked for RIFT due to the greater temperature gradient caused by the small thermal inertia of the flexible mould.

The feasibility of extending the LTE model as used in RTM to non-isothermal RIFT manufacturing processes will be discussed in this work. Although the LTE equation can include microscale flow phenomena, it requires knowledge of parameter values that are difficult to determine. This work assumes that the influence of the heat dispersion coefficients in this technique is not significant and that neglecting these terms does not cause a remarkable impact in the final accuracy of the analytical method. This is a fair assumption because of the typical slow velocity of this method. Under this assumption, the neglect of these terms will not cause a significant impact on the overall accuracy of the proposed analytical method.

7.2 Analytical background

7.2.1 Model considered

The Non-Local Thermal Equilibrium (NLTE) model, alternatively known as the two equations model, (presented in Equation 7.1 and Equation 7.2), explicitly reproduces the heat transfer phenomena inside the mould cavity by means of independent expressions for each of the constituents inside the mould cavity.

$$\begin{aligned} \phi(\rho C_p)_f \frac{\partial \langle T_f \rangle}{\partial t} + (\rho C_p)_f \nabla (\langle v_f \rangle \langle T_f \rangle) = \\ = \nabla (K_f \bullet \nabla \langle T_f \rangle) + H(T_f - T_s) + \phi \dot{s} \end{aligned} \quad (7.1)$$

$$(1 - \phi)(\rho C_p)_s \frac{\partial \langle T_s \rangle}{\partial t} = \nabla (K_s \bullet \nabla \langle T_s \rangle) - \alpha_{fs} h_{fs} (T_f - T_s) \quad (7.2)$$

In the equations above, the subscripts f and s stand for the fluid (resin) and the solid (fibre) respectively.

In these equations, ρ stands for density, C_p for the heat capacity of the materials, $\langle v_f \rangle$ for the injection average velocity, T for the temperature, K for the heat conductivity tensor, H for the heat exchange parameter, ϕ for the porosity, \dot{s} for the curing reaction heat and h_{fs} for the heat exchange coefficient between fluid and solid respectively. α_{fs} is the specific area representing the laminate architecture at tow scale and is defined in Equation 7.3.

$$\alpha_{fs} = \frac{4}{d_p} \frac{\phi}{1 - \phi} \quad (7.3)$$

In Equation 7.3, d_p corresponds to the diameter of a fibre tow and ϕ to the bed or fabric porosity.

Although this equation system has been proven as an accurate model to reproduce the heat transfer inside the mould cavity, difficulties arise in the determination of all the involved parameters for each constituent. The need of complex laboratory task to obtain the full characterization of the constituents pushed the necessity of alternative models to become suitable for industrial applications.

Under the principle that resin and fibre local temperature become equal as soon as they come into contact with each other, the Local Thermal Equilibrium (LTE) model (Equation 7.4) is the proposed alternative to the NLTE model. The LTE model stands for simplicity in the determination of involved parameters but has some limitations with the applicability range and precision [17].

$$\begin{aligned} & (\phi(\rho C_p)_f + (1 - \phi)(\rho C_p)_s) \frac{\partial \langle T \rangle}{\partial t} + (\rho C_p)_f \langle v_f \rangle \cdot \nabla \langle T \rangle = \\ & = (k_{zz} + K_{Dzz}) \frac{\partial^2 T}{\partial z^2} \nabla \cdot (((\phi K_f + (1 - \phi)K_s) + K_D) \cdot \nabla \langle T \rangle) + \phi \dot{s} \end{aligned} \quad (7.4)$$

Terms of the equation will be carefully described in the following chapter. The background behind the modelling of non-isothermal infusion techniques has solid foundations established in works of Advani et al. [18], Tucker and Dessenberger [19] or Chang et al. [20]. These works discuss the suitability of the previously stated Equations 7.1 and 7.2 to reproduce the thermal evolution inside mould cavities enclosed in rigid moulds.

It has been reported that the LTE model loses accuracy as the velocity of the fluid moving inside the cavity increases [21, 22]. At larger velocities, local convection phenomena become dominant over conduction, causing usually an over prediction of the temperatures in the mould. For the specific production process addressed in this publication, the resin velocity is limited by the pressure gradient inside the mould cavity, driven by vacuum suction.

To define an applicability range as a function of the fluid velocity, dimensionless parameters are proposed, such as the Graetz number or the Péclet number [23, 24].

The Graetz number is a relationship between the filling speed and the heat conduction. When the filling speed is slow in comparison with the heat conduction, the conduction terms are larger than the convection terms, and they dominate the energy equation. Imprecision for Graetz numbers larger than one ($Gz \gg 1$) have been reported for temperature predictions using LTE models [25].

The Péclet number is a dimensionless evaluation of the fluid velocity, usually expressed as the product of the Prandtl number and the Reynolds number [26]. Alternatively, the Péclet number can be expressed as defined in Equation 7.5.

$$Pe = Pr \cdot Re = \frac{w \cdot L}{a} \quad (7.5)$$

Where w stands for flow front velocity, L is the characteristic length and a the thermal diffusivity of the resin as stated in Equation 7.6.

$$a = \frac{k_T}{\rho_r \cdot C_{p,r}} \quad (7.6)$$

In equation 7.6 Discussion opens at this point for the selection of the right parameters for the definition of the Péclet number. Many author do use the fibre tow diameter as a representative length (L) in Equation 7.5, while other do use the mould cavity thickness [23]. The determination of the right Péclet number needs consensus for the definition of the analysis scale. According to that, in this work tow diameter is used as reference.

7.2.2 Term by term analysis

The Local Thermal Equilibrium model is composed by five different terms representing different phenomena occurring inside the mould cavity.

The first term of the equation, (Equation 7.7) corresponds to the change of internal energy occurring in the process (heating of the resin). The term consists in a law-of-mixtures of the specific heat and density of both constituents, as a function of the temperature evolution over time. For most of the materials used and usual temperature ranges (25°C to 200°C), the specific heat and the density are considered as a constant.

$$(\phi(\rho C_p)_f + (1 - \phi)(\rho C_p)_s) \frac{\partial \langle T \rangle}{\partial t} \quad (7.7)$$

Second term of the equation, (Equation 7.7) stands for convection of heat in the plane due to averaged Darcy velocity (heat transport due to moving resin). Dependent of velocity and the resin gradient of temperature, it can be affected by the slight velocity differences occurring due to the inhomogeneity of the fibre bed. However, considering the macroscale level, the velocity variation can be tracked easily and implemented in the model, restricting the possible uncertainty of this term.

$$(\rho C_p)_f \langle v_f \rangle \cdot \nabla \langle T \rangle \quad (7.8)$$

Third term (Equation 7.9) is for the through-the-thickness conduction and dispersion (due to dissipation and chemical reaction). The term reflects the gradient of temperature through the thickness of the sample. As in RIFT one mould presents little thermal inertia, the through-the-thickness gradient is of notable consideration and can be a possible source of accuracy improvement for this specific setup.

$$(k_{zz} + K_{Dzz}) \frac{\partial^2 T}{\partial z^2} \quad (7.9)$$

Fourth term (Equation 7.10) corresponds to the in plane conduction and dispersion (due to diffusion of heat from the mould walls into the resin and microscopic resin motion not accounted for convection). It is also presented in this equation as a law-of-mixtures for conductivities, as a square function

of temperature evolution. Previous studies [17] advice discarding this term as the effects caused by the square dependency are small when compared to the rest of the terms for slow velocities.

$$\nabla \cdot (\phi K_f + (1 - \phi)K_s) \cdot \nabla (\langle T \rangle) \quad (7.10)$$

Finally, the last term (Equation 7.11) stands for the heat generation due to the exothermic process of the resin cure. Usual production process design methodologies agree in the use of filling periods smaller than the resin life time, in order to avoid the sudden viscosity increase related to the crosslinking of the resin. Therefore, it is a safe decision to neglect this term under the assumption that crosslinking will never occur during the infusion period of time.

$$\phi \dot{s} \quad (7.11)$$

The third term, (Equation 7.9, arises as a discussion motive due to the preform structure in which the resin flows. The laminar flow is disturbed creating local convection effects. In the term description, the conductivity is presented as $(k_{zz} + K_{Dzz})$, but usually the thermal dispersion coefficient K_{Dzz} is neglected in its implementation.

7.3 Experimental setup

In order to investigate the applicability of the model for the specific production setup proposed, an experimental rig was developed to extract thermal information of RIFT produced samples.

The rig was designed to conduct non-isothermal infusions using a RIFT configuration. Heat is introduced into the system from the rigid mould side by means of an electric heating device. The device is placed underneath the rigid mould (aluminium slab) with a close loop feedback calibration system to keep a constant surface temperature. The aluminium slab used as a mould has a considerable thickness (40 mm.) which gives thermal inertia to the system, ensuring thermal stability of the mould and a constant temperature at the

mould surface. If needed, the resin itself can be heated beforehand in an oven and infused through an isolated gate. A scheme of the entire setup is depicted in Figure 7.2.

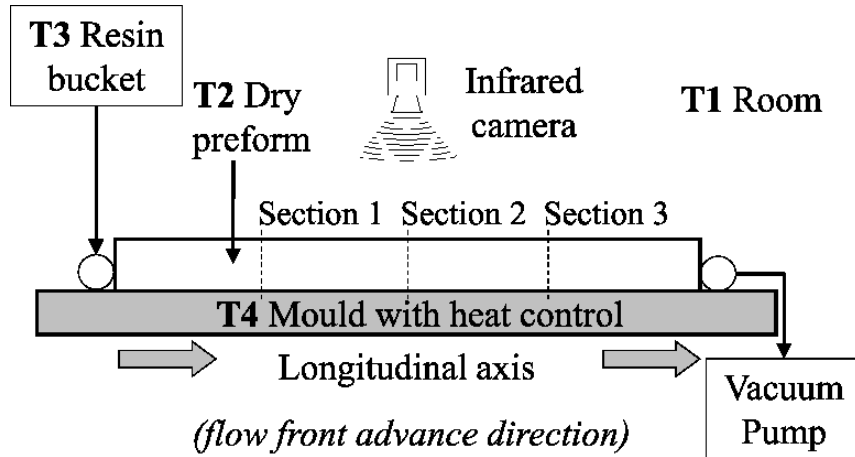


Figure 7.2: Scheme of a longitudinal cut of the experimental rig. T_1 , T_2 , T_3 and T_4 stand for the different temperatures involved in the set-up.

Resin is placed in a bucket and is driven to the mould cavity, where a distribution channel configures a linear gate across the entire edge. The rigid mould tool consists in a flat thick aluminium slab on one side, and a vacuum bag is used as a flexible tool in the other side. The resin goes through the different control section (Section 1, Section 2 and Section 3) and finally reaches the end of the mould cavity, where a vacuum pump is connected.

Type K thermocouples were embedded in these sections of the preform, lined up in layers corresponding to midplane, first quarter and third quarter of the thickness of the sample. Once the entire preform is assembled, the disposition of the thermocouples configures a 9 points grid. Three different control points are in the longitudinal axis for each instrumented layer and three control points are in the through-the-thickness direction for each section. These thermocouples are used first to determine the temperature of the dry preform (T_2), and later to determine the evolution of the temperature during the infusion and cure processes.

In addition, temperatures at top and bottom of the sample need to be recorded to monitor the interaction of the mould and the part. To this purpose, three thermocouples were embedded in the surface of the aluminium

slab in contact with the part (T4), and an infrared camera was placed on top. This camera not only verified the evolution of the temperature on the analysed top layer but was also useful to monitor the shape of the flow front advance and the temperature on the entire sample surface. Linear advance of the resin through the sample was controlled visually.

Two extra thermocouples were used to monitor the room temperature (T1) and the temperature of the resin at the inlet point (T3) during the infusion stage. A detailed transversal view of a control section (Section 1 in Figure 7.2), can be observed in Figure 7.3, where the position of each control point and its nomenclature its detailed.

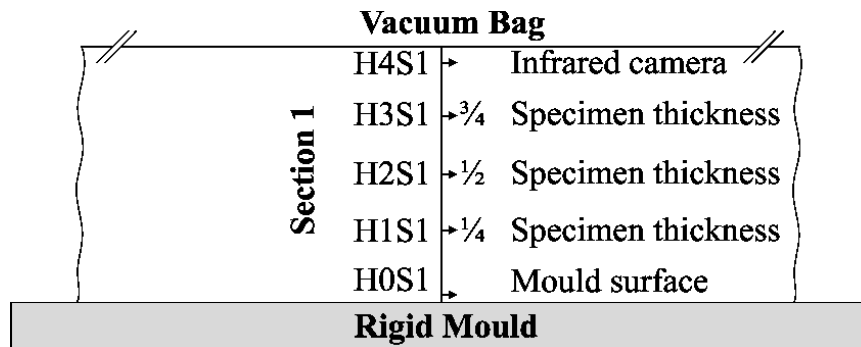


Figure 7.3: Representative (not scaled) detail of the transversal section of the sample with position and nomenclature of the recorded points.

All signals of the tests are handled through a data acquisition device. An acquisition GUI was developed in-house using a Labview environment. Temperature was recorded in real time at 1Hz frequency. Synchronized with the thermocouple measurement, the amount of resin transferred to the mould cavity is recorded to obtain the exact flow rate and flow front velocity at any time of the test.

An insulated tube was used to connect the bucket with the inlet of the mould to ensure the temperature stability of the incoming resin. A thermocouple is placed at the mould cavity inlet to provide the temperature in the entrance of the system. This point is chosen to avoid temperature variations in the short path between the bucket and the entrance of the mould cavity. Data provided from this thermocouple confirms the supposition of a constant temperature at the entrance.

Six samples were infused according to the details described in Table 7.1.

Sample dimensions and materials			
Dimensions	Length	Width	Thickness
	250 mm.	150 mm.	30 mm.
Materials	Fibreglass multi-axial/non-crimp fabric		
	Epoxy resin with amine base hardener		
Details of the experimental program			
Repetitions	Mould T ^o	Fibre T ^o	Resin T ^o
6	60°C	variable	Room

Table 7.1: *Main dimensions, material description and experimental program information.*

The samples used for the tests consisted of glass fibre reinforced epoxy rectangular plates. Extremely thick samples were used in order to insulate the measurement points of the direct influence of the boundary condition in the measurements. No flow enhancement layers or other ancillary materials are used.

7.4 Results

7.4.1 Data handling

From the LTE equation, (Equation 7.1), terms on the left are dependent on properties inherent to the own material. These properties can be directly extracted from material data sheet, and are obtained conducting common tests in material characterization process. The following Table 7.2 summarizes the used data.

Terms on the right side present variables such as the through-the-thickness conduction and dispersion term, which can be obtained with this setup.

Last term in the right side of the equation, corresponding to the exothermic reaction, is ruled out due to the supposition that no curing occur during

Material data			
		Resin	Fibre
Heat capacity	[KJ/KgK]	1800	344
Density	[Kg/m ³]	1245	2550
Conductivity	[W/mK]	0.25	1
Porosity	[%]	50	

Table 7.2: Auxiliary data extracted from the test configuration.

infusion process. Consequently, the third and fourth term (Equations 7.9 and 7.10) are left to be discussed.

Other simplifications should be considered when using the LTE equation to simulate RIFT infusions. The pressure and the velocity profile is assumed uniform through the thickness, and the variation of the viscosity once the working temperature is achieved is not strongly dependent on temperature, which is acceptable for most of the thermoset formulated resins.

Temperatures needed for the evaluation of this two terms are extracted directly from the data provided by the computing grid, depicted in Figure 7.4. In this figure, the disposition of the points and its nomenclature inside the system is presented.

H is the height, with zero being the mould and four the top layer, and S standing for section, being 1 the closest to the gate and 3 the closest to the vent. Distances between control points (thermocouples) can be found in Table 7.2. The vertical distance between points is 6.25 mm and the horizontal distance between sections is 75 mm.

The test developed is designed to understand the thermal evolution of the central point (H2S2). Taking this point as a reference, one can obtain the time partial derivation of temperatures from the values recorded at 1Hz frequency. For the distance partial derivation of temperature as a function of longitudinal displacement, one can use the data recorded at the point H2S1.

As the test is designed to provide a linear flow front advance of the resin, only one longitudinal path is evaluated in this direction, by means of the temperature at points H2S1 and H2S3. For the through-the-thickness tempera-

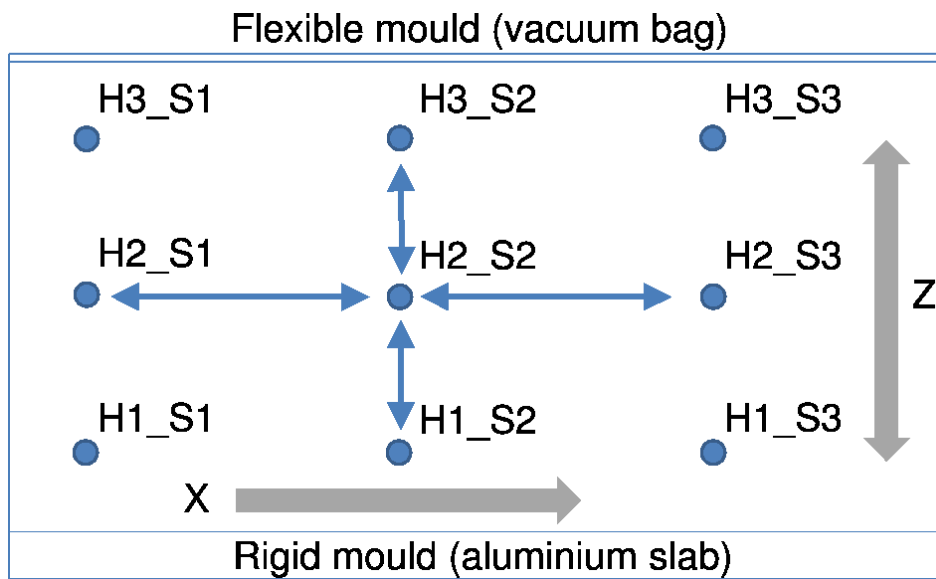


Figure 7.4: Detail of a longitudinal cut of the sample, where the disposition of the control points, and the through-the-thickness grid that they configure can be observed.

ture evolution, one uses control points H1S2 and H3S2. Figure 7.5 shows an infrared image of the infusion process, where the linear flow front advance during the process can be verified.

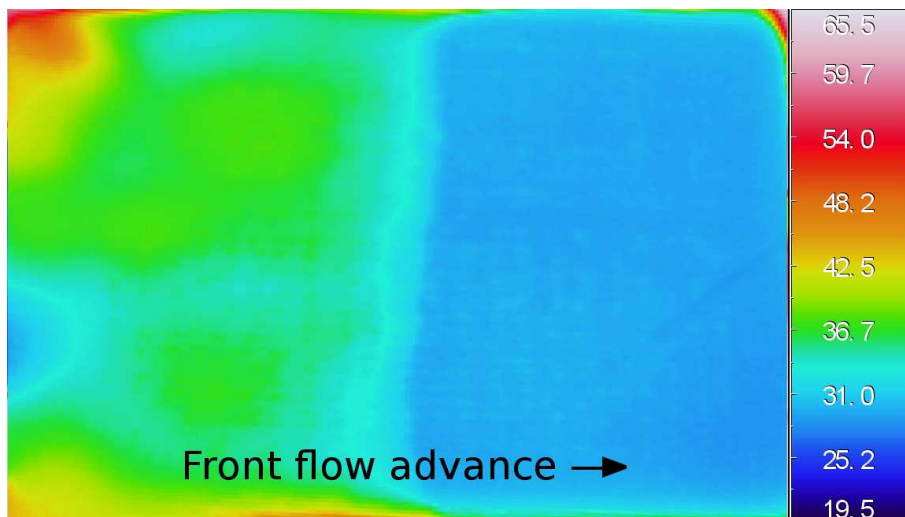


Figure 7.5: Infrared image of the upper surface of one of the samples. Temperature in $^{\circ}\text{C}$

7.4.2 Through-the-thickness conduction and dispersion evaluation

It is proposed to study the through-the-thickness conduction and dispersion term by means of its isolation in the general LTE model as is shown in the following Equation 7.12.

$$(k_{zz} + K_{Dzz}) = \frac{S_e \frac{\partial T}{\partial t} + (\rho C_p)_f \langle v_f \rangle - \nabla (K_e + K_D) \cdot \nabla \langle T \rangle}{\frac{\partial^2 T}{\partial z^2}} \quad (7.12)$$

Where S_e refers to the volumetric heat capacity as described in following Equation 7.13

$$S_e = (\phi(\rho C_p)_f + (1 - \phi)(\rho C_p)_s) \quad (7.13)$$

and K_e as it is defined in Equation 7.14

$$K_e = K_s \cdot \phi + K_f \cdot (1 - \phi) \quad (7.14)$$

One can now evaluate the magnitude of the in-plane conduction and dispersion term. Its square dependence should suppose a small influence when compared to the rest of the terms. For the tests conducted, it is confirmed that the magnitude of this term is of 2 orders of magnitude smaller than the rest of terms. One can then obviate this term from the general equation and present the following variable isolation of Equation 7.15 to evaluate the through-the-thickness conduction and dispersion term.

$$(k_{zz} + K_{Dzz}) = \frac{S_e \frac{\partial T}{\partial t} + (\rho C_p)_f \langle v_f \rangle}{\frac{\partial^2 T}{\partial z^2}} \quad (7.15)$$

7.4.3 Output analysis

The data extracted from the thermocouples provides a thermal map of the sample while the resin flows, depicted in Figure 7.6.

In Figure 7.6, the trends of the temperature evolution can be observed. Knowing the position of the thermocouples, one can use the temperature evolution to derive the flow front position and verify the linear advance of the flow

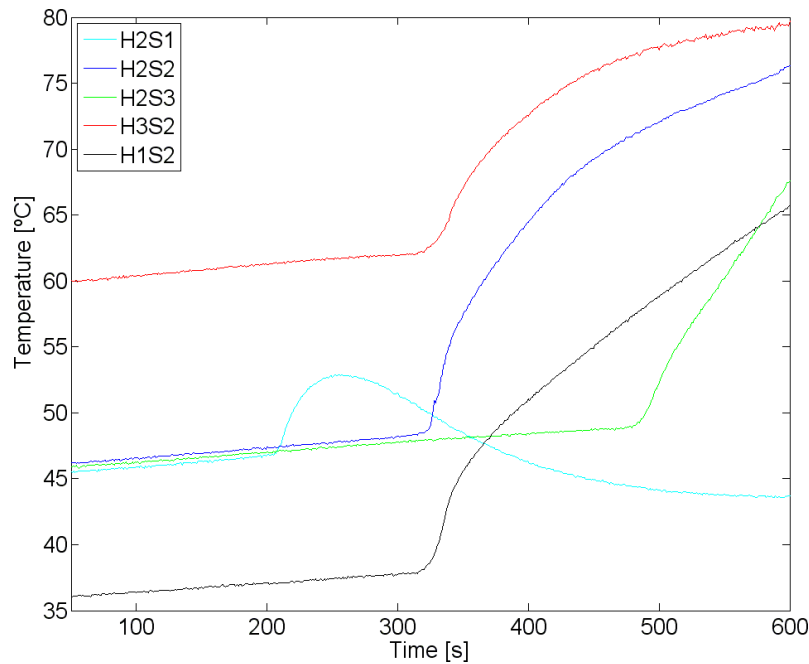


Figure 7.6: Temperature recorded from one of the infused samples, illustrative of the temperature profile typology.

in the studied direction. This is verified by the alignment in the time-scale of the tracers corresponding to Section 2.

Velocity profiles were extracted with mass loss measurements of the infusion bucket, placed over a precision scale. After data treatment, the following velocity profiles, presented in Figure 7.7 were obtained.

Velocity trends correspond with typical quadratic velocity expressions, characteristic of constant pressure infusions. Using these profiles, the different Péclet numbers were extracted for any instant of the infusion time, according to its previously stated definition. For all tests, low Péclet numbers (< 1) were obtained. Therefore, for all cases, the flow typology is slow and laminar, and matches the scope of this work.

For the purpose of this study, a limited period of time needs to be defined. This period encompasses from the first instant where resin has gone through all thermocouples until the resin reaches the mould end. This time period lasts an average of 250 seconds \pm 20 seconds for all tests.

Analysing the obtained profiles, the outputs remain constant until the resin reaches the thermocouples. At this moment, a transient period in which

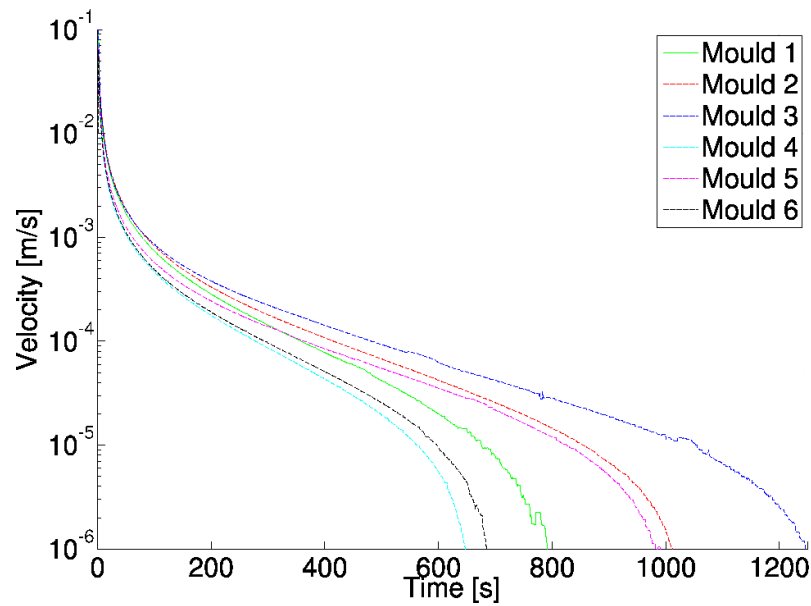


Figure 7.7: Velocity profiles for the different infusions conducted.

some thermocouples are wet and some not occurs. After that, the value stabilizes again, and the resin flow through all the control points.

The energy equation that dominates the temperature field have been formulated with and without the fourth term, related to the heat dispersion. The difference between them is unnoticeable as can be shown in the trends depicted in the following Figure 7.8.

During tests, thermal lab conditions as well as infusion procedure was kept as constant as possible. However, different profiles were obtained for different infusions, which is reasonable due to the lack of control of some parameters such as room temperature.

In addition, one must notice the existing variability in infusions 3 and 5. The analysis of the data logs does not provide any specific reason for these disturbances, so the variability was suggested to come from a physical problem. Incorrect wire connection in the measurement point or equipment end arises as the most probable cause. This leads to results with large oscillations when using this data for calculation.

After a comparative overview of the tests, the analysis of the heat dispersion term for each infusion is evaluated. The term is presented for each test as a function of the Péclet number in order to check for its variation as a function

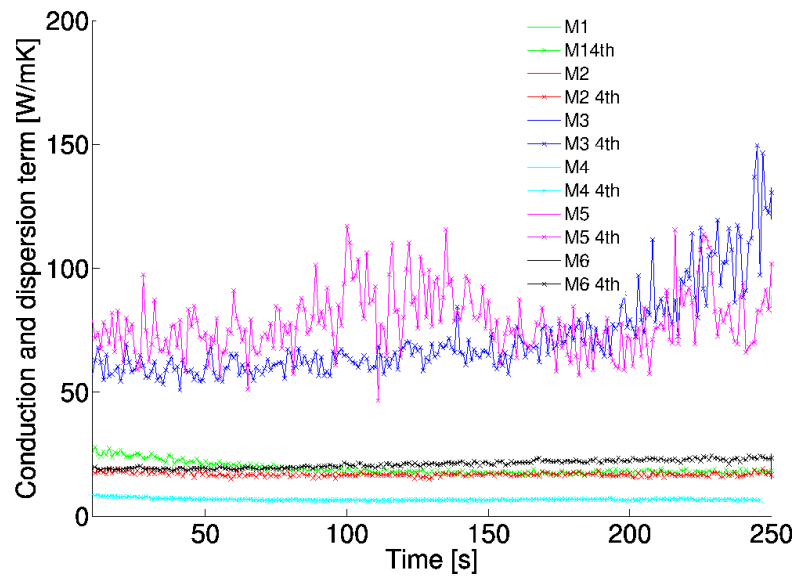


Figure 7.8: Comparison of the term obtained with and without the fourth term of the LTE model

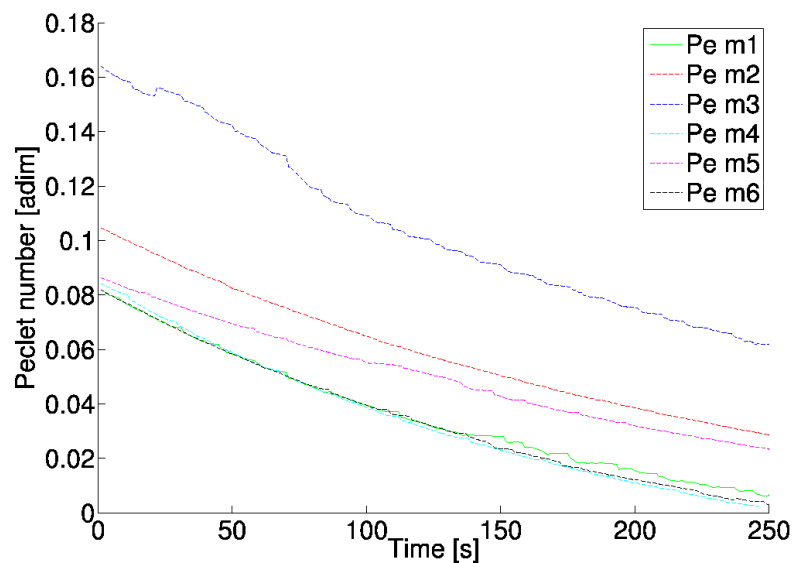


Figure 7.9: Through-the-thickness heat dispersion term as a function of the Péclet number for different test conducted

of the front flow velocity. Figure 7.9 shows the values of the Péclet number for the studied period. Magnitude of the velocity differences between different infusions conducted can be observed.

Figure 7.10 provides an overview of the through-the-thickness conduction and dispersion term for the time period considered in the analysis. Although

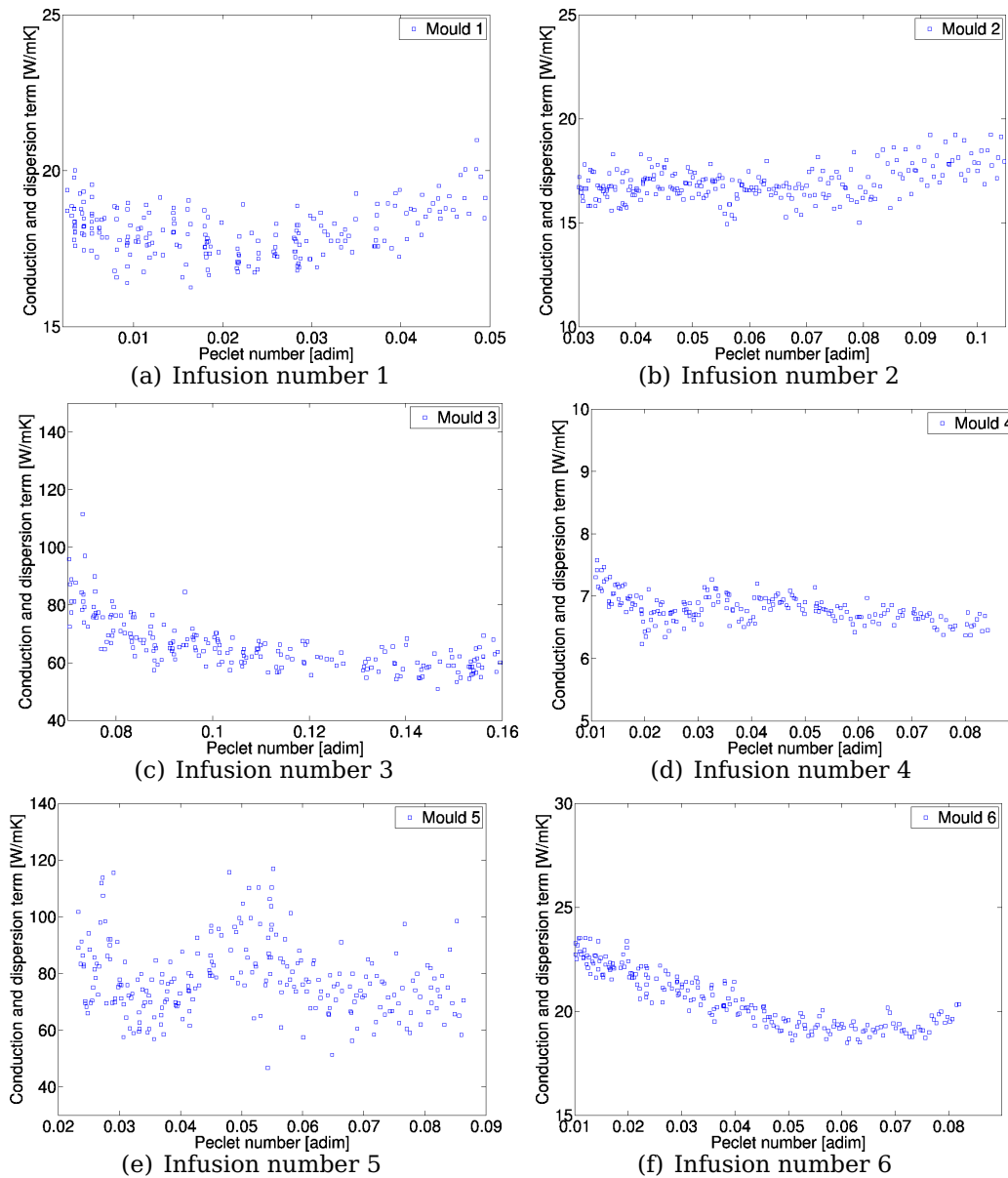


Figure 7.10: Presentation of the different conduction and dispersion terms as a function of the Péclet number for the different tests conducted

different values are obtained for each test, the shape of the term along the Péclet range considered in vacuum bagged infusion processes remains stable.

The author points the high dispersion range observed in image 7.10(e), to the previously stated causes. Even considering this dispersion, a flat trend is observed, in accordance with the results of the rest of tests.

7.4.4 Discussion

According to the observations described in literature [25, 26], one should expect a dependency between the heat dispersion coefficient and the Péclet number.

Metzger et al. [27] illustrate a methodology to obtain typology and shape of heat dispersion coefficient by means of thermocouples lectures. Although their work shows the linear evolution of the heat dispersion coefficient as a function of the Péclet number, it considered a Péclet range much larger (adequate for RTM) than the one used in the selected infusion technique.

Hsiao et Advani [28], also state the dependence of the heat convection on the Péclet number. They also notice that, for low Péclet numbers, the heat transfer is dominated by conduction, while as it increases the convection term gains weight and becomes dominant in heat transfer. However, the specific production technique cover in this work is different that the one used in the work of Hsia et Advani (RTM). With the presented data, one can confirm the validity of extending the proposed methodology to this production technique.

Their work [28], proposes a modified thermal conductivity parameter to include these phenomena and cover the entire range of production processes for composite materials, results obtained in this work show that in the specific studied technique one can obviate the convective term.

For RIFT technique, the low velocity that is used (due to the limited suction that can be done by vacuum pump), situates the value of the heat dispersion coefficient in a range were the velocity influence can be almost negligible, and therefore it is not dependent of the resin velocity. The stability of the obtained term points conduction as the main source of heat transfer for this production process. If the dispersion effect were noticeable one should expect

a linear tendency in the obtained results, which only can be identified in Figure 7.10(c), which has the larger Péclet numbers.

7.5 Conclusions

An experimental validation of proposed simplifications for the Local Thermal Equilibrium equation has been proposed in the present work.

The results confirm the low Péclet number associated to this production process which results in a heat transmission process based mainly in the conduction phenomena. Local convection is therefore negligible and the suppression of its related term is consistent with obtained results, leaving a simple, easy to implement, version of the general equation.

The obtained simplified method will suppose lighter computing expressions in simulation codes which will result in faster prediction without critical loss of precision. This fact is of great interest for the prediction of thermal maps in sizeable parts, which are every time more common of being produced with this technique.

Future work will include the implementation of this thermal simulation expression in a full-scale model in order to check its application in a real part.

Bibliography

- [1] C. Williams, J. Summerscales, S. Grove, Resin infusion under flexible tooling (RIFT). A review, *Composites Part A: Applied Science and Manufacturing* 27 (7) (1996) 517–524.
- [2] S. Mazumdar, *Composites Manufacturing. Materials, Product and Process Engineering*, CRC Press, Boca Raton, FL, USA, 1997.
- [3] C. Seeton, Viscosity temperature correlation for liquids, *Tribology Letters* 22 (1) (2006) 67–78.
- [4] C. Rudd, A. Long, K. Kendall, C. Mangin, *Liquid Moulding Technologies*, Woodhead Publishing and SAE International, Warrendale, PA, USA, 1997.
- [5] W. Schulz, D. Myers, T. Singer, P. Ifju, R. Haftka, Determination of residual stress and thermal history for im7/977-2 composite laminates, *Composites Science and Technology* 65 (13) (2005) 2104–2024.
- [6] J. Xiong, R. Shenoi, J. Gao, An analytical model to predict residual thermal stress in 2d orthogonal plain weave fabric composites, *International Journal of Solids and Structures* 46 (9) (2009) 1872–1883.
- [7] L. You, X. You, A unified numerical approach for thermal analysis of transversely isotropic fiber-reinforced composites containing inhomogeneous interphase, *Composites: Part A-Applied Science and Manufacturing* 36 (6) (2005) 728–738.
- [8] R. Gauvin, F. Trochu, Key issues in Numerical simulation for liquid composite moulding processes, *Polymer Composites*, 19(3) (1998) 233–240.

- [9] P. Simacek, S. Advani, Desirable features in mould filling simulations for liquid composite moulding processes, *Polymer Composite* 25 (4) (2004) 355–367.
- [10] M. Skinner, New application and approaches expand market for composite software, *Reinforced Plastics*, 50 (6) (2006) 24–28.
- [11] O. Mai, A. Courniot, F. Dupret, Non-isothermal simulation of the resin transfer moulding process, *Composites Part A-Applied Science and Manufacturing* 29 (1-2) (1998) 189–198.
- [12] M. Delèglise, C. Binètruy, P. Castaing, P. Krawczak, Use of non local equilibrium theory to predict transient temperature during non- resin flow in a fibrous medium, *International Journal of Heat and Mass Transfer* 50 (11-12) (2007) 2317–2324.
- [13] A. Abbassi, M. Shahnazari, Numerical modelling of mold filling and curing in non-isothermal RTM process, *Applied thermal engineering* 24 (16) (2004) 2453–2465.
- [14] M. Lin, M. Kang, H. Hahn, A finite element analysis of convection problems in RTM using internal nodes, *Composites Part A-Applied Science and Manufacturing* 31 (4) (2000) 373–383.
- [15] A. Shojaei, S. Ghaffarian, S. Karimian, Simulation of the three-dimensional non-isothermal mold filling process in resin transfer molding, *Composites Science and Technology* 63 (13) (2003) 1931–1948.
- [16] K. Pillai, M. Munagavalasa, Governing equations for unsaturated flow through woven fiber mats. Part 2. non-isothermal reactive flows, *Composites Part Part A-Applied Science and Manufacturing* 35 (4) (2004) 403–415.
- [17] P. Simacek, S. Advani, Approximate numerical method for prediction of temperature distribution in flow through narrow gaps containing porous media, *Computational Mechanics* 32 (1-2) (2003) 1–9.

- [18] S. Advani, M. Brusckhe, R. Parnas, Resin Transfer molding flow phenomena in polymeric composites. In *Flow and Rheology in Polymer Composites Manufacturing*, S.G. Advani, Amsterdam, NE, 1994.
- [19] C.L. Tucker III, R. Dessenberger, Governing equations for flow and heat transfer in stationary fiber beds. In *Flow and Rheology in Polymer Composites Manufacturing*, S.G. Advani, Amsterdam, NE, 1994.
- [20] W. Chang, N. Kikuchi, Analysis of non-isothermal mold filling molding and structural reaction process in resin transfer molding (RTM) and structural reaction injection molding (SRIM), *Computational mechanics* 16 (1) (1995) 22–35.
- [21] C.L. Tucker III, Heat transfer and reaction issues in liquid composite moulding, *Polymer Composites* 17 (1) (1996) 60–72.
- [22] H. Chiu, B. Yu, S. Chen, L. Lee, Heat transfer during flow and resin reaction through fibre reinforcement, *Chemical Engineering Science* 55 (17) (2000) 3365–3376.
- [23] M. Huysmans, A. Dassargues, Review of the use of Peclet numbers to determine the relative importance of advection and diffusion in low permeability environments, *Hydrogeology Journal* 13 (2005) 895–904
- [24] A. Caba, Verification of a three-dimensional resin film infusion process simulation model, Master thesis, Virginia State University (1998).
- [25] M. Quintard, S. Whitaker, Local thermal equilibrium for transient heat conduction: theory and comparison with numerical experiments, *International Journal of Heat and Mass Transfer* 38 (15) (1995) 2779–2796.
- [26] M. Henne, P. Ermanni, M. Deléglise, P. Krawczak, Heat transfer of fibre beds in resin transfer moulding: an experimental approach, *Composites Science and Technology* 64 (9) (2004) 1191–1202
- [27] T. Metzger, S. Didierjean, D. Maillet, Optimal experimental estimation of thermal dispersion coefficients in porous media, *International Journal of Heat and Mass Transfer* 47 (2004) 3341–3353.

- [28] K. Hsiao, S. Advani, Modified effective thermal conductivity due to heat dispersion in fibrous porous, *International Journal of Heat and Mass Transfer* 42 (1999) 1237-1254.

Part III

Conclusions

The field of design and manufacturing of fibre reinforced thermoset composite parts is known to encompass a wide variety of methods and a broad selection of process variations. The work presented here tries not to embrace the full range of study within this field. Instead, it focuses on selected topics that are of importance and particular interest to both the industrial user who is faced with technical challenges in changing markets as to the scientific community that investigates the underlying physical phenomena of the manufacturing process.

Following an introduction in Chapter 1 accompanied by a list of scientific papers in Chapter 2, Chapter 3 reviews the current state-of-the-art in the dominant manufacturing methods available by using the example of a widely used industrial part i.e. pressurised vessels. The study places fibre reinforced thermoset vessels against tanks made of different materials, as well as compares the prevailing manufacturing techniques from a structural, production process, and economical point of view. One can extract from this chapter the necessity of co-existence of different methods with various degrees of automation to best answer the current market needs of extended range of product sizes, shapes and structural requirements.

Although in the review, cutting edge technologies such as Advanced Fibre Placement or Pre-preg moulding are analysed, special attention is given to a currently mature technology, liquid composite moulding. Two main families, Resin Transfer Moulding (RTM) and Resin Infusion under Flexible Tooling (RIFT) are specifically covered. Due to the pressure on energy savings in manufacturing, such out-of-autoclave techniques are being considered as cost-effective alternatives to AFP and Pre-preg moulding for the production of structural parts in aeronautic and aerospace markets.

A method to select the best liquid composite moulding method for a particular part is proposed in Chapter 4. Although it is of a generic nature, the multidisciplinary decision tool proposed improves the efficiency and performance of design engineers. The evaluation of the material configuration, structural performance, cost analysis and production rates by means of single variable optimization makes the decision tool a valuable assistant in the time and cost consuming stage of initial conception and prototyping of a new industrial com-

posite product.

The necessity to ensure quality and repeatability has now increased the need of virtual assessment tools for RTM and RIFT to fully characterize and simulate the entire manufacturing process. Virtual tools can also help to adapt the established LCM processes to new sector requirements. Thus, based on the research and experience acquired in the first part of the dissertation, deeper analysis of the two main representative families of liquid composite moulding (RTM and RIFT) is conducted, in order to contribute to the development of advanced simulation tools for each technique.

For RTM, a strategy to obtain more precise viscosity expressions has been developed in Chapter 5. The work concludes that implementing in-situ characterization of the viscosity value considering the effect of the surrounding fibre provides more accurate injection simulation results than using traditional expressions, based on neat resin characterizations. The method, experimentally validated, discusses the sensitivity to variations in process and material parameters such as fibre volume fraction and permeability. Finally, a real application case study was included, highlighting the industrial relevance of adopting the proposed model over other non-linear viscosity models.

Moving to RIFT, advanced virtual simulation techniques are starting to include temperature effects to model the flow front advance in non-isothermal setups. An efficient, low cost algorithm is vital to encourage the practical adoption in industrial environment. So, Chapter 6 proposes a through-the-thickness temperature prediction technique that evolves from a bi-dimensional thermal analysis and extrudes the temperature profile constrained by the mould boundary conditions. The result offers a good level of agreement between experiment and simulation across the temperature range, with the exception of a slight overprediction tendency in zones close to the inlet gate.

Finally, a term by term analysis of the LTE model used for the determination of the energy balance occurring inside the mould is conducted. The analysis determines that the dominant heat transfer phenomenon during the infusion process is thermal conduction. An experimental validation of the possible simplification for the LTE equations is presented. The study demonstrates that neglecting local convection and therefore suppressing its related term in the

LTE model is consistent with obtained experimental results, thus leaving a simple, easy-to-implement version of the general equation without a critical loss of accuracy.

Main Contributions

The main contributions presented in this thesis are listed below

- A state of the art of the current manufacturing techniques including an analysis from its initial application to cutting edge technologies through one of the most common products for the industrial environment, pressure tanks. The state of the art includes technique analysis and general evaluation from a performance, production rate and economic point of view.
- The creation of a strategy to handle the information needed in each step of the design process into a multidisciplinary tool, through a single control parameter. The strategy links together material selection, structural performance, production process analysis, production rates and costs. The output evaluates the effects of design variations throughout the design steps in parallel and provides numerical support to the decision process.
- The development of a time-dependent resin viscosity expression, incorporating non-linear viscosity behaviour, which takes into account the impact of reinforcement fibre sizing and fibre bed architecture. These are not identifiable in neat resin viscosity characterization tests but are thought to have substantial impact on in-situ viscosity values during infusion, especially for large parts and slow infusion processes.
- The proposal of an analytical through-the-thickness temperature gradient model derived for resin transfer moulding, and its numerical implementation. An experimental validation study has been performed using representative set-ups of typical vacuum bagging processes and denotes the correct precision of the methodology despite its simplified nature.

- An analysis to validate the consideration of a conduction-dominant heat transfer process using the LTE equation for parts produced using heated mould setups. The analysis is done through an experimental task designed with this aim and confirms that the effect of heat dispersion caused by micro scale flow can be neglected due to the low velocity characteristic of this technique.
- The design, development and construction of a fibre reinforced thermoset composites manufacturing facility for the research group AMADE. The facility includes an instrumented vacuum bagging mould and an RTM setup with temperature control capability, to be used for further research and consolidation of the line activities.

Future Work

Based on both the results obtained and the difficulties found during the conducted research, the following points are proposed as future investigations lines.

- The introduction of effects related to the exothermic nature of the resin is an improvement to be included to the presented numerical tools. The models are thought for low-exothermic resins, which currently cover a wide range of the available thermoset resins in the market. The proposed improvement can make the tools extensible to exothermic and high-exothermic resins, where the cure effects are more noticeable and can have a considerable effect on the viscosity variation.
- The experimental validation of the proposed virtual assessment tools have been carried out at sample levels due to the limitations of the research group. A next step of the process encompasses experimental testing at sub-component and component level in order to test the viscosity model and temperature prediction precision when used in large parts.
- To continue the process of a complete virtual assessment tool to ensure the repeatability and quality of LCM produced part, the effects of the production process into the final part should be taken into account. Coupling the temperature history obtained for the infusions with structural information of the material will lead to a multi-physical tool capable to predict distortions caused by the production process into final part, as well as thermal and cure related residual stresses. This continuation work is considered as an actual topic of research for the main industrial partners of the aeronautical and aerospace sectors, as well as a specific funding topic of European research programs.